2018

Stabilization of Hypoxia Inducible Factor by Cobalt Chloride Can Alter Renal Transepithelial

Subhra Sankar Nag
Cleveland State University

STABILIZATION OF HYPOXIA INDUCIBLE FACTOR BY COBALT CHLORIDE CAN ALTER RENAL TRANSEPITHELIAL TRANSPORT

SUBHRA SANKAR NAG

Bachelor of Technology in Biotechnology

West Bengal University of Technology, India

August 2007

Master of Science in Molecular Sciences and Nanotechnology

Louisiana Tech University

March 2010

Master of Science in Bioengineering

Clemson University

May 2012

Submitted in partial fulfillment of requirement for the degree

DOCTOR OF PHILOSOPHY IN REGULATORY BIOLOGY

at CLEVELAND STATE UNIVERSITY

August 2018

We hereby approve this Dissertation for

Subhra Sankar Nag

Candidate for the Doctor of Philosophy in Regulatory Biology degree for the Department of Biological, Geological, and Environmental Sciences

and the CLEVELAND STATE UNIVERSITY

College of Graduate Studies

_____Date: _____

Dr. Andrew H. Resnick Dissertation Chairperson

BGES/ GRHD/ Physics, Cleveland State University

_____Date: _____

Dr. Crystal M. Weyman Dissertation Committee Member

BGES/GRHD, Cleveland State University

_____Date: _____

Dr. Roman V. Kondratov Dissertation Committee Member

BGES/GRHD, Cleveland State University

_____Date: _____

Dr. Aaron F. Severson Dissertation Committee Member

GRHD/BGES, Cleveland State University

_____Date: _____

Dr. Thomas M. McIntyre Dissertation Committee Member

Department of Cellular and Molecular Medicine, Cleveland Clinic
BGES, Cleveland State University

_____Date: _____

Dr. Joseph C. LaManna Dissertation Committee Member

Physiology and Biophysics, Case Western Reserve University

Student's Date of Defense: July 26, 2018

DEDICATION

I would like to dedicate this dissertation to my mom (Nina Nag), dad (Biswapati Nag), and brother (Souma Sankar Nag) for their unconditional love and support. I would also like to dedicate this dissertation in the memory of my high-school biology teacher (Chobi di) who always encouraged me to pursue higher education.

ACKNOWLEDGEMENTS

First, I would like to express my sincere gratitude to my major advisor Dr. Andrew Resnick for giving me the opportunity to work in his laboratory. He has been an awesome mentor to me. He has always been very supportive in every aspect regarding my education, research, and career. He always encouraged me to think and work independently. He was always available whenever I needed any help. Moreover, he is easily approachable, and I never felt any hesitation to ask him any questions. I would like to thank him again for all his help and providing me this excellent learning opportunity.

I would like to thank my research advisory committee members Dr. Roman Kondratov (CSU), Dr. Crystal Weyman (CSU), Dr. Thomas McIntyre (Cleveland Clinic), and Dr. Joseph LaManna (Case Western Reserve Univ.) for their valuable time to give me suggestions and critical inputs to improve my dissertation. I still recall my first committee meeting in 2014, when I had a vague research idea and the committee meeting was for more than three hours, and the advisory committee members stayed some extra time to help me figure out a clear plan of action. I am glad that my project evolved over the years by discussing it with Dr. Resnick, advisory committee members and by presenting my research in numerous conferences. I am very grateful to my advisory committee members for all their guidance during this process. I would also like to thank Dr. Aaron Severson (CSU) for agreeing to act as an internal reader in my PhD defense committee. In addition, during departmental presentations, Dr. Severson gave me some important suggestions that helped me to improve my project, and I am thankful for them.

I am grateful to the NIH and CSU-GRHD for the research funding support to Dr. Resnick and very thankful to the CSU Office of Research for a dissertation research award.

I am grateful to American Physiological Society (APS), Epithelial Transport Group (ETG) of APS, Ohio Physiological Society (OPS), and Society for Experimental Biology and Medicine (SEBM) for giving me opportunities to present my research and get some valuable input. I am also very thankful to APS, APS-ETG, and SEBM for research awards recognizing my dissertation work.

I would like to express my sincere gratitude to CSU-GRHD Director Dr. Anton Komar. He has always been very kind and supportive to me and provided conference travel funds whenever I requested them. Dr. Komar, as a previous graduate program director, played a crucial role in recruiting me in the program, and I will always be thankful for that. I would like to thank our current graduate program director, Dr. Girish Shukla, and department chair, Dr. Weyman, for their valuable time, guidance, and support whenever I needed it. I am very thankful to them and Department of BGES for providing me the opportunity to work as a teaching assistant throughout my program. I am grateful to my teaching mentors Dr. Dennis Sampson, Dr. Tobili Sam-Yellowe, Dr. Ralph Gibson, and late Dr. Donald Lindmark for all their help and guidance. I would like to thank our awesome technical and administrative staff: Ms. Michele Zinner, Ms. Susan Moreno-Molek, Ms. Carolee Pichler, Ms. Monica Warner, Ms. Lisa Pasquale, Mr. Miroslav Bogdanovski and Ms. Tara Peppard. I would like to express my sincere gratitude to Dr. Nigamanth Sridhar, Dr. Donna Schultheiss, Prof. John Plecnick, Ms. Maribeth Kralik and Ms. Patricia Otcasek of CSU College of Graduate Studies for all their help and support. I highly appreciate their efforts to organize workshops and initiate new events for graduate students, such as 3-MT thesis competition. I am very thankful to Dr. Mary McDonald and

the tutors of the CSU Writing Center for their time and efforts to check and edit my dissertation and other research or academic papers throughout my graduate program.

I would like to thank my fellow graduate students Rabbani, Anwesh, Arnab, Nikhil, Soumyaditya, Amra, Art, Raghav, and Supriya for helping me with techniques and reagents. I would like to express my sincere gratitude to Rabbani since he helped me a lot in trouble-shooting western blot issues. I would like to thank students in Dr. Resnick's lab: Vik, Brianna Boslett, Brianna McGinnis, Joe, Dave, Tara, along with BGES, Physics, Chemistry, GRHD faculty members, staff members, and students for maintaining an interactive learning environment. I would like to thank Jayeeta, Sonal, Tiyash, Raghav, Praveen, Akshay, Saikrishna, Kaushik, Banu, Atanu, Mainak, Ovishek, Dr. Shyamasree Datta (Pishi) for all their help and encouragement. I would like to thank my mom, dad, brother, and sister-in-law for all their love and support.

I apologize if I forgot to mention your name here. Thanks to all who helped me in my research and learning at CSU. All your encouragement and support really meant a lot to me. Thank you!

STABILIZATION OF HYPOXIA INDUCIBLE FACTOR BY COBALT CHLORIDE CAN ALTER RENAL TRANSEPITHELIAL TRANSPORT

SUBHRA SANKAR NAG

ABSTRACT

Kidney cyst expansion, stagnant fluid accumulation, and insufficient vascular supply can result in localized chronic ischemia-hypoxia in kidney cysts, as well as in normal renal epithelia adjacent to a cyst. We hypothesize that in normal epithelia near a cyst, the stabilization of Hypoxia Inducible Factor 1α (HIF1α), a major regulator of cellular response to hypoxia, can cause altered paracellular and transcellular transport, transforming a normal absorptive phenotype to a secretory and paracellularly leaky phenotype, leading to cyst expansion.

Using 100 μmol/L cobalt chloride ($CoCl_2$), HIF1α was stabilized in cellular nucleus of a mouse cortical collecting duct cell line (mCCD 1296 (d)), which resulted in an increased level of erythropoietin, an effector and reporter molecule of HIF1α. The mCCD monolayers have a high transepithelial resistance (TER) value (~3000 Ω-cm^2) and around 95% amiloride-sensitive voltage value. Equivalent current was calculated to compare active ion transport. Our results showed that TER values decreased significantly after 48 and 72 hours of HIF-stabilization. The decrease of TER value was consistent with the increase in the permeability of 70 kDa FITC-dextran molecules, supporting the hypothesis that HIF-stabilization altered paracellular transport. Stabilization of HIF caused a significant decrease in the protein level of zonula occludin 1 (ZO1), which controls paracellular transport through tight junctions. Decrease in the ZO1 protein level was

consistent with the decreased TER value and the increased paracellular permeability. Similarly, HIF-stabilization was found to increase paracellular permeability in Mardin-Darby Canine Kidney (MDCK) epithelial monolayers. In mCCD monolayers, HIF-stabilization for 48 hours caused loss of active sodium ion (Na^+) transport, and very interestingly, 72 hours of HIF-stabilization caused a switch in the direction of net active ion transport. HIF-stabilization caused a significant decrease of protein level of sodium-potassium-ATPase (Na^+/ K^+-ATPase) α1 subunit, the catalytic subunit of the enzyme responsible for active Na^+ transport, consistent with the loss of active transport of Na^+.

Our results indicate that HIF-stabilization can transform a normal absorptive epithelium to a paracellularly leaky and cyst-like secretory epithelium by reversing net Na^+ transport and increasing monolayer permeability due to alterations of tight junctions, and thereby HIF-stabilization may contribute to cyst expansion.

TABLE OF CONTENTS

Page

Page

Page

Page

LIST OF TABLES

LIST OF FIGURES

Figure Page

Figure Page

LIST OF ABBREVIATIONS

AC	Alternating current
ACE	Angiotensin converting enzyme
ADH	Antidiuretic hormone
ADPKD	Autosomal dominant PKD
AE	Anion exchangers
Ag/AgCl	Silver/ Silver chloride
AJ	Adherens junctions
AKI	Acute kidney injury
ANOVA	Analysis of Variance
APDM	Apical differential media
AKF	Acute kidney failure
ARPKD	Autosomal recessive PKD
AQP	Aquaporin
ATP	Adenosine triphosphate
ATPase	Adenosine triphosphatase
BLDM	Basolateral differentiation media
Ca^{2+}	Calcium ions
cAMP	Cyclic adenosine monophosphate
CCRCC	Clear cell renal cell carcinoma
CD	Collecting duct
CF	Cystic Fibrosis
CFTR	Cystic fibrosis transmembrane conductance regulator

CER	Cytoplasmic Extraction Reagent
cGMP	Cyclic guanosine monophosphate
CKD	Chronic kidney disease
Cl^-	Chloride ions
CO	Cardiac output
Co^{2+}	Cobalt
$CoCl_2$	Cobalt chloride
CT	Collecting tubule
DC	Direct current
DO_2	O_2 delivery
DMEM	Dulbecco's Modified Eagle Medium
DMOG	Dimethyloxallylglycine
DFX	Desferrioxamine
ECM	Extracellular matrix
EGF	Epidermal growth factor
ENaC	Epithelial Na^+ channels
EPO	Erythropoietin
ESRD	End-stage renal disease
FA	Focal adhesion
FAK	Focal adhesion kinase
FBS	Fetal bovine serum
FITC	Fluorescein isothiocyanate
GAPDH	Glyceraldehyde 3-phosphate dehydrogenase

GFP	Green fluorescent protein
GFR	Glomerular filtration rate
GLUT	Glucose Transporter
G_p	Paracellular conductance
GPCR	G-protein coupled receptor
G_t	Transepithelial conductance
G_{trc}	Transcellular conductance
H^+	Hydrogen ion or proton
HCO_3^-	Bicarbonate ion
HEPES	4-(2-hydroxyethyl)- 1- piperazineethanesulfonic acid
HIF	Hypoxia inducible factor
HO-1	Heme oxygenase-1
HRE	Hypoxia response element
HRP	Horseradish peroxidase
Hz	Hertz
I_{eq}	Equivalent current
IFT	Intraflagellar transport
I_{sc}	Short-circuit current
Isc_{eq}	Equivalent short-circuit current
JAK-STAT	Janus kinase-STAT
K^+	Potassium ions
mCCD	Mouse cortical collecting duct (Epithelial Cells)
MDCK	Madin-Darby Canine Kidney (Epithelial Cells)

MMPs	Matrix metalloproteinases
mTOR	Mammalian target of rapamycin
Na^+	Sodium ions
NaCl	Sodium Chloride
$NaHCO_3$	Sodium Bicarbonate
Na^+/ K^+-ATPase	Sodium-Potassium ATPase
NCC	Sodium-chloride cotransporter
NCX	Na^+/Ca^{2+} exchanger
NER	Nuclear Extraction Reagent
NHE	Na^+/H^+ exchanger
NKCC	Na^+-K^+-Cl^- cotransporter
NO	Nitric oxide
NPPB	5-nitro-2-(3-phenylpropylamino) benzoic acid
ODD	Oxygen-dependent degradation domain (ODD)
PAGE	Polyacrylamide gel electrophoresis
P_{app}	Apparent permeability
PAS	Per-Arnt-Sim
PC1	Polycystin 1
PC2	Polycystin 2
P_{Cl}	Permeability of Cl^-
PCP	Planar cell polarity
PCT	Proximal Convoluted Tubules
PHA	Pseudohypoaldosteronism

PHD	Proline hydroxylase
PKA	Protein Kinase A
PKC	Protein Kinase C
PKD	Polycystic kidney disease
PKG	Protein Kinase G
P_{Na}	Permeability of Na^+
P_o	Opening probability
PVDF	Polyvinylidene difluoride
pVHL	von Hippel-Lindau tumor suppressor protein
ROS	Reactive oxygen species
R_a	Apical membrane resistance
RAS	Renin-angiotensin system
R_b	Basolateral membrane resistance
R_{gap}	Gap resistance
R_{ic}	Intracellular resistance
$R_{meas.}$	Measured resistance
R_p	Paracellular Resistance
R_{tj}	Tight junction resistance
R_{trc}	Transcellular Resistance
R_s	Solution resistance
SDS	Sodium Dodecyl Sulfate
SEM	Standard error of mean
SLGT	Sodium/glucose cotransporter

SNGFR	Single nephron glomerular filtration rate
STAT	Signal Transducer and Activator of Transcription
T3	3,39,5-triiodo-L-thyronine
TAL	Thick ascending limb
TBST	Tris-buffered Saline-Tween 20
TER	Transepithelial resistance
TEER	Transepithelial electrical resistance
TGF	Tubuloglomerular feedback
TRP	Transient receptor potential
TRPM4	TRP melastatin-4
TRPV4	TRP vanilloid 4
TTX	Tetrodotoxin
VEGF	Vascular endothelial growth factor
WPI	World Precision Instruments
ZO1	Zonula occludens 1

CHAPTER I

INTRODUCTION

1.1 General Introduction

The function of a kidney is to maintain electrolyte (ion) and pH balance in our body. Excess ions are removed from the blood in the form of urine and thereby the kidney helps in controlling blood pressure. A kidney is made of around a million of filtering units, called nephrons (Pitts 1968). As shown in figure 1, kidney tubules are lined with epithelial cells having primary cilia. A renal cilium senses fluid flow and helps in maintaining normal function and physiology of the kidney. Thus, cilia, fluid flow, and epithelial cells are related to each other to maintain kidney anatomy and physiology, and thereby kidney homeostasis.

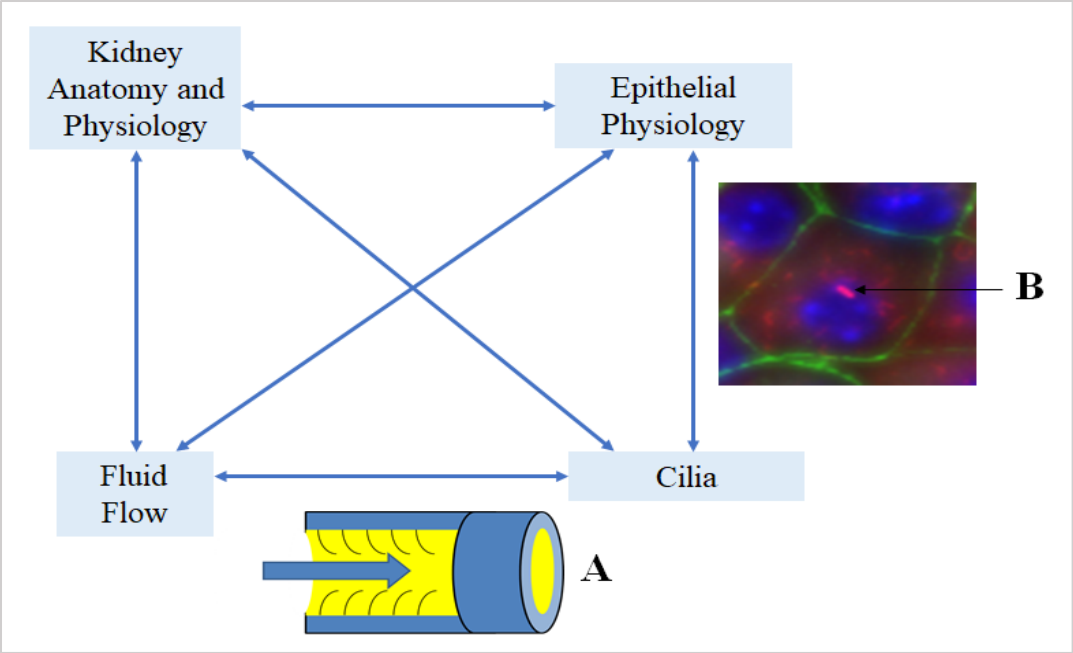

Figure 1: Kidney physiology maintained by epithelial cells containing primary cilia which sense fluid flow. The diagram A shows fluid flow through a cylindrical kidney tubule lined with epithelial cells having primary cilia. The diagram B shows an immunocytochemistry of renal epithelial cell and red protruding structure shows a primary cilium.

Around 600,000 people in the United States alone have polycystic kidney disease (PKD), which is characterized by the formation of fluid-filled pouch like structures called cysts, as shown in figure 2. The cysts expand over the years and finally causes kidney failure. Kidney cysts can compress onto blood vessels and can create kidney localized ischemic-hypoxic condition (Bernhardt, Wiesener et al. 2007). Kidney cystic epithelium was shown to have altered epithelial physiology and kidney localized hypoxia may affect the normal epithelia near a cyst (Yu, Kanzawa et al. 2008; Wilson 2011).

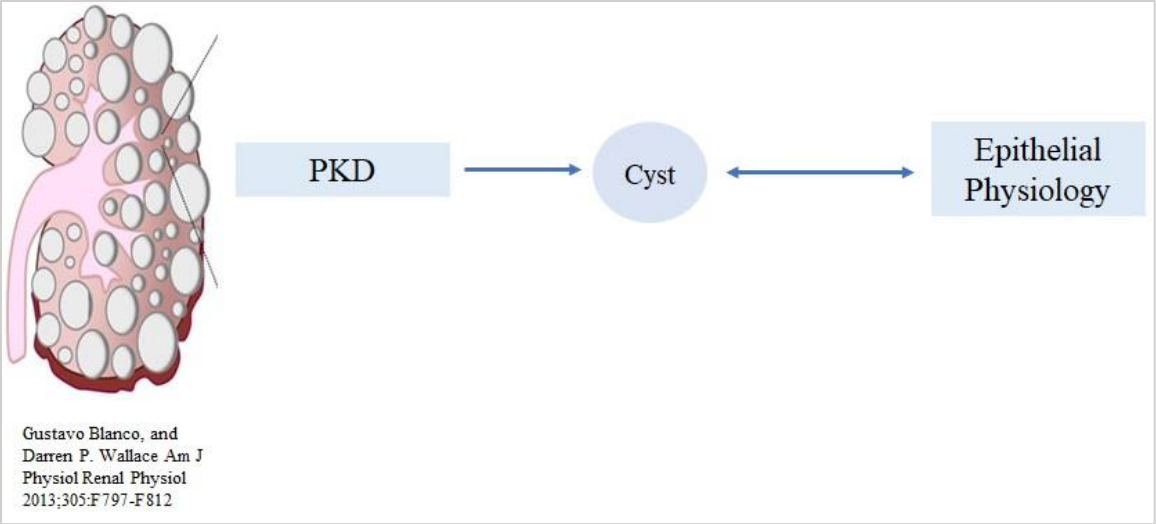

Figure 2: Polycystic kidney disease and epithelial physiology. Kidney cysts have altered epithelial physiology and kidney cysts may affect physiology of normal non-cystic epithelia.

As shown in figure 3, kidney cysts can block fluid flow. Renal cilia sense fluid flow and are believed to play an important role in maintaining normal kidney function. Blockage of kidney fluid flow can affect the cilia. Kidney localized ischemic-hypoxic condition can affect normal epithelial physiology. Kidney localized hypoxia can affect renal cilia. Hypoxia can affect renal ciliary length and ciliary biomechanics and thereby may affect ciliary flow-sensing (Verghese, Zhuang et al. 2011; Resnick 2016). Alterations of renal cilia can affect normal renal epithelial physiology. Ciliary length and fluid flow were found to control active transport of sodium ions (Resnick and Hopfer 2007; Resnick 2011). Hypoxia can affect renal epithelial transport (Husted, Lu et al. 2010). Thus, cyst and cyst induced hypoxia may affect normal renal fluid flow and cilia, thereby affecting ion transport and physiology of normal epithelial cells. The different aspects are discussed in detail in this section of introduction.

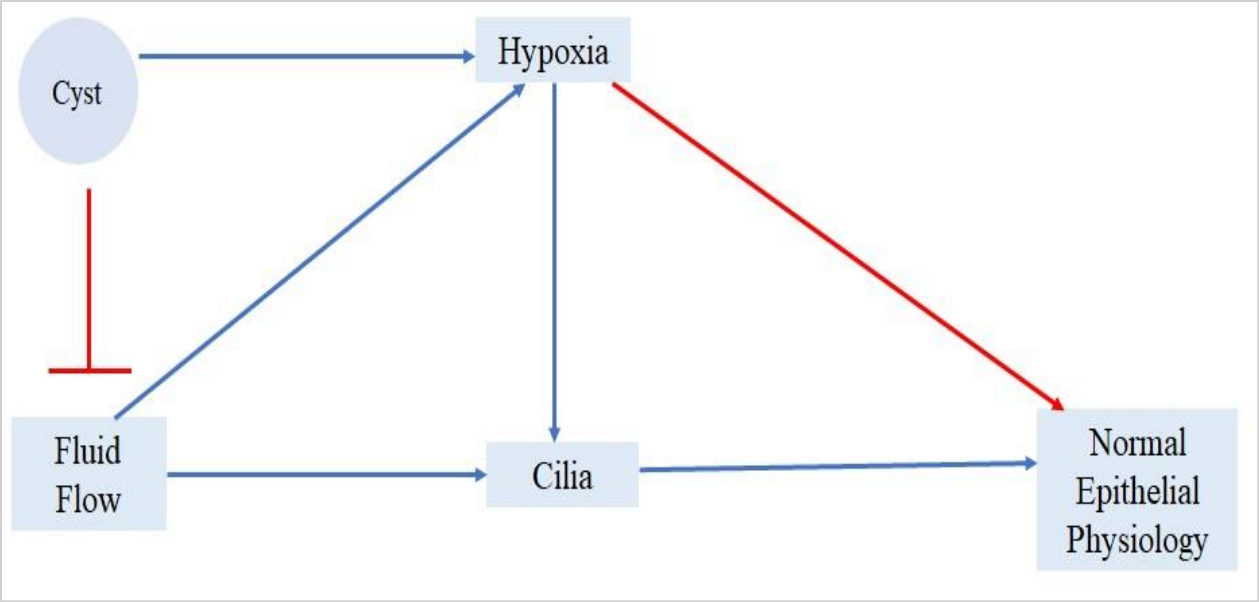

Figure 3: Effect of kidney cysts and cyst-induced localized hypoxia on normal renal epithelial physiology.

1.2 Overview of Kidney Anatomy and Function

1.2.1 Kidney Anatomy

A kidney, which is a compound organ made of tubules, can be divided into three major sections: 1) outer medulla, 2) inner medulla, and 3) cortex. Inner and outer medulla together is called the medulla (Layton 2012). Functional and structural identical units of a kidney are called nephrons (Pitts 1968). A kidney is composed of around one million to one and one fourth of a million nephrons in humans and around 38,000 nephrons in rats (Pitts 1968; Layton 2012). As shown in figure 4, a nephron is composed of a renal corpuscle consisting of glomerulus and Bowman's capsule, a proximal convoluted tubule, a loop of Henle and the distal convoluted tubule (Pitts 1968). Inside the glomerulus, blood plasma first goes through endothelial fenestrations and fluid enters Bowman's capsule, followed by the fluid traveling through the nephron (figure 4). During this fluid flow through nephrons, water and solutes are actively and passively transported across epithelial

cell layers with the help of transporters and ions channels. Many nephrons put their contents into a multibranched collecting duct. Numerous collecting ducts combine and pass their contents through a duct of Bellini, finally disposing into a renal calyx (Pitts 1968). The collecting duct is considered as the terminal part of the nephron and acts as an osmotic exchanger to control hypertonicity of urine (Pitts 1968).

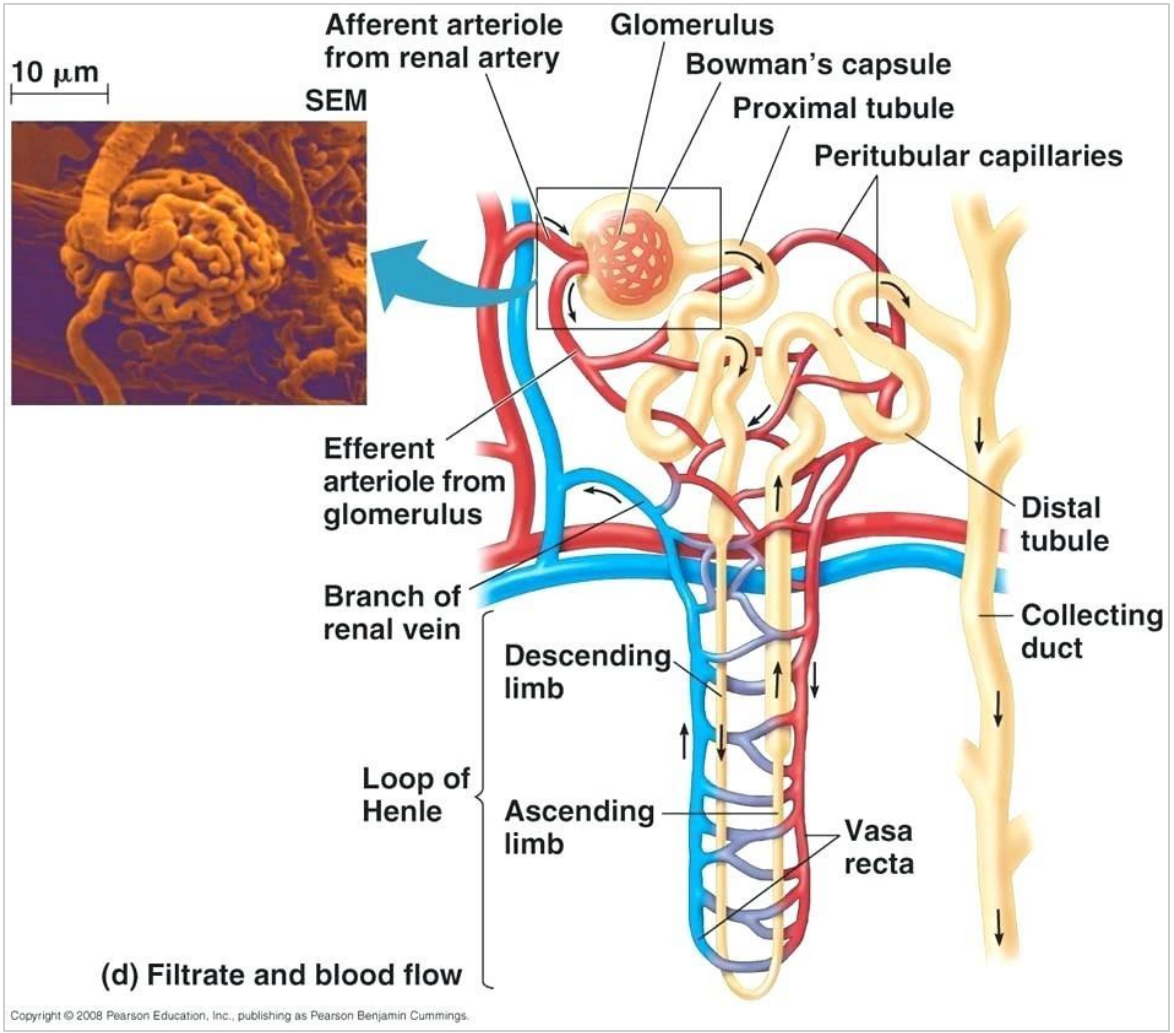

Figure 4: Structure of a nephron. Figure credit: Pearson Education.

1.2.2 Function of Kidney

A kidney performs various essential regulatory functions in our body. The most well-known function is to remove metabolic wastes and toxins from our blood and excrete

them in the form of urine. The kidney also helps in maintaining homeostasis in our body by regulating water, electrolytes, and acid-base balance. The kidney is also known to be responsible for synthesis or activation of hormones that are associated with erythropoiesis, metabolism of calcium, and control of pressure and flow of blood (Layton 2012).

1.2.3 Mechanisms Involved in Urine Production

Three separate mechanisms result in the production of urine: 1) glomerular ultrafiltration 2) tubular reabsorption 3) tubular secretion.

1) Glomerular ultrafiltration removes or filters colloidal matters such as, proteins and lipids and other particulates. However, this process cannot prevent molecules with small dimensions such as crystalloidal solutes (Pitts 1968).
2) In tubular reabsorption, glucose is completely reabsorbed in this process while traveling through the first half of the proximal tubule (Walker and Hudson 1936). Sodium ions are thought to be actively reabsorbed, whereas chloride ions are thought be passively reabsorbed in the proximal tubule. The tubule is known to be freely permeable to water. Reabsorption of ions creates an osmotic gradient which drives the reabsorption of water to maintain the osmotic balance(Pitts 1968). In the distal tubule, ions are reabsorbed faster than water, thereby urine is diluted. Thus, without proportionally high loss of ions, water is removed in the distal tubule (Pitts 1968).
3) Reabsorption of water does not account for increased concentration of certain molecules in the urine (Pitts 1968). For example, the increased concentration of

urea in the urine can be caused by the process of tubular secretion (Marshall Jr and Crane 1924; Pitts 1968).

1.2.4 Urine Concentrating Mechanism

The actual mechanism by which a mammalian kidney is able to concentrate urine when deprived of consumption of water still remains an unsolved mystery and have hypothetical predictions even after many decades of research attempts (Sands and Layton 2000; Layton 2012). The urine concentrating mechanism is known in the outer medulla of the kidney where counter-current multiplication can concentrate urine by absorbing salt in between parallel and opposing flows in descending and ascending tubes which stay in direct contact with each other. However, the urine concentrating mechanism in the kidney inner medulla, which is known to be the site for main urine concentrating function in mammals, is still vaguely understood (Layton, Layton et al. 2009; Layton 2012). Normal blood plasma osmolality is around 300 mOsm/kg H_2O. The capability of the kidney to concentrate urine during deprivation of water consumption varies among different animal species. For example, humans can concentrate urine up to a maximum at around 3.8 times higher osmolality than blood plasma and normal mice and rats around 9-10 times; whereas the Australian hopping mouse, which lives in the desert, can concentrate urine at around 30 times higher osmolality than blood plasma (Beuchat 1996; Layton 2012). For this reason, the sea water should be avoided for human consumption to quench thirst since sea water is known to have osmolality around 2,000 to 2,400 mOsm/kg H_2O (Layton 2012).

1.3 Fluid Flow in the Kidney

Hydrodynamic pressure gradients are known to drive fluid flow through kidney tubules (Layton 2012). Fluid flow in the kidney may be quantified as volumetric flow rates

in terms of single nephron glomerular filtration rate (SNGFR), or flow can also be expressed as wall shear stress (Nag and Resnick 2017). Micropuncture studies reported SNGFR rates in kidney proximal tubule around 25-45 nl/ min in rats and 60-85 nl/ min in dogs and around 125 nl/min in humans (Gottschalk and Mylle 1959; Nag and Resnick 2017). Similarly, using fluorescence markers, SNGFR was measured to be around 32 nl/ min in rats(Kang, Toma et al. 2006). A rise in the blood pressure within the glomerulus can result in the increased SNGFR and can cause increased fluid flow rate throughout the tubule(Layton 2012). Fluid flow through kidney is not a steady flow, rather it has time-dependent oscillatory or pulsatile flow pattern (Layton 2012; Nag and Resnick 2017). In the glomerulus, endothelial fenestrations and podocyte slit diaphragm can absorb high frequency pressure oscillations. Rhythmic contractions of pelvicalyceal wall around the inner medulla creates unsteady fluid flow pattern within the nephron (Young and Marsh 1981; Sakai, Craig et al. 1986; Holstein-Rathlou and Marsh 1989; Pruitt, Knepper et al. 2006; Nag and Resnick 2017). Pressure, flow, and solute concentrations in the proximal tubule show oscillatory patterns with frequencies in the range of 0.015-0.2 Hz (Young and Marsh 1981; Sakai, Craig et al. 1986; Holstein-Rathlou and Marsh 1989; Pruitt, Knepper et al. 2006; Nag and Resnick 2017). Tubular flow was found to show oscillatory pattern with oscillations of 0.1 to 0.02 Hz (Kang, Toma et al. 2006; Rosivall, Mirzahosseini et al. 2006). In mouse kidney, green fluorescent protein (GFP) expressing cilia in the proximal tubule region showed ciliary oscillation having frequency of 4.8 Hz (O'Connor, Malarkey et al. 2013; Nag and Resnick 2017). Thus, oscillatory fluid flow in the kidney tubule can cause oscillatory motion of renal cilia (Nag and Resnick 2017).

Fluid flow was found to decrease active sodium transport in cultured epithelial monolayers derived from kidney cortical collecting duct as compared to no flow. The cell cultures under dynamic or variable fluid flow culture conditions showed dedifferentiated pro-growth like phenotype, whereas cells under stable flow conditions maintained differentiated cellular phenotype (Resnick 2011). Therefore, fluid flow seems to be important in maintaining the normal functional phenotype of renal epithelial cells.

Normal function of kidney is maintained by a narrow range of fluid flow through glomerulus and nephron. The tubular fluid flow rate is important in maintaining the balance of water and sodium in our body and gets adjusted according to the body's requirements. The flow rate in the tubules is mainly controlled by glomerular filtration rate which includes tubuloglomerular feedback (TGF) and myogenic mechanism (Layton 2012).

1.3.1 Tubuloglomerular Feedback

The TGF mechanism plays a crucial role in the regulation of glomerular filtration rate. The TGF system is controlled by the chloride concentration in the macula densa, a bundle made of specialized cells located in the thick ascending limb of the Henle's loop, named the "Juxtaglomerular apparatus" (Layton 2012). When the chloride concentration in the macula densa is very low, this feedback mechanism induces vasodilation (i.e., widening of blood vessels) of afferent arterioles leading to a rise in the pressure of glomerular filtration. A rise in blood pressure in the glomerulus increases the rate of fluid flow in the kidney tubule. Increased flow results in decreased tubular transport period and allows less absorption of sodium chloride (NaCl). Similarly, when chloride concentration in the macula densa is very high, then vasoconstriction of afferent arteriole is induced, and

followed by decreased flow rate and increased NaCl absorption (Layton 2012). This TGF mechanism can cause a continuous oscillation of around 30 mHz in nephron fluid flow (Leyssac and Baumbach 1983).

1.3.2 Myogenic Effect

Vascular smooth muscle in the afferent arteriole in the glomerulus develops active forces and compensatory vasoconstriction to adjust to the increased stretch generated by transmural pressure. This intrinsic feature or response of vascular smooth muscle to be able to constrict when intraluminal pressure increases is known as the myogenic effect. This myogenic response is known to be important in the autoregulation of blood flow and capillary blood pressure (Layton 2012). The renal afferent arteriole is known to have rhythmic activity, also referred as vasomotion as seen in other arterioles and small arteries. This vascular oscillation is independent of heart beat or respiration. This oscillatory pattern is believed to be controlled by resident cells in the arterial wall. Myogenic responses are known to be blocked by membrane channel blockers, such Ca^{2+} and K^{+} channel blocker (Layton 2012). Mathematical models to study myogenic response predict that voltage-gated channels and voltage-calcium-gated channels control Ca^{2+} and K^{+} fluxes respectively, these two ion fluxes interact and a rhythmic transport pattern of these two ions result (Chen, Sgouralis et al. 2010; Sgouralis and Layton 2012). Ion flux interactions and rhythmic transport process can lead to periodic variation in the cytoplasmic calcium concentration and can cause myosin light chain phosphorylation, and finally result in the development of muscle stress. Therefore, rhythmic oscillations in cytosolic calcium concentration can cause sudden vasomotion in the afferent arteriole, and the findings of the

mathematical models were reported to be consistent with the experimental results (Steinhausen, Endlich et al. 1997; Layton 2012).

1.3.3 Fluid Flow Related Forces Acting on Kidney Tubule

Fluid flow through elastic kidney tubules can generate three different forces, two forces (normal and shear stress) acting on tubular walls lined with epithelial cells and the third force (hydrodynamic drag) acts on protruding renal primary cilia (Nag and Resnick 2017). Hydrodynamic drag acts only on a primary cilium whose distal end is free to move, and cilia can bend in response to fluid flow. This ciliary bending mechanism is believed to be responsible for ciliary mediated intracellular calcium influx and cellular signaling (Nag and Resnick 2017).

1.4 Overview of Primary Cilia Anatomy and Function

Epithelial cells in the kidney control transport of solutes and water using ion channels and transporters. Primary non-motile cilia are found on epithelial cells in renal duct and renal tubule and these protruding or antenna-like structures are made of microtubules. Renal cilia act as the cellular fluid flow sensor and also regulate cellular differentiation (Praetorius and Spring 2003; Zhang, Taulman et al. 2004). Ciliary defects can lead to dysregulation of proliferation and differentiation of epithelial cells and polycystic kidney disease (Calvet 2002; Deane and Ricardo 2007).

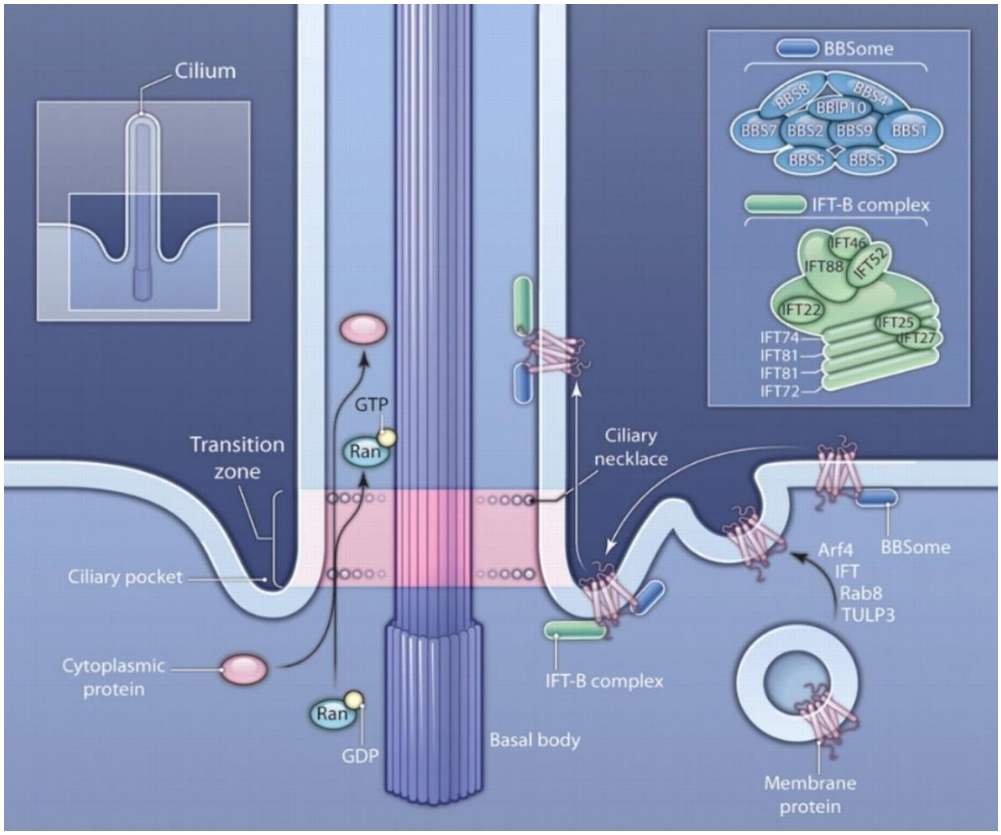

Figure 5: Structural components of a primary cilium. Figure credit (Smith and Rohatgi 2011)

1.4.1 Major Structural Components of a Primary Cilium

The microtubule-based cytoskeleton in the inner core of a cilium is called the axoneme, which remains covered by a lipid bilayer membrane continuous with the cellular plasma membrane. Ciliary membrane is known to contain a different subset of receptors and cell signaling molecules as compared to cellular plasma membrane (Veland, Awan et al. 2009). The basal body of a cilium helps in keeping the cilium connected to a cell as well as provide the platform for 9-fold symmetry formation of the ciliary axoneme. As shown in figure 5, the ciliary 'necklace' is a structure which keeps the ciliary and plasma membrane compartment separated (Gilula and Satir 1972; Veland, Awan et al. 2009). Transition fibers connect the ciliary necklace to the transition zone of the basal body of a

cilium. These fibers are believed to form 'ciliary pore complex', which selectively allows proteins to get inside the ciliary compartment (Rosenbaum and Witman 2002). A renal cilium is non-motile and is designated as (9+0) as compared to designation of (9+2) for a motile cilium, where '9' shows the number of outer doublet microtubules in the axoneme and '0' or '2' shows the number of central microtubules that are present (Veland, Awan et al. 2009). Central microtubule pair and structures, such as dynein arm and radical spokes which are responsible for motility, are absent in a non-motile renal cilium (Veland, Awan et al. 2009). Intraflagellar transport (IFT) is a very conserved mechanism in a cilium and involves bidirectional passage of IFT particles (i.e., protein complexes) within the axoneme of the cilium (figure 5). Anterograde (base to tip of a cilium) movement is driven by motors of kinesin-2 and retrograde movement is guided by cytoplasmic dynein 2 (KozMINSKI, Johnson et al. 1993; Scholey 2008; Veland, Awan et al. 2009). Mutations of IFTs, such as *ift88*, in mice showed formation of kidney cysts along with a number of developmental defects (Lehman, Michaud et al. 2008).

1.4.2 Mechanosensory Functions of a Cilium

1.4.2.1 Ciliary Flow Sensing and Calcium Influx

The mechanical links connecting bending of a cilium to increased levels of intracellular Ca^{2+} influx is not clearly understood. Bending of the cilia by fluid flow is known to increase cytosolic levels of calcium, a second messenger, and lead to calcium induced calcium release (Praetorius and Spring 2001; Praetorius, Frokiaer et al. 2003; Praetorius and Spring 2003). Increase in the cilioplasmic Ca^{2+} concentration results in the increase in cAMP and cytosolic concentration of Ca^{2+}, causing activation of protein kinase A (PKA) and initiate downstream signalling pathways (Jin, Mohieldin et al. 2014; Nag and Resnick 2017). Loss of renal cilia was found to cause uncontrolled influx of intracellular

Ca^{2+} (Siroky, Ferguson et al. 2006). A study, contradicting the existing ciliary calcium influx model, reported that the application of fluid flow increases cytoplasmic Ca^{2+} concentration rather than cilioplasmic Ca^{2+} concentration and non-ciliary site was the initial site for increased levels of Ca^{2+} in response to fluid flow (Delling, Indzhykulian et al. 2016). Previous studies did not specifically isolate and study the effect of hydrodynamic drag force which acts on protruding cilia and is responsible for ciliary bending. In experimental set up involving fluid flow, the shear and stretch act on renal epithelial cells and initiate cell signalling responses which can mask the ciliary flow sensing response (Nag and Resnick 2017).

Major suspects responsible for ciliary mechanosensation are believed to be the polycystin and polycystin-like proteins encoded by PKD1/PKD2 and PKD1L1/PKD2L2 genes respectively. Polycystin 2 (PC2) proteins form the calcium channel (Luo, Vassilev et al. 2003) and Polycystin 1 (PC1) has been suggested to be a G-protein coupled receptor (GPCR) and acts as a sensor (Patel and Honoré 2010; Trudel, Yao et al. 2016). Renal cilia are known to contain several transient receptor potential (TRP) proteins acting as ion channels, such as TRP melastatin-4 (TRPM4), TRP vanilloid 4 (TRPV4), and TRPP2 (polycystin) (PKD2) (Flannery, Kleene et al. 2015; Phua, Lin et al. 2015; Pablo, DeCaen et al. 2016; Nag and Resnick 2017). Fluid flow sensing occurs by opening of divalent cation channel PKD2 along with opening of the TRPV4 (Lee, Guevarra et al. 2015).

1.4.2.2 Effect of Cilia on Active Sodium Transport

In kidney cortical collecting duct cells, application of fluid flow using an orbital shaker was found to enhance movement of angiotensin receptor type 1 to the apical surface and suggested that ciliary mechanosensation play some role in regulating flow dependent reabsorption of sodium (Na^{+}) ions and water in kidney proximal tubule (Kolb, Woost et al.

2004; Resnick and Hopfer 2007). The presence of an intact cilium was found to be crucial in the active Na^+ ion transport through epithelial Na channels (ENaC), since the removal of cilia caused cellular monolayer to become non-responsive to fluid flow induced changes of ENaC current (Resnick and Hopfer 2007). Presence of fluid flow in renal epithelial monolayers caused around 60% drop in the sodium current and around 30% decrease in the length of the cilium (Resnick and Hopfer 2007). Thus, the active sodium transport in renal epithelial cells is believed to be regulated by functional renal cilia. The proteins - PC1 and PC2 encoded by PKD1 and PKD2 genes respectively (Nauli, Alenghat et al. 2003), Polaris encoded by Tg737 (Taulman, Haycraft et al. 2001), and cystin encoded by cpk gene (Hou, Mrug et al. 2002) are all found to be localized in the cilia (Yoder, Hou et al. 2002), and mutations of these genes cause an absorptive epithelia to transform into a secretory cystic epithelia as seen in polycystic kidney disease (Brown and Murcia 2003; Nauli, Alenghat et al. 2003).

1.4.3 Renal Ciliary Length Alterations

Cell signaling molecules were found to affect the length of cilia. Activation of PKA by cyclic AMP (cAMP) was shown to increase ciliary length and inhibition of PKA caused decrease in ciliary length (Besschetnova, Kolpakova-Hart et al. 2010). In contrast, ciliary length altered inversely with intracellular calcium concentration (Besschetnova, Kolpakova-Hart et al. 2010; Nag and Resnick 2017). Renal ciliary length was found to increase in response to injury in mouse models (Verghese, Weidenfeld et al. 2007; Wang, Weidenfeld et al. 2008) and human kidney transplant with acute form of tubular necrosis (Verghese, Weidenfeld et al. 2007). The absence of fluid flow in renal epithelial cell culture caused elongation of renal cilia (Resnick and Hopfer 2007). Stabilization of hypoxia

inducible factor (HIF) by cobalt chloride was shown to increase the lengths of the cilia (Verghese, Zhuang et al. 2011). Another study with similar experimental approach showed that HIF-stabilization decreased the effective bending modulus of a cilium and hence the cilium became more flexible (Resnick 2016). A mouse model of polycystic kidney disease, orpk/Tg737 showed formation of much shorter cilia (Cano, Murcia et al. 2004; Liu, Murcia et al. 2005).

The change in cilia lengths could be assumed as a cellular mechanism to adapt to adverse physiological conditions, such as lack of fluid flow or hypoxia. Therefore, it is tempting to speculate that the ciliary length alterations can reflect altered ciliary biomechanical properties, such as bending modulus, and can lead to altered ciliary flow sensing and calcium signaling.

1.5 Renal Epithelial Transport

1.5.1 Epithelial Cells

An epithelial cell separates complimentary transport proteins in apical and basolateral membranes, maintaining cell polarity. An epithelial tissue has the ability to transport electrolytes and non-electrolytes in a specific direction (vectorial), since this tissue is composed of polarized cells and cellular tight junctions. Epithelial cells can perform selective transport (absorption or secretion) of electrolytes and non-electrolytes against their electrochemical gradient (Lewis 1996).

1.5.2 Overview of Cellular Transport

Transport of ions and molecules across cellular layers is crucial to maintain tissue function and homeostasis. From a thermodynamic point of view, transport of molecules and ions can be divided into two categories: active transport and passive transport

(Srivastava 2005). If the transport process is driven by cellular environment, the transport is called passive transport, which does not utilize any cellular energy. On the other hand, if the transport process uses energy generated by cellular metabolism, the transport is then called active transport (Srivastava 2005). Chloride ions having a smaller size, with diameter of 0.3 to 0.4 nm, can easily diffuse through the pores on a cellular membrane having diameter of 0.5 to 0.8 nm (Srivastava 2005). Na^+ ions in an aqueous solution maintain hydrated form with diameter of 0.51 nm, whereas hydrated form of K^+ ions maintain diameter of 0.39 nm (Srivastava 2005). Therefore, hydrated K^+ ions diffuse easily through cellular membrane pores as compared to Na^+ ions. Moreover, the interior of pores contains positively charged ions such as Ca^{2+}, therefore anions such Cl^- can pass through the pores easily, whereas the passage of positively charged cations such as Na^+ and K^+ is prevented (Srivastava 2005). Active transport can occur even if there is no electric-potential gradient and can also occur against the electrochemical gradient (Srivastava 2005).

Active transport can be divided into two categories: 1) Primary active transport 2) secondary active transport. In the primary active transport, normally hydrolysis of ATP by the transporter, e.g., ion pump or ATPase, generates the energy required to drive the transport process. All epithelia are known to have one or more ATPases, such as Na^+/ K^+-ATPase and H^+-ATPase (Reuss, Wills et al. 1996). On the other hand, secondary active transport uses the energy formed by the electrochemical gradient created due to transport one substance to drive the transport of other substance or substances. Normally the secondary active transport is coupled to active Na^+ transport. The electrochemical gradient created by Na^+ pump acts as the energy source to transport of Na^+ and other substances

(Reuss, Wills et al. 1996). The sodium-coupled secondary active transport is called cotransport, when Na^+ ion and the other substance both move along the same direction of electrochemical gradient of Na^+, and the transport proteins are referred to as the cotransporters or symporters. For example, in the kidney proximal tubule, sodium/ glucose cotransporter (SLGT1) transports 2 Na^+ ions along with 1 glucose molecule into the cell. When the transport of a substance occurs in the opposite direction of Na^+ electrochemical gradient, then the secondary active transport is called counter-transport, and the transport proteins are referred to as the exchangers or antiporters. For example, Na^+/Ca^{2+} exchanger (NCX) 1, which is found in kidney distal tubule, is known to move 3 Na^+ ions inside the cell in exchange for moving 1 Ca^{2+} ion out of the cell (Magyar, White et al. 2002).

1.5.3 Epithelial Transport Pathways

The epithelial transport pathway can be divided into two categories:

1) Intercellular or paracellular pathway: This process involves transport across cellular tight junction and then movement along the intercellular spaces in between two adjacent cells.
2) Transcellular pathway transport: This mode of transport begins by the entrance of ions or molecules through apical membrane and existing through basolateral membrane of a cell (Reuss, Wills et al. 1996).

1.5.4 Properties of Epithelial Cells

The basic building block of an epithelium consists of 1) epithelial cells 2) tight junctions 3) Basement membrane. The basement membrane provides structural support and acts as the site for cellular attachment. Tight junctions help in keeping cells bound

together and can also restrict passage of substances among epithelial cells. Tight junctions keep the apical membrane separated from the basolateral membrane (Lewis 1996).

1.5.4.1 Epithelial Junctional Complex

Other than tight junction, the junctional structure consists of 1) gap junction 2) desmosomes, and 3) zona adherens (Lewis 1996). Cell to cell communication occurs via gap junctions. Spot junctions, also known as desmosomes, provide integrity of cellular structures. The cellular actin filaments from lateral membrane bind to the site in the junctional region, called zona adherens. The space that exists between cells is referred as the lateral intercellular space. The lateral intercellular space can be very small, around 10 nanometers (nm), and can be as large as 1-3 micrometers (μm) depending on the specific type of epithelia. The transport through paracellular space is determined by the tight junctions and lateral intercellular space (Lewis 1996).

The junctional complex has three major functions:

1) The tight junction in the junctional complex separates the apical membrane and the basolateral membrane. The junctional complex creates a barrier that prevents migration of apical membrane protein to basolateral side and basolateral membrane protein to apical side. Thus, the junctional complex helps in maintaining the cell membrane polarity (Lewis 1996).
2) The junctional complex provides epithelial structural integrity by keeping epithelial cells bound together.
3) The junctional complex controls paracellular route of transport of electrolytes and non-electrolytes. Hydrophilic substances can move transcellularly using ion channels and membrane proteins on apical and basolateral membranes. The junctional complex

selectively allows passage of hydrophilic substances on the basis of charge and size (Lewis 1996).

Leaky and Tight Epithelia

Electrical resistance is the inverse of electrical conductance. An epithelium belongs to one out of the two categories based on the electrical resistance by tight junctions. An epithelium having low tight junction resistance (less than 100 Ω-cm^2) is called a leaky epithelium, whereas an epithelium having high tight junction resistance (more than 500 Ω-cm^2) is termed as the tight epithelium (Fromter and Diamond 1972).

A leaky epithelium has low transepithelial (combined transcellular and paracellular) voltage for two possible reasons:

1) Voltage generated by active ion transport can be leaked through the low resistance epithelial junctions.
2) A leaky epithelium can actively transport ions in an electroneutral process. For example, cotransport of a cation and anion together or absorption of a cation causing secretion of another cation does not develop any electrical current (Lewis 1996).

A leaky epithelium cannot maintain an ion concentration gradient for two possible reasons:

1) Epithelial junctions have high permeability for ions since the junctional electrical resistance is low. Ions can freely move from high concentration gradient to low concentration gradient by the process of diffusion, resulting in the loss of ion concentration gradient (Lewis 1996).

2) A leaky epithelium cannot maintain an ion concentration gradient because water molecules easily pass through the epithelial layer through osmosis (Fromter and Diamond 1972).

A tight epithelium due to high junctional resistance can maintain high voltage. The tight epithelium's junction is very less permeable to solutes and the passive transport does not have any significant effect on the ion concentration gradient created by the active transport. Due to low water permeability and low junctional solute permeability, a tight epithelium can create and maintain ionic gradients. A leaky epithelium can transport large amounts of electrolytes, non-electrolytes, and water as compared to a tight epithelium, whereas a tight epithelium can maintain high concentration gradients of electrolytes and non-electrolytes. The transport process across a tight epithelium is known to be hormone regulated but not in case of a leaky epithelium (Lewis 1996).

In a tight epithelium, such as kidney cortical collecting duct, Na^+ ions are known to be transported actively and Cl^- is known to be transported passively. In this tight epithelium, Na^+ ions enter the cells through apical epithelial Na channels (ENaC). With the help of Na^+/ K^+-ATPase 3 Na^+ go to the basolateral side and $2K^+$ ions enter cells. This transport is a transcellular or active transport process (figure 6). There are low conductance K^+ channels, which help in removing intracellular K^+ build up. Movement of Na^+ ions actively produce negative value of equivalent (short circuit) current. Using sodium channel blocker 95% of current can be blocked (Resnick and Hopfer 2007; Resnick 2011). By active sodium transport sodium ions are reabsorbed from urine back to blood. Active Na^+ transport creates electrochemical gradient which drives passive transport of negatively charged Cl^- ions through tight junctions as shown in figure 6. In some epithelia, such as

frog skin epithelia or sweat gland, Cl^- can pass transcellularly since those epithelial apical and basolateral membrane have chloride conductance (Lewis 1996).

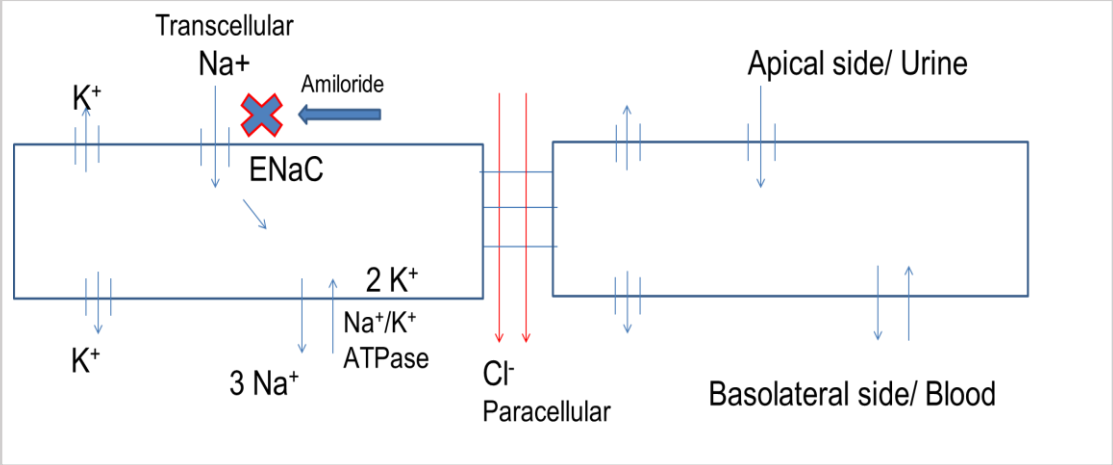

Figure 6: Epithelial transport in a tight epithelium (e.g., kidney cortical collecting duct). Na^+ ions are known to be transported through transcellular route using epithelial sodium channels (ENaC) and Na^+/ K^+-ATPase. Cl^- ions are known to be transported paracellularly.

1.5.4.2 Epithelial Na+ and K+ Transport

In almost all types of epithelial cells, Na^+/ K^+-ATPase is found to be present in the basolateral membrane (Lewis 1996). As discussed previously, the Na^+/ K^+-ATPase transports 3 Na^+ ions from cellular cytoplasm to the serosal solution, and during this process 2 K^+ ions are transported from serosal solution to the cellular cytoplasm. The process is called electrogenic, since during one cycle one positive charge moves out of the cell. In this process, one ATP molecule is utilized in each cycle. This process is called primary active transport since Na^+ and K^+ ions are transported against their concentration gradient. The basolateral membrane is known to maintain a negative voltage between -30 and -80 mV. The concentration of K^+ ions inside the cells is higher as compared to the extracellular fluid. For example, cellular K^+ concentration is > 100 mmol/L and extracellular K^+ concentration is 5 mmol/L in mammals (Lewis 1996). The concentration of Na^+ is known to be lower inside the cell as compared to the extracellular fluid. Cellular

concentration of Na^+ is around 10-20 mmol/L and extracellular fluid concentration of Na^+ is around 135-145 mmol/L in humans (Lewis 1996; Wills, Reuss et al. 2012; Staruschenko, Ilatovskaya et al. 2016). Each kidney glomeruli can filter 25,000 mEq of Na^+ ions per day (Staruschenko, Ilatovskaya et al. 2016). The glomerulus freely allows Na^+ ions to pass through, and the epithelial cells of different segments of nephron reabsorb the majority of Na^+ during the fluid flow and urine formation (Staruschenko, Ilatovskaya et al. 2016).

1.5.5 Epithelial Transport Mechanisms

A hydrophobic or lipid soluble substance can pass through lipid bilayer by a process known as solubility-diffusion, a passive transport process. A hydrophilic solute can be transported by primary or secondary active transport or passive transport process (Reuss, Wills et al. 1996).

1.5.5.1 Passive Transport

Passive transport can occur in two ways: 1) through lipid layer of cell membrane 2) using transport proteins such as channels and carrier proteins. Passive transport is driven by an already existent electrochemical gradient and result in the transport of a single substrate.

The driving force for the passive transport is the electrochemical potential difference ($\Delta\mu_j$) which is denoted as:

$$\Delta\mu_j = z_j V_m F + RT \ln\left(\frac{C_j{}^i}{C_j{}^0}\right)$$

Where z_j = valency of ion j, V_m = membrane voltage= $V_i - V_0$, i= inside of membrane, o= outside of membrane, F= Faraday's constant, R= Gas constant, T= temperature, $C_j{}^0$ = concentration of ion j outside of the membrane, and $C_j{}^i$ = concentration of ion inside of the membrane (Reuss, Wills et al. 1996).

1.5.5.2 Epithelial Transporters

The transporters onto epithelial cellular membrane can be categorized into three types: 1) Ion pumps 2) Carriers 3) Channels.

1) Ion Pumps

The ion pumps include ATPase which is known to use the energy produced due to hydrolysis of ATP and transport ions against the electrochemical gradient. Thus, ion pumps drive active ion transport. The ion pumps can transport around 100-200 molecules per second, referred to as the turnover number. ATP hydrolysis causes conformational change of the subunit of ATPase and dissociation of substrate which was previously associated (Läuger 1991; Reuss, Wills et al. 1996). In this section, among the different ion pumps, primary emphasis will be given on Na^+/ K^+-ATPase.

Major Epithelial Ion Pumps

a) H^+ pumps: H^+-ATPases are expressed in the kidney proximal tubule and distal nephron and helps in maintaining acid-base homeostasis (Gluck, Underhill et al. 1996). This pump causes K^+ reabsorption and H^+ secretion and is known to be present in the intercalated cells from cortical collecting duct and distal regions of nephrons. The activity of H^+,K^+-ATPase acts independent of Na^+, is stimulated by K^+, and can be blocked by vanadate (Reuss, Wills et al. 1996).

b) Ca^{2+}-ATPase: This ATPase drives the active transport of Ca^{2+} from cellular cytoplasm to the interstitial fluid and this pump is found in renal tubule cells. Each transport cycle with Ca^{2+}-ATPase pump causes removal of 2 Ca^{2+} ions. This ATPase pump is known to be inhibited by vanadate (Carafoli 1994).

c) Na^+/ K^+-ATPase: This ion pump helps in maintaining high concentration of K^+ and low concentration of Na^+ inside the cells. The Na^+/ K^+-ATPase maintains the membrane

potential and osmotic balance of cells (Blanco and Mercer 1998). In the kidney, Na^+/ K^+-ATPase helps in the reabsorption of Na^+ ions and water and thus this enzyme is crucial in maintaining homeostasis of water and electrolytes in our body (Glynn 1985; Jørgensen 1990). The turnover number for Na^+, K^+-ATPase is around 100-200/ second. Ouabain is known to block the pump activity and aldosterone, a hormone, is known to increase the pump density (Lingrel, Van Huysse et al. 1994).

Table I: Intracellular and extracellular Na^+ and K^+ concentrations.

Intracellular [Na^+]	Extracellular [Na^+]	Intracellular [K^+]	Extracellular [K^+]
10-20 mmol/L	135-145 mmol/L	> 100 mmol/L	5 mmol/L

Subunits of Na^+/ K^+-ATPase

The Na^+/ K^+-ATPase pump is an oligomer and is made of two subunits, α and β in a 1:1 stoichiometric ratio (Reuss, Wills et al. 1996). Another subunit γ of Na^+/ K^+-ATPase has been identified whose function is controversial and not clearly understood (Blanco and Mercer 1998). The three isoforms of α: α1, α2, and α3 have molecular mass of around 120 kDa and two isoforms of β: β1 and β2 have molecular mass around 50 kDa (Reuss, Wills et al. 1996). The α and β isoforms show tissue specific expression patterns (Blanco and Mercer 1998). The expression of α1 isoform along with β1 isoform is normally seen in all tissue (Lingrel 1992; Levenson 1994). In the kidney α1β1 is the major isozyme (Jørgensen 1990; Blanco and Mercer 1998). The presence of other isoforms of Na^+/ K^+-ATPase such as α2 and α3 and their functional contributions have been debatable (Farman, Corthesy-Theulaz et al. 1991; Ahn, Madsen et al. 1993; Blanco and Mercer 1998). The mRNA and protein level detection of α2 and α3 isoforms suggested that they are equivalent to 0.01%

of α1β1 enzyme in the kidney tissue (Lucking, Nielsen et al. 1996). The α subunit is the catalytic subunit and is mainly responsible for ATPase activity and transport of ions (Lingrel, Van Huysse et al. 1994; Reuss, Wills et al. 1996; Wills, Reuss et al. 2012). The α subunit is known to contain the site to bind cations, ATP, inhibitor, and ouabain (Mercer 1993; Pressley 1996; Blanco and Mercer 1998). The β subunit is needed to assemble and target the pump to be delivered onto the basolateral membrane of epithelial cells (Lingrel, Van Huysse et al. 1994; Reuss, Wills et al. 1996; Wills, Reuss et al. 2012). The β subunit is crucial in the function of Na^+/ K^+-ATPase and it regulates the affinity of the enzyme for Na^+ and K^+ (Eakle, Kabalin et al. 1994; Eakle, Lyu et al. 1995; Blanco and Mercer 1998). The β subunit acts as a chaperone and guides correct folding of the α subunit to be correctly directed to the basolateral membrane (McDonough, Geering et al. 1990).

Regulation of Na^+/ K^+-ATPase

Different isoforms of Na^+/ K^+-ATPase have different affinities for Na^+, K^+, and ATP (Blanco and Mercer 1998). Intracellular Na^+ concentration, a rate limiting step, controls Na^+/ K^+-ATPase function. Intracellular Ca^{2+} and endogenous ouabain may control sodium pump activity for a short period (Blaustein 1993; Blanco and Mercer 1998). Intracellular cAMP and exogeneous derivatives of cAMP can inhibit this pump (Bertorello and Katz 1993; Blanco and Mercer 1998). Phosphorylation/ dephosphorylation process can regulate activity of this pump. Protein kinase A (PKA) mediated phosphorylation of serine residue at the position of 943 of α subunit causes inhibition of this pump's activity (Fisone, Cheng et al. 1994). Activation of protein kinase C (PKC) causes phosphorylation of serine residue at the position 16 of α subunit and can result in the inhibition of the pump activity (Beguin, Beggah et al. 1994). In the kidney, protein kinase G (PKG) and cGMP shows an

inhibitory effect on the active sodium pumping (McKee, Scavone et al. 1994); (Scavone, Scanlon et al. 1995). Thus, activation of PKA, PKC, and PKG can regulate the function of Na^+/K^+ pump isozymes. Digoxin and ouabain obtained from plants are known block activity of Na/K-ATPase by binding to an extracellular region of the α subunit of this pump (Lingrel, Van Huysse et al. 1994). Ouabain was found to cause endocytosis of Na^+/ K^+-ATPase in porcine renal epithelial cells (Liu, Kesiry et al. 2004). Different isoforms of α of Na^+/ K^+-ATPase have different affinity for ouabain. The α3β1 and α3β2 isozymes show high level, α2β1 and α2β2 isozymes show intermediate level, and α1β1 isozymes show low level of reactivity or sensitivity for ouabain (Obrien, Lingrel et al. 1994; Bamberg and Schoner 2012).

2) Carriers

The carriers are known to cause secondary active transport or passive transport. The carrier which transports one substance is called uniporter. The carriers can also transport multiple substances. Electrochemical gradient created by transport of one substance can drive the transport of another substance or substances. The carrier can be either symporters (cotransporters) i.e., the movement of two substances in the same direction, or exchangers (countertransporters) i.e., the movement of two substances in the opposite direction. The turn over numbers of carriers are around 10^2-10^4 molecules per second (Stein and Litman 2014). Normally carriers act in conjunction with a pump. Carriers and/ or channels act in series or in parallel with a pump. For example, Na^+- glucose cotransporter or amiloride-sensitive sodium channel acts in series with the Na^+/ K^+-ATPase located in the basolateral membrane of an epithelium which absorbs Na^+ (Reuss, Wills et al. 1996).

Major Renal Epithelial Carriers

a) Sodium-glucose cotransporter: These apical cotransporters belonging to SGLT gene family are used in the absorption of salt and water in the kidney proximal tubule (Reuss, Wills et al. 1996). Outward passage of glucose through basolateral membrane occurs using glucose uniporters belonging to GLUT gene family (Thorens 1993).

b) Sodium-chloride cotransporter: This cotransporter (NCC) is normally present in the apical membrane distal convoluted tubule (DCT) and is known to reabsorb 5-10% of Na^+ and Cl^- (Reilly and Ellison 2000). In the DCT, this cotransporter is known to interact and regulate epithelial Na^+ channels (Mistry, Wynne et al. 2016).

c) Other Na^+ organic solute transporters: Na^+ electrochemical gradient generated by Na^+, K^+ pump drives secondary active transport i.e., intracellular uptake of vitamins, bile salts, and anions (Reuss, Wills et al. 1996).

d) Na^+/H^+ exchanger: This NHE is the carrier which causes exchange of a Na^+ for a H^+. This is an electroneutral process. The NHE has two functions: 1) apical NHE causes Na^+ absorption and H^+ secretion 2) basolateral NHE maintains cellular pH and volume. The expression of NHE3 is majorly noticed in the kidney proximal tubule (Pouysségur 1994; Reuss, Wills et al. 1996).

e) Na^+-K^+-Cl^- cotransporter: The NKCC cotransporter has important roles in the function of chloride transporting epithelia. This cotransporter performs transport of Cl^-, Na^+, and K^+ in a stoichiometric ratio of 2:1:1 in an electroneutral manner. The NKCC driven transport can be inhibited by loop diuretics, such as furosemide and bumetanide. NKCC is normally found in the Cl^- transporting epithelium in the

opposite of the membrane in which Cl^- channel is expressed (Haas 1994). In the thick ascending loop of Henle, NKCC is found in the apical membrane. Cl^- ions exit the basolateral membrane through Cl^- channel and Na^+ ions go out using the Na^+/ K^+-ATPase. NKCC2 is seen in the mammalian kidney (Haas 1994).

f) Anion exchangers: The anion exchangers (AE) cause exchange of Cl^- and HCO_3^- in an electroneutral process. AE1b, a truncated AE1 protein, is found in the basolateral membrane of intercalated cells in the kidney collecting duct (Reuss, Wills et al. 1996).

g) Na^+-HCO_3^- cotransporter, Na^+ dependent Cl^-/ HCO_3^- exchanger: The Na^+-HCO_3^- cotransporter is known to be expressed in the proximal tubule and contribute to 90% of HCO_3^- transport through basolateral membrane of the epithelia (Boron and Boulpaep 1989). The Na^+ dependent exchange of Cl^-/ HCO_3^- is an electroneutral process and is also seen in the basolateral membrane of cells in the kidney proximal tubule. This exchanger contributes to a much less extent in the HCO_3^- transport as compared to the Na^+-HCO_3^- cotransporter (Reuss, Wills et al. 1996).

3) Channels

Ion-channels are formed by pore-forming proteins and allow the passage of ions according to cell's electrochemical gradient (Nadeau 2017). The process of the passage of ions through channels is a passive transport. The channels are maintained in either one of two states: open or closed. The transition in between these two states is called gating (Reuss, Wills et al. 1996). Thus, in addition to selectivity, ion channels also show gating effect, i.e., these channels open in response to a stimulus. For example, voltage-gated channels open in response to transmembrane potential (Nadeau 2017). Channels in open

state allows free passage of ions. The typical turnover number for channels is around 10^6 to 10^7 ions per second (Reuss, Wills et al. 1996). Numerous ion pumps are needed to match up with the flow of ions through a channel. It has been suggested that there are around 5000 to 10000 Na^+ pumps per one K^+ ion channel present (Hille 2001). In this section, among the various epithelial ions channels, a major emphasis will be given on the epithelial sodium channel (ENaC).

Major Epithelial Channels

a) Sodium channels: The sodium channels can be classified into three categories:

   i. Highly selective Na^+ channel: These Na channels have high Na^+ selectivity over K^+ i.e., $P_{Na}/ P_K \geq 10$, low conductance (ca. 5 pS), and the channel open and close times are long (0.5 second to 5 second).

   ii. Moderately selective Na^+ channel: These Na^+ channels have relatively low selectivity for Na^+ as compared to highly selective Na^+ channels, i.e., $P_{Na}/ P_K =$ 3-4; higher conductance (7-15 pS), and very short open or closed times ($\leq$ 50 ms).

   iii. Non-selective channel: These channels show little selection preference or no selection preference for Na^+ over K^+ i.e., $P_{Na} / P_K \leq 1.5$; high conductance 23-28 pS or low conductance $\geq$ 3 pS (Reuss, Wills et al. 1996).

All these three types of Na^+ channels are amiloride-sensitive (Garty 1994). The channel blockage occurs by a plug-type process. Highly selective Na^+ channels are expressed in the tight epithelia having high electrical resistance, such as the ENaC present in the renal distal tubule and cortical collecting duct (Palmer 1995). The aldosterone-sensitive and vasopressin-sensitive epithelia showed increase in the open channel

probability and numbers of sodium channels in response to hormones. Channel activity is known to decrease by intracellular Na^+ concentration, which may be due to activation of PKC. The moderately selective Na^+ channels are known to coexist along with highly selective Na^+ channels in epithelial cells cultured onto impermeable supports. These moderately selective Na^+ channels are controlled by G proteins and cellular actin filaments. Non-selective Na^+ channels were reported to be present in the primary cell cultures of inner medullary collecting ducts. The increased level of cGMP is known to cause phosphorylation of channels and can decrease the open probability of these non-selective Na^+ channels (Garty 1994; Palmer 1995; Reuss, Wills et al. 1996).

Epithelial Na^+ Channel (ENaC)

The final stages of Na^+ reabsorption occur in the convoluted and collecting tubules and collecting duct using the epithelial Na^+ channel (ENaC). Sodium reabsorption is known to control extracellular fluid volume and regulate blood pressure (Pratt 2005; Rotin and Schild 2008; Hamm, Feng et al. 2010). ENaCs are distinct compared to Na^+ channels of excitable membrane (Reuss, Wills et al. 1996). The ENaC forms a heterotetramer and consists of two α, one β, and one γ homologous subunits (Canessa, Schild et al. 1994; Kellenberger, Hoffmann-Pochon et al. 1999). Each subunit is known to have two transmembrane domains: M1 and M2, short intracellular N and C termini of 9-10 kDa, and large extracellular loops of around 50 kDa with numerous sites for N-linked glycosylation. The αENaC (78 kDa) subunit helps in forming the Na^+ ion selective and amiloride sensitive conductive pore. The β and γ subunits are needed in the enhancement of channel expression (Garty 1994; Palmer 1995; Reuss, Wills et al. 1996). All three, α, β, and γ ENaC subunits on a single channel level show a higher selection for

Na^+ than K^+ and relatively low value of conductance (~5pS) and also exhibit channel gating with long channel opening time (Butterworth 2010). Thus, ENaCs act as the highly selective Na^+ channel. Half-life of ENaC in the apical side was found to be around 20-30 minutes using cell culture studies (Balda and Matter 2000; Hanwell, Ishikawa et al. 2002; Butterworth 2010).

Regulation of ENaC

ENaC is known to control the Na^+ absorption rate in the distal nephron (Bhalla and Hallows 2008; Loffing and Korbmacher 2009; Butterworth 2010; Hamm, Feng et al. 2010). The ENaC mutations and conditions can result in upregulation and downregulation of ENaC activity, such as seen in Liddle syndrome, type I Pseudohypoaldosteronism (PHA-I), and cystic fibrosis (CF) (Bhalla and Hallows 2008). Glycosylation, cleavage by proteolysis, and other post translational modifications are important in the expression and activity of ENaC (Bhalla and Hallows 2008). Sodium reabsorption through ENaC can be altered by two different mechanisms: i) the variation of surface density or number of channels on the apical surface and ii) a change in the open probability of channels by gating the channel or by proteolytic cleavage of the extracellular loops α and γ (Butterworth 2010).

i) Variation of ENaC Surface Density

The downregulation of apical ENaC involves ubiquitination of ENaC by ubiquitin ligase Nedd4-2 and removal from apical surface by the process of endocytosis (Kabra, Knight et al. 2008). Endocytosed ENaC can go back to apical surface after removal of ubiquitin molecules and recycling or these ubiquitinated ENaC molecules are degraded (Butterworth 2010). Aldosterone is known to bring ENaC from intracellular and cytoplasmic region to apical surface of principal cells from the distal nephron area. With

long term application of aldosterone, ENaC production and protein half-life are increased (Niisato, Taruno et al. 2007; Bhalla and Hallows 2008; Frindt, Ergonul et al. 2008; Butterworth 2010). Short term application of aldosterone increases numbers of ENaC on the surface (Frindt, Ergonul et al. 2008). The cAMP agonist was found to increase channel density of ENaC in the apical side of kidney collecting duct epithelial cells (Morris and Schafer 2002; Butterworth, Edinger et al. 2005).

ii) Change in Channel Open Probability

Intra and extracellular concentrations of Na^+ regulate ENaC activity. A rapid change of channel activity, which is seen within seconds due to increased extracellular Na^+ concentration, is known as Na self-inhibition (Fuchs, Larsen et al. 1977). Noncleaved channels maintain low channel opening probability (P_o) when extracellular Na^+ concentration is high (Sheng, Carattino et al. 2006). The Na-self inhibition mechanism is relieved by proteolytic cleavage of extracellular loops of ENaC α and γ subunits (Bhalla and Hallows 2008).

Feedback inhibition is a slow change in channel activity that occurs after a few minutes to hours due to increased intracellular Na^+ concentration (MacRobbie and Ussing 1961). The application of Na^+/ K^+-ATPase inhibitors does not cause swelling of cells (Sheng, Carattino et al. 2006; Bhalla and Hallows 2008) and indicates the importance of feedback inhibition.

Na-self inhibition and feedback inhibition of ENaC are especially important specially in high-salt environments or diets (Bhalla and Hallows 2008).

b) Potassium Channels: Epithelial potassium channels are responsible for three functions:

i. High intracellular concentration of K^+ ions as compared to extracellular fluid concentration of K^+, which creates the negative potential and provides the electrochemical gradient to move other ions.

ii. These channels allow transepithelial absorption or secretion of K^+ ions.

iii. During cellular swelling, these K^+ channels get activated to control cellular volume (Wang, Sackin et al. 1992; Taglialatela and Brown 1994).

ROMK1 channel: This channel is an inwardly rectifying K^+ channel, i.e., it allows easier movement of K^+ ions into the cells than out of. It is an ATP sensitive K^+ channel, which is known to have conductance around 39 pS and high sensitivity to K^+ than Na^+. This channel shows increased open probability at membrane potential, which is at a more positive value than -60 mV. The ROMK1 expression is seen in the renal cortex and outer medulla (Ho, Nichols et al. 1993).

Other Maxi-K^+ channels have been found in the apical membrane in the areas of renal proximal tubule and cortical collecting duct (Reuss, Wills et al. 1996).

c) Chloride Channels: Chloride channels play a crucial role in the epithelia, such secretion of Cl^-, absorption of NaCl, and regulation of cell volume. Major chloride channels include: cystic fibrosis transmembrane conductance regulator (CFTR) and swelling activated Cl^- channels. CFTR is an ATP-dependent and cAMP regulated channel and can be blocked by 5-nitro-2-(3-phenylpropylamino) benzoic acid (NPPB) and glibenclamide (Fong and Jentsch 1995; Reuss, Wills et al. 1996). CFTR is found in the apical membrane of most exocrine glands. The intracellular cAMP-controlled opening of CFTR channels is diminished in the individuals with cystic fibrosis. In the kidney

cysts, CFTR channels are believed to be associated with active chloride secretion (Brill, Ross et al. 1996; Hanaoka, Devuyst et al. 1996).

Swelling activated Cl^- channels are found in the culture of cortical collecting duct and inner medullary cells. The permeability preference of this channel is P_{Cl}> P_{HCO3} > P gluconate > P_{Na}, and these channels can be blocked by the chloride channel blocker NPPB (Fong and Jentsch 1995; Reuss, Wills et al. 1996; Wills, Reuss et al. 2012).

d) Calcium Channels: The calcium channels play crucial roles in Ca^{2+} absorption by renal epithelial cells, and are thereby important in intracellular signalling. The voltage-dependent calcium channels get activated due to the depolarization of membrane potentials and can be inhibited by $Co^{2+.}$ These channels are similar to L-type Ca^{2+} channels. The role of these Ca^{2+} channels in the kidney epithelial cellular function is unknown (Friedman and Gesek 1993; Reuss, Wills et al. 1996).

e) Non-selective Cation Channels: These channels have been reported to be present in the renal inner medullary collecting duct, renal distal tubule cells, and M-1 cortical collecting duct cell line (Reuss, Wills et al. 1996).

f) Water Channels (Aquaporins): Lipid membranes are known to have high water permeability by osmosis and do not actually require water channels or pores. An epithelium with high osmotic water permeability, such as a leaky epithelium and antidiuretic hormone (ADH) stimulated epithelium, is known to have pores or water channels called aquaporins. The aquaporin 1 (AQP) 1 is a tetramer in which each subunit is known to act as a pore. The AQP1 has high selectivity for water molecules and almost no permeability for electrolytes or non-electrolytes. AQP1 is known to

express in the apical and basolateral membranes of the epithelial cells from kidney proximal tubule and in the descending thin limb belonging to loop of Henle. Some other water channel proteins have also been identified, such as ADH regulated water channels: AQP-CD or AQP2 in the apical membrane of the renal collecting duct cells. The water channel AQP3 is found in the basolateral membrane of renal collecting tubule (Engel, Walz et al. 1994; Sabolic and Brown 1995; Reuss, Wills et al. 1996).

1.5.6 Overview of Renal Epithelial Na^+ Transport

In the kidney, along with Na^+, other ions, such as chloride and bicarbonate ions, also get reabsorbed heavily (Staruschenko, Ilatovskaya et al. 2016). The main mode of sodium reabsorption in the kidney is the active transport through transcellular pathways. Passive transport is also known to contribute partially in the total Na^+ transport in the kidney. Sodium reabsorption in known to occur through both active and passive transport mechanisms in proximal convoluted tubules (PCT) and the thick ascending limb (TAL) of Henle's loop (Breiderhoff, Himmerkus et al. 2012; Muto, Furuse et al. 2012). Passive transport of Na^+ ions is majorly seen in the PCT, where the paracellular resistance is low. (Staruschenko, Ilatovskaya et al. 2016). Claudin-2 in the tight junction is known to be responsible for reabsorption of Na^+ (Kiuchi-Saishin, Gotoh et al. 2002). Around 30% of Na^+ ions, absorbed from urine to blood by transcellular transport mechanisms, are known to go back to the urine in the proximal tubule by paracellular transport process (Staruschenko, Ilatovskaya et al. 2016). The electrogenic pump Na^+/ K^+-ATPase is known to be localized in the basolateral membrane of kidney epithelial cells. This pump is found in abundance in the TAL of Henle's loop, distal convoluted tubule (DCT), collecting tubule (CT), and principal cells belonging to collecting duct (CD) (Staruschenko, Ilatovskaya et

al. 2016). The kidney segments having high active transport is generally known to have increased level of Na^+/ K^+-ATPase activity (Féraille and Doucet 2001). The absorption of Na^+ is known to be maximum in the region of kidney proximal tubule and decrease as the fluid travels through the distal segments of the kidney tubule. As shown in figure 7, the SGLT cotransporter and NHE3 exchanger account for transcellular reabsorption of Na^+ ion in the proximal tubule and Na^+-K^+-Cl^- cotransporter NKCC2 accounts for the transcellular reabsorption of Na^+ ions in Henle's loop. The Na^+-Cl^- cotransporter NCC drives transcellular Na^+ reabsorption in the distal convoluted tubule, and ENaC channels in the collecting duct allow transcellular entry of Na^+ ions for reabsorption. Proximal tubule reabsorbs around 60-70% of Na^+ ions, and distal convoluted tubule and collecting duct are each known to contribute to around 5% of Na^+ ion reabsorption and are known to be precisely controlled by physiological factors (Féraille and Doucet 2001).

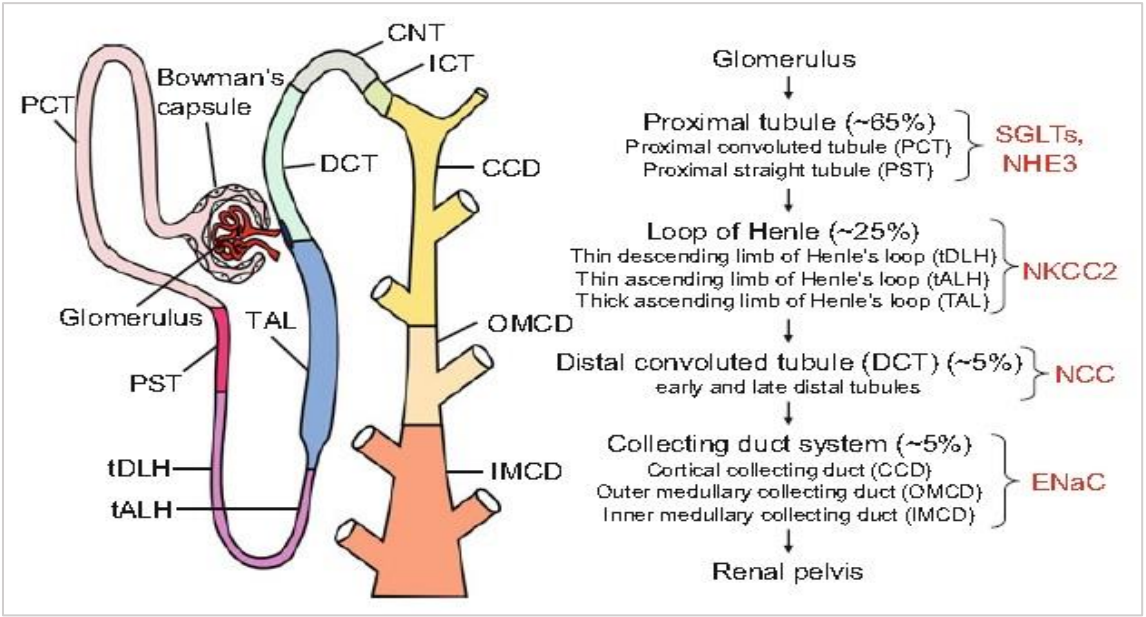

Figure 7: The percentage of Na^+ transport involving major ion channels and transporters in the different segments of a nephron. Image credit (Staruschenko, Ilatovskaya et al. 2016). SGLT= Sodium-glucose cotransporter, NHE= Na^+/H^+ exchanger, NKCC= Na^+-K^+-Cl^- cotransporter, NCC=Na^+–Cl^- cotransporter, ENaC= Epithelial sodium channel.

1.5.7 Regulation of Epithelial Permeability by Cellular Tight Junctions

1.5.7.1 Epithelial Tight Junctions

In epithelia, tight junctions act as barriers and form morphological and functional boundaries between apical and basolateral sides and regulate selective movement of solutes through paracellular pathways (Balda and Matter 2000; Cereijido, Shoshani et al. 2000; Anderson 2001; Denker and Sabath 2011). Epithelial tight junctional complex is made of tight junction, adherens junction, and desmosomes (Farquhar and Palade 1963). The paracellular permeability is mainly determined by the unique tight junction composition of specific claudin types, which occupy and control the paracellular space (Furuse, Fujita et al. 1998). Signalling proteins and pathways are important in maintaining the function of tight junctions to regulate permeability. Zonula occludens 1 (ZO1), a scaffolding protein, acts as a connector which links tight junction protein to each other and to actin cytoskeleton, and also to signal transduction molecules (Denker and Sabath 2011). Tight junctions can regulate signals for gene expression by transporting DNA binding proteins from tight junction to the cellular nucleus (Denker and Sabath 2011). Through tight junction signalling process involving ZO1 associated nucleic acid binding proteins, cells can estimate cellular density and accordingly initiate cell proliferation (Balda and Matter 2000; Lima, Parreira et al. 2010).

1.5.7.2 Transepithelial Resistance

Transepithelial resistance (TER), also known as transepithelial electrical resistance (TEER), is the inverse of electrical conductance. TER is a combined value of transcellular and paracellular resistance arranged in parallel and is therefore calculated as: $1/TER = [1/TER_{transcellular} + 1/TER_{paracellular}]$(Matter and Balda 2003). In epithelia with low TER values, the paracellular resistance is much larger than transcellular resistance (Cereijido,

Gonzalez-Mariscal et al. 1983; Stefani and Cereijido 1983; Gonzalez-Mariscal, De Ramirez et al. 1989). Therefore, the TER values of low resistance epithelia, such as Madin-Darby Canine Kidney Epithelial Cells II (MDCKII), mostly indicate paracellular resistance which is a combination of junctional resistance and resistance by the paracellular space (Matter and Balda 2003). Permeability of ions through epithelial cells can be roughly estimated by measuring TER values (Matter and Balda 2003). TER of cellular monolayers using cell culture media primarily indicates Na^+ permeability (Matter and Balda 2003). Measurement of TER is a convenient method to test for cellular monolayer formation onto permeable support membrane, and TER values indicate integrity of tight junctions. Therefore, TER is useful in determining barrier functions of epithelial monolayers (Lea 2015).

1.5.7.3 Renal Epithelial Tight Junctions and TER

Major tight junction proteins of kidney epithelial cells are shown in figure 8A. Claudins are the major integral membrane proteins which help in maintaining barrier function and allow paracellular transport selectively. Proteins, such as ZO1 and occludin, also help in the maintenance of epithelial tight junction barrier. Tissue injury causes phosphorylation of tight junction proteins and disruption of epithelial barrier function. As shown in figure 8A, tight junction disruption or injury causes loss of selective paracellular permeability and increase in TER values. Recovery of tight junction proteins help in restoring barrier function by regaining selective paracellular permeability and decrease of TER values (Denker and Sabath 2011).

TER values of different segments of nephron are inversely proportional with permeability as shown in figure 8B. In the nephron of a mammalian kidney, the paracellular permeability decreases from proximal tubule to the collecting duct as the unique

composition of different claudin changes (Kiuchi-Saishin, Gotoh et al. 2002), and higher ZO1 and occludin protein levels are expressed in the lower segments of the nephron (Gonzalez-Mariscal, Namorado et al. 2000). A major claudin normally found in the proximal tubule is claudin-2 which creates high conductance pores for cations, such as sodium ion, and therefore proximal tubule shows low electrical resistance (Muto, Hata et al. 2010). Proximal tubule is known as the leaky region of the nephron and one third of the fluid reabsorption occurs by paracellular pathway. Thus, starting from glomerulus, the lower segments of nephrons are less and less permeable and show more selective transport and high TER values (figure 8B). The distal region of the nephron, such as collecting duct, is considered as a tight epithelium with high resistance and very selective permeability i.e., low cation permeability due to the presence of cation barrier forming claudins such as claudin-4 and 8 (Denker and Sabath 2011). The permeability difference between proximal tubule and collecting duct is around 100 fold (Denker and Sabath 2011).

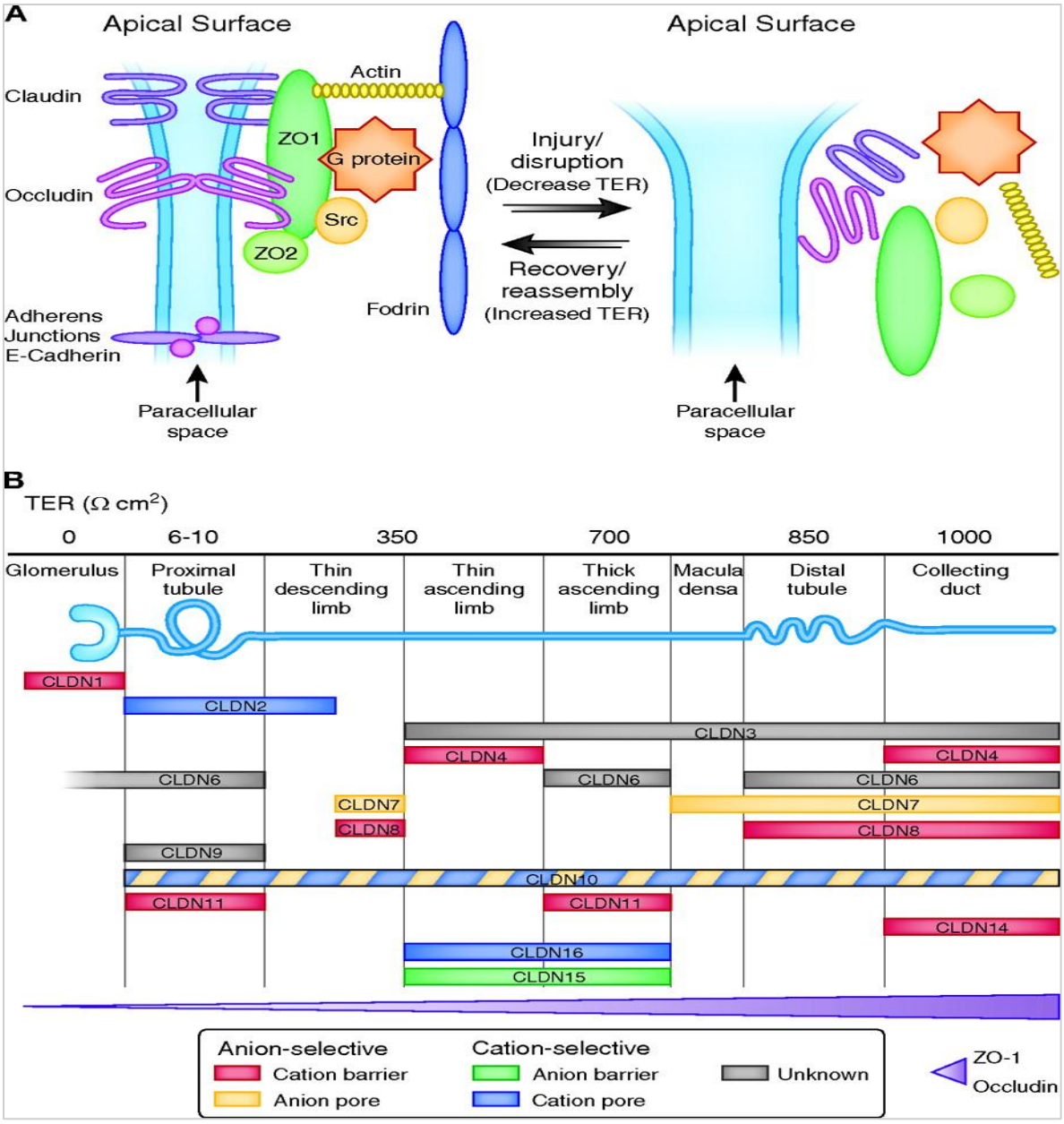

Figure 8: Epithelial tight junctions and TER of a nephron. Image credit (Denker and Sabath 2011). (A). Major Tight junction proteins in kidney epithelial cells. (B) Different segments of the nephron with major claudins.

1.5.7.4 Tight Junction Integrity and Paracellular Transport

Tight junctions maintain two functions 1) as a fence and 2) as a gate. The junction fence prevents the intermixing of lipid molecules in the outer phospholipid layer of the cell membrane (Matter and Balda 2003). Fluorescence conjugated lipids such as sphingomyelin

or glycolipids are commonly used to label outer leaflet of plasma membranes in order to estimate to "fence function" (Meer and Simons 1986; Mandel, Bacallao et al. 1993; Balda, Whitney et al. 1996). The diffusion of lipids is studied by confocal microscopy in cells or fluorometric analysis is performed with cell lysates (Matter and Balda 2003).

The gate function of tight junctions controls the paracellular transport pathway. Paracellular transport is generally considered as passive transport and is driven by electro-osmotic gradient created due to active transport. Epithelial paracellular transport can occur through two separate pathways: 1) through charge and size selective 4 Å sized pores made by claudins and 2) large discontinuities in the tight junction which allows large molecules to pass through irrespective of charge and size (Anderson and Van Itallie 2009). Several orders of magnitude difference of permeability can be seen between a tight and leaky epithelium (Anderson and Van Itallie 2009). An epithelium with "tight" tight junctions can have high electrochemical gradient due to active transport of ions or charged species (Anderson and Van Itallie 2009). Nearly all leaky epithelia preferentially allow transport of sodium ions than chloride ions i.e. the ratio of Permeability of Na^+ (P_{Na})/ Permeability of Cl^- (P_{Cl}) will be around 10 to 1.5 (Anderson and Van Itallie 2009).

1.5.7.5 Experimental Measurement of Epithelial Paracellular Permeability

Epithelial permeability can be measured using hydrophilic tracers such as fluorophore labelled dextrans or radiolabelled inulin or mannitol. Variable sized tracer molecules can be analysed by labelling dextran molecules with FITC or rhodamine, and different fluorophore tags allow analysis of more than one tracer in a single cellular monolayer in one experimental set up (Matter and Balda 2003). In simple ion selective

experiments, filters with cellular monolayers are tested in the presence NaCl or LiCl to test for Na or Li permeability. Tracers, such as mannitol (radius= 4.2 Å) in radius, inulin (radius= 15 Å), and FITC-conjugated dextran molecules (3, 10, 70 kDa, etc), go through the non-pore pathway i.e., temporary breaks in the tight junction, rather than the pathway involving claudin pores (Anderson and Van Itallie 2009). Fluorescence of FITC-dextran molecules that can permeate through epithelial monolayer can be detected by measuring fluorescence values at time intervals and the transepithelial permeability can be quantified in terms of the apparent permeability (P_{app}) values (Nag and Resnick 2017). TER or small tracer permeability cannot estimate only paracellular permeability but combined transcellular and paracellular permeabilities. Dextran molecules with size around 4 kDa can be transported across epithelial monolayer through paracellular pathway as well as through fluid-phase transcytosis (Matter and Balda 2003). Fluid-phase transcytosis can be estimated by allowing cells to uptake horseradish peroxidase (HRP) and after washing and incubating transcytosed HRP can be detected using enzymatic reactions (Miettinen, Matter et al. 1992; Balda, Whitney et al. 1996). Application of large sized tracers such 40-400 kDa can show only paracellular transport (Matter and Balda 2003). Thus, by choosing a variety of tracer molecules, paracellular transport can be estimated.

1.6 Epithelial Electrophysiology

Epithelial transport can be characterized by measuring electrical properties, such as transepithelial potential difference, transepithelial resistance, short circuit current, and capacitance (Lewis 1996). Cellular lipid bilayer is resistant to charged molecules, therefore simple diffusion cannot produce an electrical current, rather transport needed to occur through ion channels which are pore-forming proteins allowing selective ion-transport,

although some non-selective ion channels can also be present allowing either all cations or anions to pass (Nadeau 2017). Some of the majorly used electrophysiological analysis systems are discussed below.

1.6.1 Transepithelial Electrical Resistance

Transepithelial resistance (TER), also known as transepithelial electrical resistance (TEER), can be measured by passing a current ΔI across the epithelial layer and measuring the resultant change in voltage (ΔV) in a current-clamp mode. The TER can also be measured in a voltage-clamp mode by passing a voltage (ΔV) and measuring the change in current (ΔI) which is needed to maintain at that voltage (Lewis 1996). The resistance is determined from Ohm's law i.e., the resistance is equal to the transepithelial voltage change divided by transepithelial current change (Lewis 1996).

$$R_{meas.} = \frac{\Delta V_t}{\Delta I_t} \times A$$

Where, A= area of epithelial layer

Unit of resistance is expressed in the units of ohm-cm^2. Measured resistance ($R_{meas.}$) is a sum of transepithelial resistance and series resistance of the measuring solution (R_s). Actual transepithelial resistance TER can be measured by subtracting measuring solution resistance from total measured resistance i.e., TER= $R_{meas.} - R_s$ (Lewis 1996). The value of the series resistance can be measured by measuring the resistance of an empty cell culture insert without any epithelial cells. For epithelia with high resistance, the value of R_s accounts for very minor corrections. Transepithelial conductance= $G_t = G_{trc} + G_p$

Where, G_t= transepithelial conductance, G_{trc}= transcellular conductance, and G_p= paracellular conductance. Electrical resistance is the inverse value of conductance.

Therefore, transepithelial resistance is calculated as:

$$G_t = \frac{1}{TER} = \frac{1}{R_{trc}} + \frac{1}{Rp}$$

Where, TER= Transepithelial Resistance, R_{trc}= Transcellular Resistance, and R_p= Paracellular Resistance (Lewis 1996).

1.6.1.1 Equivalent Electrical Circuit of an Epithelial Monolayer

The transcellular and paracellular resistances act in parallel. The detailed equivalent electrical circuit of an epithelial monolayer is shown in figure 9. Apical membrane and basolateral membrane contribute to total resistance separately and they act as series resistances. Transcellular resistance, R_{trc} is the sum of apical resistance (R_a) and basolateral resistance (R_b). The paracellular resistance (R_p) is the main contributor in the total resistance, especially in the beginning of the cellular monolayer barrier formation, when tight junctions and adherent junctions are not yet formed in between cells (Bertrand, Durand et al. 1998; Benson, Cramer et al. 2013; ávan der Meer, JungáKim et al. 2015). Generally, any experimental manipulation causing a change of TER value, indicates the change of R_p (Matter and Balda 2003). This model is applicable to measurement using DC currents with frequency of 0 Hz, however AC current with very low frequency can also be used in this model (ávan der Meer, JungáKim et al. 2015). Total monolayer resistance can be expressed as:

$$\frac{1}{R_T} = \frac{1}{R_a + R_b} + \frac{1}{R_P} + \frac{1}{R_g}$$

Since, R_a and R_b resistances act in series. (R_a+ R_b), R_p, and R_g act all in parallel.

$$\mathrm{TER} = \mathrm{R_T} + \mathrm{R_f}$$

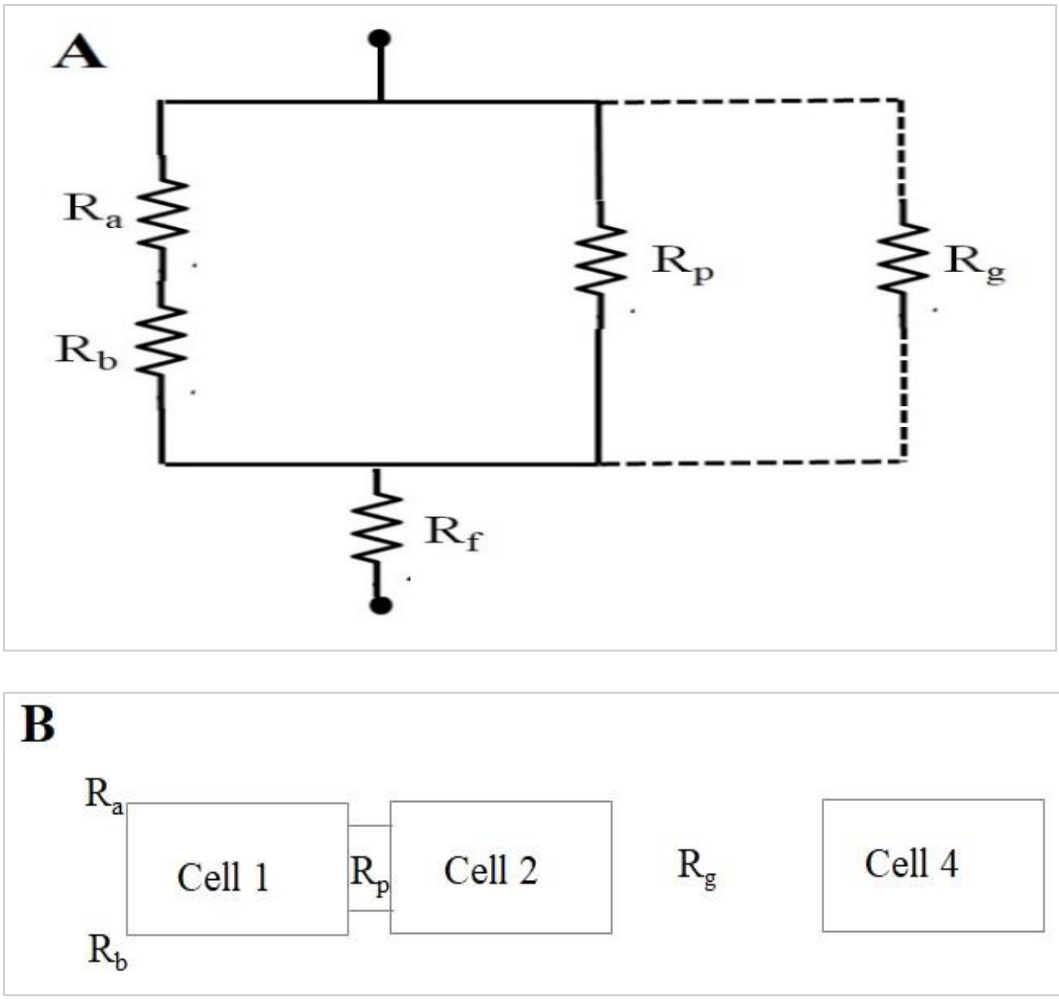

Figure 9: Equivalent circuit model for TER of an epithelial monolayer. (A) Different resistance components of a confluent epithelial monolayer. R_f= fluid resistance, R_a= apical membrane resistance, R_b= basolateral membrane resistance, R_p= paracellular resistance, and R_{gap}= gap resistance which is absent in a confluent monolayer. (B) Resistances contributed by epithelial cells of a cellular monolayer.

R_g shows the gap resistance of a partial cell coverage of the cellular monolayer. If a cellular layer has 99.6% cell coverage or confluence the measured TER value can be 80% lower than the TER value of a culture with 100% cell coverage or confluence (ávan der Meer, JungáKim et al. 2015). Thus, a drastic decrease of TER indicates a loss of cellular confluence and thereby can help to monitor monolayer health.

1.6.1.2 TER Measurement Methods

For TER measurement, two electrodes are used (one electrode in the upper compartment and second one in the lower compartment), and a cell culture insert with cellular monolayer is placed in between. TER can be measured by applying a direct current (DC) voltage across a cellular monolayer and by measuring the resulting current and then calculated as the ratio of voltage and current following Ohm's law. Direct current can damage electrodes and cells due to charging effects on electrodes and cellular layer. To avoid this issue, an alternating current (AC) with low frequency (12.5 Hz) is applied (Srinivasan, Kolli et al. 2015). In a current-clamp mode, first the membrane potential is set to zero, then an AC current (12.5 Hz) is applied with one pair of electrodes and deflection of voltage is measured with a second pair of electrodes (Matter and Balda 2003; Srinivasan, Kolli et al. 2015). TER values are calculated using Ohm's law R= V/I. A silver-silver chloride chopstick electrode (such as, STX2 from World Precision Instrument or Millicell STX probe from Millipore) or a small electrode chamber system (such, Endohm chamber from World Precision Instrument) connected to an epithelial voltmeter (such as, EVOM from World Precision Instrument or Millicell-ERS Voltmeter from Millipore) are used to measure the TER values in cell culture inserts (Matter and Balda 2003; ávan der Meer, JungáKim et al. 2015). Properly performed, a TER experiment will ensure equal current distribution throughout the membrane. Use of cell culture media acting as a conductive interphase ensures a close-to-an-equal drop in the potential throughout the whole membrane (ávan der Meer, JungáKim et al. 2015).

1.6.1.3 Factors that Can Affect TER Measurements

Transfer of filters into a measurement chamber can cause fluctuation in TER value, and the fluctuation can be nullified by equilibrating the filter in the measurement chamber

for around 15 minutes. The same fluid levels need to be maintained in the inner and outer chamber (Matter and Balda 2003). The cultures or cell culture media should be maintained at 37°C since temperature strongly affects TER values (Gonzalez-Mariscal, De Ramirez et al. 1985). For example, lowering of temperature to ambient temperature causes TER value to increase more than three times in MDCK, kidney epithelial cells (Matter and Balda 2003). Media change or washing right before measure can show a large change in the TER values (Matter and Balda 2003).

1.6.1.4 Other TER Measurement System

A DC based TER measurement system may have a few drawbacks, such as restricted measurement range, possible measurement errors due to electrode surface alterations after prolonged usage, and possible adverse effects on cellular health due to silver ions released by overused electrodes (ávan der Meer, JungáKim et al. 2015). To overcome these limitations, complex-impedance based system has been also used to obtain TER values (Benson, Cramer et al. 2013). Currently, AC based systems: cellZscope system72 from nanoAnalytics GmbH and the ECIS system from Applied Biophysics are commercially available to determine TER in Transwell systems (ávan der Meer, JungáKim et al. 2015).

1.6.2 Impedance Analysis

Another way of monitoring epithelial transport is the use of impedance analysis which measures frequency dependent characteristics of epithelia by measuring voltage by applying a small current. Impedance analysis involves modelling of epithelia as an electrical model made of capacitors and resistors (Lewis, Clausen et al. 1996). Therefore, impedance measures the resistance of an electric circuit which exhibits sinusoidal signal at a fixed frequency. Impedance measurements include capacitance i.e., the ability of a

biological membrane to store charge and acting as a capacitor (Lewis, Clausen et al. 1996). Therefore, understanding capacitance of membrane may help to understand the information about membrane area, for example, geometry of epithelial crypts or extracellular structures. The drawback of impedance analysis is the complexity of coming up with the actual or physiologically relevant equivalent circuit model to extract meaningful data (Lewis, Clausen et al. 1996).

1.6.3. Short Circuit Current

The amount of transepithelial movement of total charged species can be quantified by determining the current that needs to pass through an epithelial layer to reduce the potential or transepithelial voltage to zero. This current is referred as the short-circuit current (I_{sc}) (Lewis 1996). In simple terms, the current that short-circuits the tissue is the I_{sc}. This current can be measured using a voltage-clamp to detect the amount of current needed to bring the epithelial voltage to zero millivolts (Lewis 1996).

In an Ussing chamber, when identical bathing solution is present on both sides of epithelial monolayer, and only one specific ion gets actively transported, the I_{sc} is equal to the rate of transport of that ion. When more than one ion species is involved in the active transport, then I_{sc} will be equal to the algebraic sum of all active ion transport mechanisms (Lewis 1996). In the frog skin model to study Na^+ transport from a pond to the blood of a frog, the net Na^+ transport was found to be equal to the value of I_{sc} (Koefoed-Johnsen and Ussing 1958).

The relation between current and ion transport can be expressed as:

$$J_i = \frac{I_{sc}}{zF}$$

Where, J_i denotes net flux of ion i, I_{sc} is the short circuit current.

F= Faraday's constant and z= valency of the transported species (e.g., $Na^+ = 1$).

Generally, spontaneous electrical potential can be created across an epithelium due to passive transport forces, such as osmotic and electrochemical gradients. An Ussing chamber omits the effect of passive transport by clamping the epithelial potential to zero by passing an external current across the epithelium and thereby eliminates the possible effects of transepithelial diffusive forces (Clarke 2009). Thus, an Ussing chamber only detects the active transport process, and the I_{sc} is known to be equivalent to the algebraic sum of active transport of electrogenic ions (Clarke 2009).

Commercially available electrode systems as used for TER measurement, such as Endohm chamber or chopstick electrode connected to EVOM or Millicell voltmeters are used to obtain voltage values. The equivalent current (I_{eq}) or equivalent short circuit current (Isc_{eq}) can be calculated from voltage and resistance read outs following Ohm's law i.e., I= V/ R (where, I= current, v= voltage, R= resistance) (Resnick and Hopfer 2007; Resnick 2011; Nag and Resnick 2017).

Channel Blockers

Ion channel activity can be isolated by using specific agents that can block the channel. Use of channel blockers and measurement of electrical current help to get a clear knowledge about a specific ion channel, omitting the possibility of any background noise. Tetrodotoxin (TTX) is obtained from puffer fish and acts as a channel blocker for voltage gated Na^+ channels (Nadeau 2017). Other channel blockers have been developed from snakes, spiders, and insects. In case of ligand-gated ion channels, agonists and antagonists can be effective in blocking channels. Agonist and antagonists can bind at the same site as the ligand or somewhere else, disabling channel activity. Most channel blockers can bind

to various channels with varying binding affinity (Nadeau 2017). In a mouse cortical collecting duct epithelial cells (Principal cells), application of 10 μmol/L of Na^+ channel blocker, amiloride, decreased I_{sc} by 95% and suggested 95% of I_{sc} is produced due to active Na^+ transport (Resnick and Hopfer 2007).

1.6.4 Other Methods to Study Cellular Electrophysiology

Cellular electrophysiology can be studied to understand electrical features of cells and activity of ion channels using patch-clamping or lipid bilayer recording. In patch-clamp technique electrical properties are measured by making direct contact between an electrode and a cell (Nadeau 2017). The patch refers to the patch of a cell membrane measured using a current or voltage clamp to detect voltage or current of a biological cell. The electrical recording of lipid bilayer is similar as the patch-clamp technique, although the physical set up is different. In this method, a lipid layer orifice separates two chambers of bath. Ion channels can be implanted onto the lipid layer orifice and electrical properties of the channel can be evaluated (Nadeau 2017). Measurement of single channel provide better understanding of channel activity, whereas whole-cell recordings measure hundreds to thousands of channels. Single channel measurements give a clear knowledge about channel conductance, and we can understand channel opening and closing modes of action (Nadeau 2017). Thus, by patch-clamp or lipid bilayer method, single channel or multiple channel activity of a single cell can be detected as compared to an Ussing chamber which detects all the channel activities of a cellular monolayer.

1.7 Kidney Pathology and Diseases

Kidney diseases can be divided into two categories: acute and chronic. Acute kidney injury (AKI) does not have an universal definition, rather it is diagnosed on the

basis of some physiological parameters such as changes of serum creatinine levels or absolute creatinine level (Mehta, Kellum et al. 2007). A kidney disease can be categorized as a chronic kidney disease (CKD) when the glomerular filtration rate (GFR) remains continuously less than 60 mL/minute/ 1.73 m^2 during a period of 3 months or longer (Quigley 2012).

AKI may occur during clinical procedures, such as kidney transplantation and cardiac surgery (Bellomo, Kellum et al. 2012). Diabetes, hypertension, and obesity are considered as the leading risk factors for the occurrence of CKD (Coresh, Selvin et al. 2007). In this section, among different kidney diseases, a major emphasis will be given on polycystic kidney disease.

1.7.1 Acute Kidney Injury

AKI, or acute kidney failure (AKF), is a clinical complication characterized by a sudden drop (hours to days) of kidney excretory function. AKI or AKF may result in decreased urine output and accumulation of metabolic acids and increased levels of phosphate and potassium ions. This diseased state causes an accumulation of products formed due to nitrogen metabolism, such as creatinine and urea. A small rise of serum creatinine level was found to cause patient mortality (Bellomo, Kellum et al. 2012). AKI is known to be caused mainly by hypoxia, ischemia or nephrotoxicity (Basile, Anderson et al. 2012). AKI has been studied in animal acute ischemic models in which ischemia is induced by acutely blocking the renal artery. Animal models of these AKI showed kidney localized adverse reactions such as activation of coagulation system, infiltration of neutrophils, cytokine release, and damage of the endothelium (Bellomo, Kellum et al. 2012).

1.7.2 Chronic Kidney Disease

Chronic Kidney Disease (CKD), also known as chronic kidney failure, causes a gradual loss of kidney function and finally leads to kidney failure. Earlier stages of CKD show some level of kidney damage, as determined by albuminuria, and compromised kidney function, detected as GFR by measuring serum creatinine concentration (Levey, Eckardt et al. 2005). The end stage symptom of CKD is the kidney failure which requires dialysis and kidney transplantation. CKD is also known to increase the risk of cardiovascular diseases and can result in other complications (Sarnak, Levey et al. 2003; Levey, Eckardt et al. 2005; Coresh, Selvin et al. 2007). In the United States, the number of patients with kidney failure related to CKD more than doubled in 2004 as compared to 1991 (Health 2010).

1.7.2.1 Hypertension in CKD

The renin-angiotensin system (RAS) is one of the major control systems that regulates the blood pressure as well as fluid balance. Renin is mainly produced and secreted from the kidney. Plasma renin concentration is adjusted depending on the blood pressure and salt balance (Sparks, Crowley et al. 2014). Renin cleaves angiotensinogen and creates angiotensin I. Angiotensin converting enzyme (ACE) converts angiotensin I to angiotensin II, which controls the blood pressure and flow and thereby regulates glomerular filtration rate (Sparks, Crowley et al. 2014). In CKD patients, the inability to maintain Na^+ balance can result in hypertension. Secretion of renin can worsen blood pressure related complications. Increased blood pressure further causes kidney damage and loss of kidney function (Quigley 2012).

1.7.2.2 Polycystic Kidney Disease

Polycystic kidney disease (PKD) is a genetic disease which is characterized by the formation of fluid-filled pouch-like structures, called cysts. These cysts tend to grow larger over the years causing reduction of kidney function and finally lead to kidney failure (Deane and Ricardo 2007). Thus, PKD falls under the category of chronic kidney diseases. In PKD, mutations occur in the PKD1 and PKD2 genes encoding PC1 and PC2 proteins respectively. Although the genetic cause of PKD is known, the factors which are responsible for the cyst expansion and disease progression are not clearly understood (Cowley 2004).

One in every 1000 persons becomes affected by autosomal dominant PKD (ADPKD) (Gabow 1993), whereas autosomal recessive PKD (ARPKD) occurs around one in 20,000 live births (Zerres, Rudnik-Schöneborn et al. 1998). Around 50% of ADPKD patients face end-stage renal disease (ESRD) by the age around 60 years, and most of the infants with ARPKD who are able to survive the prenatal period encounter chronic kidney failure when they reach adolescence (Rohatgi, Greenberg et al. 2003). Mutations of PKD1 and defective PC1 cause 85-90% of ADPKD, and the remaining ADPKD is caused due to the mutations of PKD2 (Wilson 2004). In ADPKD, the cysts become separated from the nephron and do not communicate with the tubules from which they were formed (Wilson and Falkenstein 1995). On the other hand, in case of ARPKD, the cysts still remain connected as the expanded forms of the collecting duct and allow fluid to flow through them (Osathanondh and Potter 1964). In both ARPKD and ADPKD, kidney cysts expand over years and cause malfunction of the rest of the functional epithelia and finally lead to renal failure (Grantham 1996).

i. Role of Primary Cilia and Cell Signaling Pathways in PKD

Renal epithelia have primary cilia which may sense fluid flow using PC1 and PC2 proteins and allow influx of Ca^{2+} in the renal epithelial cells. This Ca^{2+} influx effect is amplified due to the release of intracellular Ca^{2+} stores by epithelial cells (Pazour, San Agustin et al. 2002; Deane and Ricardo 2007). Increased levels of Ca^{2+} inside cells stimulate cell signaling (eg., B-Raf/MEK/ERK pathway) events that may help in maintaining renal epithelial phenotype (Simons and Walz 2006; Deane and Ricardo 2007). When ciliary signaling is absent, renal epithelial cells may undergo dedifferentiation which can lead to cyst formation and expansion, and during this process the level of cAMP is found to be increased (Belibi, Reif et al. 2004). Increments of extracellular concentration of Ca^{2+} were shown to reverse phenotypic abnormalities seen in the cystic epithelial cells of PKD (Yamaguchi, Hempson et al. 2006) indicating the importance of ciliary flow sensing. Decreased levels of PC1 protein were shown to result PKD in mice models (Leeuwen, Dauwerse et al. 2004); whereas decreased levels of PC2 may show early signs of cystogenesis since reduced PC2 protein levels were found to cause the proliferation of kidney tubular cells and the fibrosis of the interstitium (Chang, Parker et al. 2006).

In PKD, proteins (such as polycystins (e.g., PC1 and PC2), nephrocystins, fibrocystin, Wnt signaling proteins, and planar cell polarity (PCP) proteins) were found to be localized inside the cilium or basal body of the cilium, having altered functions (Pazour, San Agustin et al. 2002; Yoder, Hou et al. 2002; Veland, Awan et al. 2009). It has been hypothesized that epithelial cells in the nephron can undergo dedifferentiation and proliferation, and they are followed by redifferentiation in response to an injury to nephrons as an attempt to restore tissue function (Bonventre 2003; Guo and Cantley 2010). Renal

injury repair shares similar cell signaling pathways as PKD (Weimbs 2006; Weimbs 2007). In the Oak Ridge polycystic kidney mouse model, renal cilia were found to be much shorter as compared to a normal mouse renal cilia (Pazour, Dickert et al. 2000; Yoder, Tousson et al. 2002), possibly implying a relationship between flow sensing and PKD. In mouse models, kidney specific inhibition of ciliogenesis, i.e., the formation of cilia, was found to result in a PKD-like phenotype (Lin, Hiesberger et al. 2003). Ciliary flow sensing was found to affect active Na^+ transport in the normal mouse kidney cortical collecting duct epithelial monolayers (Resnick and Hopfer 2007; Resnick 2011). These findings suggested the importance of primary cilia and their flow sensing function in the context of PKD.

In PKD, mammalian target of rapamycin (mTOR) and signal transducer and activator of transcription 6 (STAT6) signaling pathways remain activated even under normal conditions (Low, Vasanth et al. 2006; Becker, Saez et al. 2010). In normal renal epithelial cell cultures, fluid flow induced by mild shaking retained the STAT6 in the cilium, and it prevented the translocation of STAT6 to cellular nucleus (Low, Vasanth et al. 2006). Thus, flow sensing of cilia can control cell division in kidney tubules (Singla and Reiter 2006), and in PKD this mechanism may be impaired. Fluid flow is also known to maintain differentiation of renal epithelial cells by blocking canonical Wnt signaling due to the elevated levels of inversin, a ciliary protein (Simons, Gloy et al. 2005; Deane and Ricardo 2007). Fluid flow is known to cleave the C-terminal domain of the PC1 protein, followed by the translocation into the cellular nucleus. This nuclear localization is thought to affect transcription of different genes (Chauvet, Tian et al. 2004; Deane and Ricardo 2007). PC1 is known to control cell proliferation since PC1 regulates the mTOR cell

signaling pathway, and this signaling pathway can be abnormally activated in case of PKD (Shillingford, Murcia et al. 2006). Combined activities of PC1 and PC2 control the cell cycle by regulating the JAK-STAT pathway (Bhunia, Piontek et al. 2002). Thus, different cell signaling mechanisms directly or indirectly related to cilia and ciliary flow sensing are responsible for controlling renal epithelial phenotype and gene expression and may be associated with PKD (Deane and Ricardo 2007).

ii. Alterations of Epithelial Transport in PKD

As discussed previously under the epithelial transport section, the collecting duct of the nephron helps in fine-tuning salt concentration by reabsorbing salt and water. In the collecting duct epithelial cells, Na^+ enter cells through ENaC, and with help of basolateral Na^+/ K^+-ATPase, these Na^+ move to the basolateral side and K^+ enter the cells (Wilson, Dillingham et al. 1985). Na^+ are reabsorbed from urine to blood through this mechanism. In mouse disease models of ARPKD, Na^+/ K^+-ATPase was detected in the apical membrane of cystic epithelial cells (Avner, Sweeney et al. 1992) suggesting similar Na^+ secretion can occur in case of ADPKD (Rohatgi, Greenberg et al. 2003). In the cystic epithelial cells of ADPKD patients, Na^+/ K^+-ATPase expression was also found to be in the apical side (Wilson, Sherwood et al. 1991; Rohatgi, Greenberg et al. 2003). Thus, the mislocalization of Na^+/ K^+-ATPase can be seen in both ADPKD and ARPKD.

Another study using immunohistochemistry reported that in human cystic kidney tissue and in mouse kidney cysts, Na^+/ K^+-ATPase α1 catalytic subunit expression levels were significantly reduced in intermediate and large cysts (Yu, Kanzawa et al. 2008). This finding suggested that active Na^+ transport may be diminished in PKD. The fluid accumulation and cyst expansion involve transepithelial fluid and solute secretion inside

the cyst lumen as opposed to the absorptive function of normal renal epithelial cells (Yu, Kanzawa et al. 2008). In kidney cysts, Cl^- are believed to be actively secreted using $Na^+/K^+/2Cl^-$ cotransporter, NKCC1 (Lebeau, Hanaoka et al. 2002; Thomson, Mentone et al. 2003) and apical c-AMP stimulated chloride channels, CFTR (Brill, Ross et al. 1996; Hanaoka, Devuyst et al. 1996). In the cyst lumen, Na^+ are thought to be secreted paracellularly due to the electrochemical gradient created by the active Cl^- transport. The accumulation of Na^+ and Cl^- results in the secretion of water in the cyst lumen by the process of osmosis involving water channels AQP1 and AQP2 (Devuyst, Burrow et al. 1996; Yu, Kanzawa et al. 2008). Thus, the secretion and accumulation of salt and water within the cysts can promote cyst expansion.

Experiments using microcysts formed by growing cells on collagen scaffolds showed that cells were capable of absorption as well as secretion similar to the epithelia from the intestine and trachea (Alton and Smith 1995; Greger, Bleich et al. 1997; Sullivan, Wallace et al. 1998). Chloride ions are secreted actively using $Na^+/K^+/2Cl^-$ cotransporter in the basolateral membrane and CFTR channel in the apical membrane as shown in figure 10 (Sullivan, Wallace et al. 1998). Two separate studies showed that they were able to reduce equivalent current or apical to basolateral Na^+ movement of kidney cysts by adding the sodium channel blocker, amiloride (Perrone 1985; Wilson, Sherwood et al. 1991). Thus, active Na^+ transport may still be present in kidney cysts. However, according to another study using ADPKD monolayers, I_{eq} remained unaffected even at 10 times higher concentration of amiloride or with other active sodium transport blocking agents, indicating the possible contribution of active chloride transport (Sullivan, Wallace et al. 1998). Thus, the contribution of active Cl^- transport in PKD may be debatable to some

extent. However, the application of a CFTR inhibitor, CFTRinh-172 (Ma, Thiagarajah et al. 2002) was found to slow the cyst expansion in the MDCK cell culture cyst model, whole embryonic kidney organ culture, and mouse ADPKD model (Li, Findlay et al. 2004; Magenheimer, John et al. 2006; Yang, Sonawane et al. 2008). These findings strongly support the role of active Cl^- transport in the PKD progression.

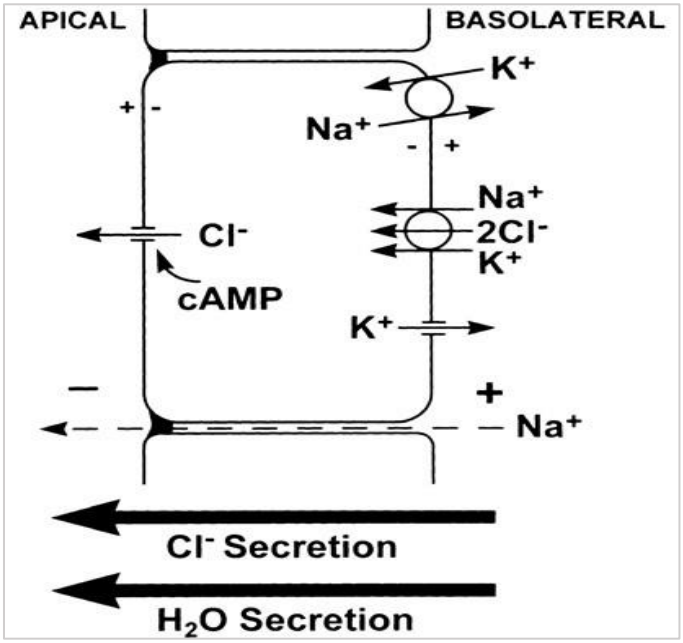

Figure 10: Epithelial Transport in PKD. Figure credit (Sullivan, Wallace et al. 1998). Chloride and water secretion seen in secretory epithelia (Liedrke 1989). The same secretory mechanism is believed to be involved in cystic epithelia of PKD (Sullivan, Wallace et al. 1998).

iii. Alterations of Epithelial Junctional Complex in PKD

a) Abnormal Adherens Junctions in PKD

Adherens junctions (AJ) keep cells attached by binding to actin filaments using cadherins and catenins. Spot-like adherens junctions, which allow cells stay attached to cellular extracellular matrix (ECM), are called the focal adhesions (FA). In ADPKD cystic epithelial cells, lateral AJ and FA show abnormalities. At the FA of an ADPKD epithelium,

the phosphorylation of focal adhesion kinase (FAK) is diminished and results in altered protein composition of FA (Wilson, Geng et al. 1999; Wilson 2011). Impaired phosphorylation of FAK complex leads to alteration in the cell shape, adhesion, and migration as seen in both ADPKD and ARPKD (Wilson, Geng et al. 1999; Israeli, Amsler et al. 2010; Elliott, Zheleznova et al. 2011; Wilson 2011).

In ADPKD, E-cadherin remains absent from the lateral membrane of AJ since E-cadherin undergoes internalization (Charron, Nakamura et al. 2000) similar to as seen in the epithelial to mesenchymal transition (Thiery and Sleeman 2006). In normal kidney epithelial cells, PC1 protein helps in forming a complex at the adherens junction with E-cadherin and β-catenins in order to maintain cell adhesion or polarity (Huan and van Adelsberg 1999). Increased phosphorylation of PC1 is seen in ADPKD cells causing disruption PC-1/PC-2/E-cadherin/β-catenin complex (Roitbak, Ward et al. 2004). Moreover, in ADPKD, the disruption of this complex is enhanced since the E-cadherin is internalized and replaced by embryonic isoform N-cadherin (Roitbak, Ward et al. 2004). E-cadherin plays a crucial role in maintaining adherens junction and thereby controls the junctional complex (Capaldo and Macara 2007). In ADPKD, the function of the adherens junctions is impaired mainly due to insufficient presence and stability of E-cadherin and can affect polarity of epithelial cells leading to cyst formation (Roitbak, Ward et al. 2004). The disruption of adherens junctions can alter the function of the epithelial tight junctions (Yu, Kanzawa et al. 2008).

b) Alteration of Tight Junctions in PKD

Cluadin-7 is known to be expressed in distal nephron and creates a transport barrier for both cations and anions (Alexandre, Lu et al. 2005; Yu, Kanzawa et al. 2008).

Overexpression of claudin-7 was shown to decrease Cl^- permeability and increase Na^+ permeability in porcine kidney epithelial cells (Alexandre, Lu et al. 2005). These findings suggested claudin-7 acts as a barrier against Cl^-, whereas forming pores that allow Na^+ through the paracellular space (Alexandre, Lu et al. 2005). In kidney cysts from human ADPKD patients, as well as in mouse kidney cysts, claudin-7 was found to be present in abundance (Yu, Kanzawa et al. 2008). It can be inferred that claudin-7 in the tight junctions of the cysts acts as a barrier preventing paracellular back-leak of Cl^- and allows Cl^- to be secreted only through transcellular transport pathway. The transcellular Cl^- movement can drive Na^+ movement paracellularly and water through osmosis into the cyst lumen (Yu, Kanzawa et al. 2008). Thus, claudin-7 in the tight junctions may contribute to cyst expansion.

iv. Abnormal Protein Sorting System and Cell Polarity in PKD

In the mouse model, lack of MALS-3, a PDZ-protein which interacts with polarity complex, resulted in cyst and fibrous tissue formation in the kidney (Olsen, Funke et al. 2007). As shown in figure 11, Na^+/ K^+-ATPase were found to be mislocalized in the apical membrane due to the apical mislocalization of trafficking protein syntaxin-4, and the membrane stabilizing proteins, ankyrin and fodrin (Wilson, Sherwood et al. 1991; Torkko, Manninen et al. 2008). The activation of Erb2 by phosphorylation causes alterations in the apico-basal polarity, and the overexpression of activated Erb2 leads to kidney cyst formation (Aranda, Haire et al. 2006; Wilson 2011). Membrane proteins are formed in the endoplasmic reticulum and undergo processing in the Golgi apparatus, followed by sorting to be directed and delivered by apical or basolateral vesicles (Wilson 2011). The trafficking of proteins in the right membrane domain is believed to be contributed by at

least partly by small G proteins belonging to Rab/sec family along with exocyst complex. Some Rab/sec family proteins (such as Rab 8, Rab 10, Rab 11, Rab 14, syntaxin-3) are known to control the delivery and transport of proteins onto the apical membrane whereas other Rab/sec family proteins, such as Rab6 and syntaxin-4, are known to cause localization and trafficking in the basolateral membrane (Wilson 2011). In ADPKD cells, abnormalities were found in Rab6/Rab8 trafficking proteins and syntaxin-4 proteins. These abnormalities in the kidney cystic epithelia affect the vesicle trafficking complex, known as the exocyst, and can cause defects in the mechanisms involving the apical docking and maintenance of membrane protein-tethering domain (Wilson 2011).

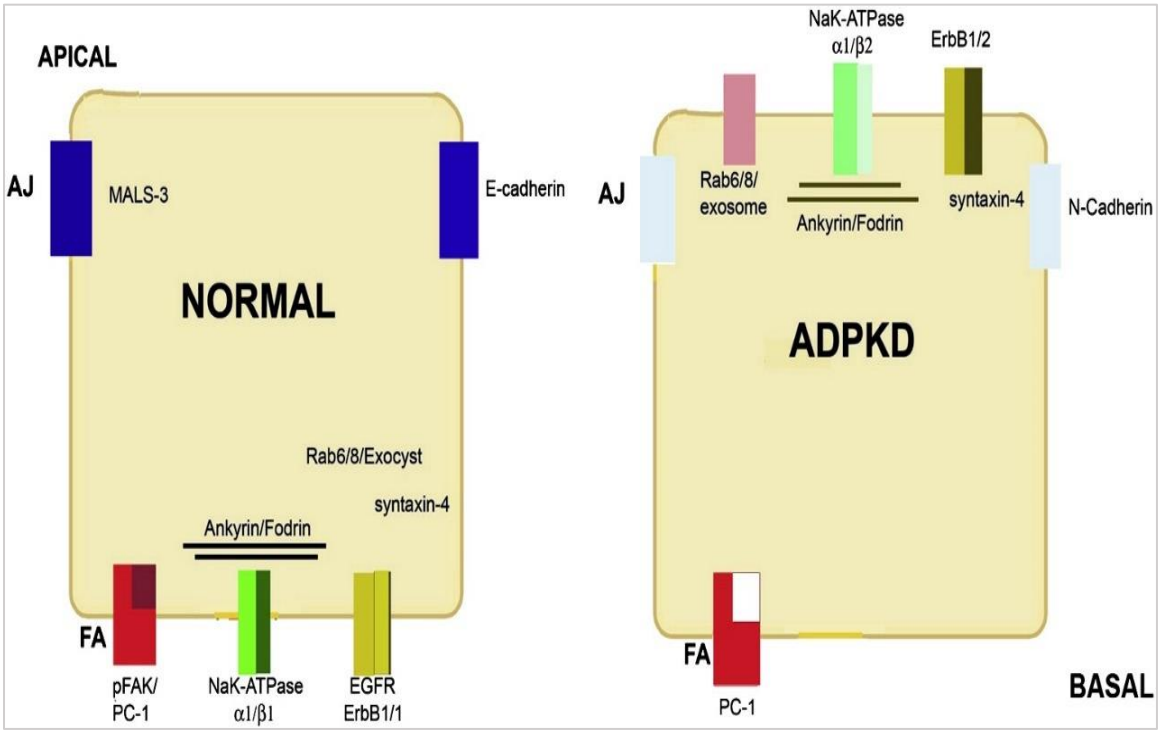

Figure 11: Polarized membrane associated proteins in normal kidney and cystic (ADPKD) kidney epithelial cells. Figure credit (Wilson 2011). In ADPKD, Na^{+}/ K^{+}-ATPase α1/β2, ErbB1/2 rab6/8 syntaxin 4, and ankyrin/fodrin are mislocalized onto the apical membrane and MALS-3 is absent from apico-lateral polarity complex. In the lateral adherens junction (AJ) of ADPKD cells, E-cadherin is substituted by N-cadherin and the pFAK is also diminished from focal adhesions (FA) of ADPKD cells (Wilson 2011).

In ADPKD cells, various changes are also noticed in the cellular cytoskeleton such as actin microfilaments, microtubules, and cytokeratin scaffolds. These cytoskeletal structures are known be associated with the process of vesicle transport and trafficking and stability of the membrane domain. Therefore, the alterations of cellular cytoskeleton are in agreement with the abnormal protein sorting system as seen in ADPKD cells (Oriolo, Wald et al. 2007; Wilson 2011). Thus, the renal epithelial polarity or functional phenotype can be impaired in PKD.

1.8 Role of Hypoxia on Cellular Functions and Diseases

1.8.1 Hypoxia and Hypoxia Inducible Factors

Oxygen (O_2) is crucial for the survival and normal function of mammalian cells and tissues. The lack of adequate O_2 supply creates a condition called hypoxia, which is known to be associated with various kidney pathologies such as AKI. Therefore, it is important to understand how cells adjust to hypoxic conditions. Hypoxia inducible factors (HIF) regulate cellular and tissue responses in an environment lacking sufficient availability of O_2 (Andringa and Agarwal 2014). HIF-1 and HIF-2 transcription factors are heterodimeric helix-loop-helix Per-Arnt-Sim (PAS) domain proteins (Haase 2009). These transcription factors form dimers and bind to the DNA of the target gene resulting in the activation of transcription (Semenza 2000). The α subunit is the O_2 sensitive and regulatory subunit, and β is the constitutively expressed subunit of HIF (Haase 2006). The binding of the HIF heterodimer to a hypoxia response element (HRE) on a regulatory region of a hypoxia responsive gene causes HIF-regulated transcription (Haase 2006). HIF-1 and HIF-2 have very little similarity in their functions (Haase 2006). HIF activation occurs when the α subunit is translocated into the nucleus and dimerizes with the β subunit and followed by

the binding of transcriptional cofactors, such as p300 (Haase 2006). Hypoxia was found to cause fast accumulation of HIF-1α protein without a significant rise in the HIF-1α mRNA levels (Huang, Arany et al. 1996). HIF-1α is known to be expressed almost in all types of tissues in humans, mice, other rodents, whereas the expression of HIF-2α is known to be more selective and is expressed primarily in the endothelium and interstitial cells of the kidney (Semenza 2000; Haase 2006). HIF is known to be involved in the regulation of different kidney function related processes, such as metabolism of glucose, angiogenesis, erythropoiesis, migration of cells, and cell-cell and cell-matrix interactions (Haase 2006). Various HIF target genes (> 100 genes) have been identified. These HIF-regulated genes include the genes that enhance O_2 delivery by promoting angiogenesis, for example vascular endothelial growth factor (VEGF), VEGF receptor-1 (Flt-1), and endoglin (CD105), the genes that enhance systemic delivery of O_2, such as erythropoietin (EPO), and the genes that favor anaerobic glucose metabolism, such as GLUT-1 (Haase 2006). Thus, HIF can control diverse cellular functions.

1.8.1.1 HIF Degradation by O_2 Sensing

During normoxia (i.e., normal O_2 level), HIF-1α and HIF-2α proteins undergo ubiquitin and proteasome-mediated degradation, and therefore these proteins cannot accumulate. HIF-α proteins have an oxygen-dependent degradation domain (ODD), containing a sequence of 200 amino acids, which plays an important role in the O_2 mediated degradation of HIF-α (Huang, Gu et al. 1998; O'Rourke, Tian et al. 1999). In normoxic condition, the ubiquitination and degradation of HIF-α is controlled by the binding of the tumor suppressor protein: the von Hippel-Lindau protein (pVHL) to the ODD domain of HIF-α (Maxwell, Wiesener et al. 1999; Kamura, Sato et al. 2000). The pVHL- mediated HIF degradation mechanism requires hydroxylation of specific proline residues (e.g.,

proline residue at the position 564) within the ODD, and thereby proline hydroxylation is important in determining HIF-α levels and the downstream hypoxia responsive gene transcription (Epstein, Gleadle et al. 2001; Ivan, Kondo et al. 2001; Jaakkola, Mole et al. 2001; Masson, Willam et al. 2001; Yuan, Hilliard et al. 2003).

1.8.1.2 Cobalt Prevents HIF Degradation

The metal cobalt (Co^{2+}) can stabilize HIF by preventing HIF degradation irrespective of the O_2 concentration. As shown in figure 12A, when a sufficient level of O_2 is present, HIF-specific hydroxylases cause hydroxylation of HIF-α and induce HIF-α degradation. Even during an adequate O_2 level, Co^{2+} can bind and block the iron binding sites on those proline hydroxylases (PHD), causing the inactivation of hydroxylase enzymatic function as shown in figure 12B (Epstein, Gleadle et al. 2001; Yuan, Hilliard et al. 2003). Moreover, as suggested in the figure 12B, Co^{2+} can still prevent the degradation of HIF-α even if the HIFs are already hydroxylated. Co^{2+} can directly bind to the hydroxylated HIF-α and inhibit the interaction between HIF-α with pVHL, and thereby block the ubiquitination and degradation of HIF-α (Yuan, Hilliard et al. 2003). Similar to Co^{2+}, dimethyloxallylglycine (DMOG) acts as the competitive inhibitor of PHD (Bruick and McKnight 2001), and iron chelator desferrioxamine (DFX) prevents the activity of PHD and thereby they can stabilize HIF by preventing its degradation (Hirsilä, Koivunen et al. 2005). Thus, using chemicals such as cobalt chloride ($CoCl_2$) and DFX, HIF can be stabilized even in the presence of adequate O_2, and the effects of HIF stabilization can be studied.

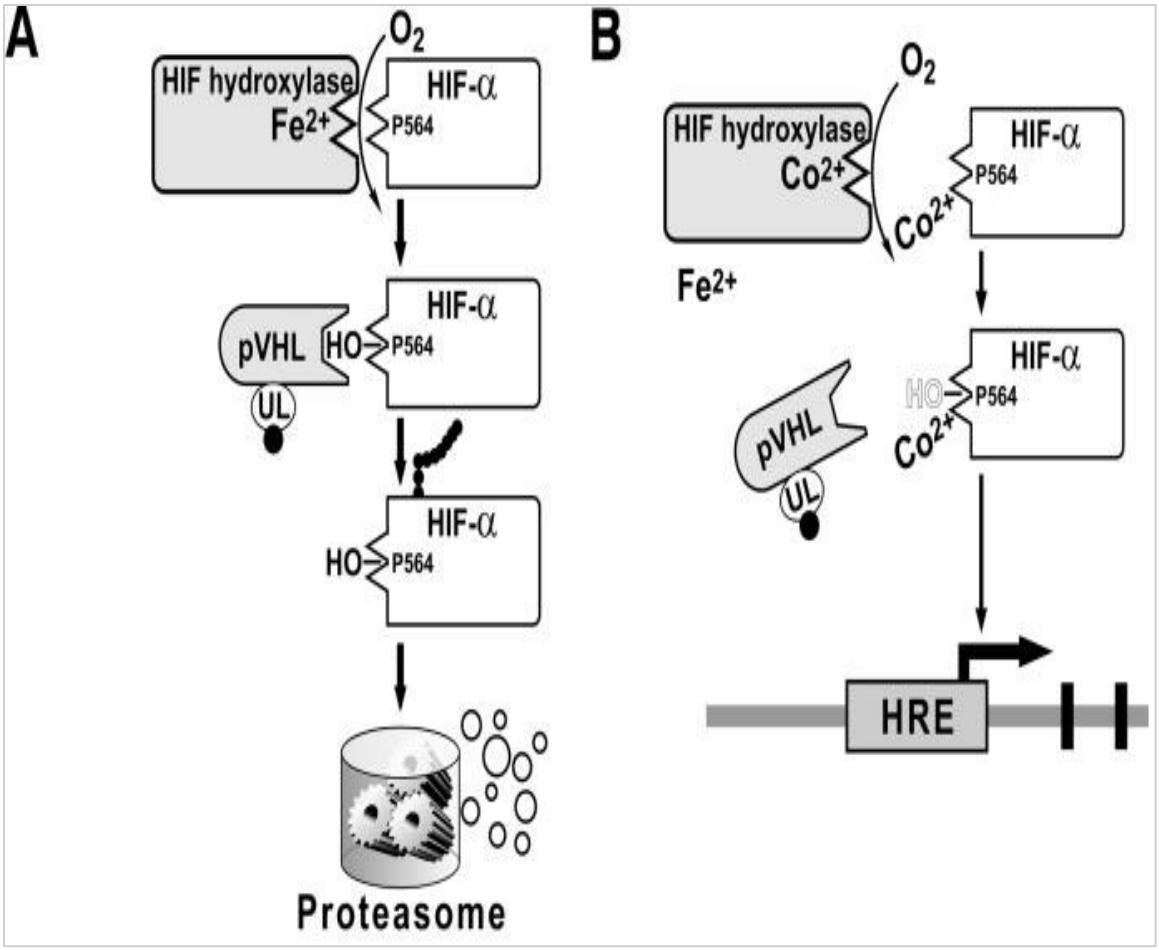

Figure 12: Mechanisms of HIF-α degradation or stabilization. Image credit (Yuan, Hilliard et al. 2003). (A) Current model of HIF-α and O_2 sensing. In the HIF-specific hydroxylase, iron acts as a cofactor. When adequate level of O_2 is present, PHD causes hydroxylation of proline residue at 564 in the peptide sequence of HIF. Hydroxylated HIF undergoes pVHL-mediated ubiquitination and is followed by proteasome guided degradation. B. Co^{2+} can prevent HIF hydroxylation by conjugating with iron-binding site of HIF hydroxylase and making the enzyme inactive. Moreover, in case HIF-α is already hydroxylated, Co^{2+} can bind directly to the hydroxylated HIF and can block the interaction between HIF-α and pVHL, and thereby prevents the degradation of HIF-α (Yuan, Hilliard et al. 2003).

1.8.2 O_2 Utilization and the Effect of Hypoxia in Kidney

Around 20 % of total cardiac output (CO) goes to the kidney, but still the O_2 tensions are found to be low in the kidney. For example, in the kidney medulla, O_2 tension is only 5 mm Hg (Lübbers and Baumgärtl 1997). Most O_2 in the kidney is used by the mitochondrial respiratory chain to produce ATPs which are mainly used in the function of

Na^+/ K^+-ATPase to drive reabsorption of Na^+ and other transport processes such as the passage of glucose and amino acids across cellular membranes (Haase 2013). Hypoxia causes a severe energy depletion and critical changes of metabolism (Devarajan 2006). Hypoxia results in the disruption of cellular cytoskeleton, leading to mislocation of polarized proteins, such as integrins and Na^+/ K^+-ATPase in the kidney (Nangaku and Eckardt 2007).

1.8.3 HIF Activation or Hypoxia in Kidney Diseases

Kidney hypoxia is found in PKD, diabetic kidney, ageing kidney, kidney injuries, and others (Nangaku 2006; Tanaka, Kato et al. 2006; Rosenberger, Khamaisi et al. 2008; Palm and Nordquist 2011). HIF-α stabilization is seen in both acute and chronic kidney diseases (Haase 2006). In diabetic nephropathy, the degree of HIF-activation was found be in correlation with the level of kidney injury (Higgins, Kimura et al. 2007). Pharmacological activation of HIF shows a protective effect in AKI, whereas similar HIF-activation can show reno-protective and pathological effects in CKD (Bernhardt, Wiesener et al. 2007; Haase 2013; Andringa and Agarwal 2014). Previous data showed that the timing of the pharmacologic activation of HIF is crucial in the renoprotective effects (Yu, Fang et al. 2012).

1.8.3.1 Hypoxia in CKD

a) Causes of Hypoxia in CKD

Chronic ischemia (i.e., obstructed or restricted blood flow) is seen in the tubulointerstitium. The damage to renal arterioles and arteries and the deformation and decrease in the number of capillaries can cause intense tubulointerstitial injury due to the ischemic-hypoxic condition (Choi, Chakraborty et al. 2000; Kairaitis, Wang et al. 2005; Nangaku 2006).

I. Role of Fibrosis in Hypoxia

In CKD kidney fibrosis may cause reduced O_2 supply due to the decreased blood supply by peritubular capillaries (Nangaku 2006). Moreover, the formation of kidney interstitial fibrotic tissue layer in between peritubular capillaries and tubular cells decreases the efficiency of O_2 diffusion from the capillaries to the cells (Nangaku 2006).

II. Role of Glomerulosclerosis in Hypoxia

During early stages of CKD, glomerulosclerosis causes a decrease in the blood supply and stagnant blood inside peritubular capillaries. These events further induce the loss of the capillaries and localized hypoxic condition, promoting tubulointerstitial injuries (Nangaku 2006).

III. Role of Vasoactive Substances in Hypoxia

During early stages of CKD, with normal glomerular structure and function, the imbalance of vasoactive substances, such as angiotensin II, may result in an intrarenal vasoconstriction, leading to kidney-localized hypoxia (Nangaku 2006). The activation of the renin-angiotensin system is known to cause the vasoconstriction of efferent arterioles, leading to a hypoxic condition in the tubulointerstitium. The administration of angiotensin II was found to reduce the numbers of peritubular capillaries in rats (Lombardi, Gordon et al. 1999; Nangaku 2006). In patients with type II diabetes and normalbuminuria, the reduced levels of peritubular capillary flow showed a correlation with the tubular dysfunction (Futrakul, Vongthavarawat et al. 2005). This finding suggested that the chronic hypoxia may lead to ESRD in CKD patients (Nangaku 2006).

IV. Role of Anemic Condition in Hypoxia

The O_2 delivery (DO_2) in the kidney or other organs is calculated using the equation: $DO_2 = CO \times (\% Sat \times 1.39 \times [Hb])$

where, CO= cardiac output, % Sat= the percentage of hemoglobin saturated with O_2, [Hb] = the concentration of hemoglobin with units of grams per liter, and 1.39= the value of the hemoglobin binding constant. The anemic conditions of CKD patients can cause decreased levels of DO_2, and thereby can result in the kidney-localized hypoxia (Nangaku 2006).

V. Role of Oxidative Stress in Hypoxia

Angiotensin II is known to be elevated in kidney diseases and creates oxidative stress by stimulating the NADPH oxidase. Moreover, the level of EPO decreases in CKD. The presence of superoxide causes decrease in the nitric oxide (NO) level. The NO suppresses mitochondrial respiration and the lack of NO elevates mitochondrial respiration process and can contribute to hypoxia (Nangaku 2006). Mitigation of oxidative stress was shown to prevent hypoxia by enhancing the delivery of O_2 to renal tissue in a study using a diabetic nephropathy model (Palm, Cederberg et al. 2003).

b) Effects of Hypoxia in CKD

Tubular cells under hypoxia are known to induce epithelial-mesenchymal transdifferentiation and be transformed into myofibroblasts (Manotham, Tanaka et al. 2004). Hypoxia is known to cause apoptosis of tubular cells as well as results in the ECM deposition and fibrosis due to the deficiency of matrix metalloproteinases (MMPs), other proteases and lysosomal enzymes (Tanaka, Hanafusa et al. 2003; Nangaku 2006) . Thus, hypoxia can cause renal necrosis and fibrosis, resulting in the loss of renal function.

1.8.3.2 Hypoxia in Kidney Cysts

Kidney cysts in ADPKD and ARPKD are known to expand over years and finally lead to kidney failure. The factors responsible for the cyst expansion and disease progression are not well understood (Cowley 2004). When kidney cysts grow, they can compress the adjacent blood vessels, decreasing the blood and O_2 supply. Moreover, the fluid inside the cysts is stagnant. Therefore, kidney cysts can be hypoxic environments. Higher levels of serum EPO were detected in ADPKD as compared to other kidney diseases (Eckardt, Möllmann et al. 1989). Arteriovenous EPO levels and cystic fluid EPO levels were found to be higher than normal in kidney cysts (Eckardt, Möllmann et al. 1989). New blood vessel formation, i.e., angiogenesis, is seen in polycystic kidneys due to the higher expression level of VEGF and VEGF receptors. Angiogenesis can allow enough nutrient and O_2 supply for cellular proliferation in order for cyst to expand (Bello-Reuss, Holubec et al. 2001; Wei, Popov et al. 2006). HIF-1α and HIF-2α proteins were found to show strong expression levels in rat kidney cysts similar to a kidney from a normal rat under hypoxia (Bernhardt, Wiesener et al. 2007). In cysts from human ADPKD patients, HIF-1α protein expression was detected in the cystic epithelial cells of renal medulla and HIF-2α protein was found to be expressed in the interstitial and endothelial cells. Consistent with the increased expression levels of HIF-1α, elevated levels of VEGF were found in the kidney cysts and collecting duct in PKD (Bernhardt, Wiesener et al. 2007). The mRNA levels of HIF effector molecules: heme oxygenase-1 (HO-1), Glut-1, and EPO were found to be higher in kidney cysts as compared to normal kidneys under normoxia and hypoxia (Bernhardt, Wiesener et al. 2007). In cystic kidney, HO-1 and Glut-1 protein levels were also found to be higher in the polycystic kidney than a kidney from a rat under systemic hypoxia (Bernhardt, Wiesener et al. 2007). In the cystic kidney epithelial cells,

Glut-1 and VEGF proteins were detected. The angiogenic factor, endoglin is an indicator of new blood vessels and the protein expression levels of endoglin were consistent with HIF-2α expression levels in the cysts of a human kidney (Bernhardt, Wiesener et al. 2007). Thus, the kidney cysts were found to be hypoxic and the HIF pathway seemed to remain continuously upregulated in the cysts. The kidney-localized hypoxia in the cysts showed signs of a higher level of hypoxia (i.e., chronic hypoxic response) as compared to a normal kidney from an individual encountering systemic hypoxia.

1.8.3.3 Effect of HIF-1α on Kidney Cyst Growth and Ion Transport

Forskolin is known to stimulate the growth of cysts having secretory functions (Magenheimer, John et al. 2006). In MDCK *in vitro* cyst models, the stabilization of HIF-1α by PHD inhibitors increased the level of GLUT-1 and promoted the forskolin-stimulated cyst growth. The knock down of HIF-1α by short hairpin RNA (shRNA) against HIF1α or the application of HIF-1α inhibitor was found to prevent cyst growth and also inhibited the stimulation of cysts with forskolin (Buchholz, Schley et al. 2013). Similarly, in embryonic mouse kidneys, the stabilization of HIF-1α was shown to increase Glut-1 and promoted cyst growth, and the inhibition of HIF-1α decreased Glut-1 and resulted in the formation of smaller cysts (Buchholz, Schley et al. 2013). In the rat kidney cyst models, the correlation between Glut-1 and cystic index supported the role of HIF-1α on the *in vivo* cyst growth. In the MDCK *in vitro* cystic model, even the treatment with selenium, insulin, dexamethasone, transferrin for two weeks could not regain the ENaC or active Na^+ transport. The application of CFTR inhibitor, CFTRinh-172 was found to prevent *in vitro* cyst growth (Buchholz, Schley et al. 2013). The stimulation of cystic epithelial cells with extracellular ATP molecules is known to increase intracellular concentration of Ca^{2+} promoting cyst growth due to the stimulation of purinergic receptors (Paulmichl and Lang

1988). The HIF1α deficient *in vitro* cysts could not grow in response to ATP or PHD inhibitor. These results suggested that the stabilization of HIF-1α induces calcium-activated chloride secretion, leading to cyst expansion. Ionomycin, which is an ionophore, is known to cause an increase in intracellular Ca^{2+} concentration for a relatively extended period of time. In the presence of ionomycin, the I_{sc} was generated due to the luminal Cl^- secretion process in normal MDCK cells, and this I_{sc} was abolished in cells in which HIF-1α was knocked down (Buchholz, Schley et al. 2013). Thus, in the MDCK *in vitro* cyst model, active Cl^- secretion seems to be the major active transport which is regulated by HIF-1α.

1.8.4 Effects of Hypoxia on Active Na^+ Transport and Cellular Junctions

1.8.4.1 Effects of Hypoxia/ Ischemia or HIF-stabilization on Renal Epithelial Cells

The comparison of I_{sc} values in the kidney collecting duct monolayers showed that as compared to an ambient O_2 concentration of 20%, an O_2 concentration of 40%, increased the ENaC activity by 50%. Similarly, when the ambient 20% O_2 concentration was reduced to 8%, ENaC activity was found to decrease by 40%. As compared to 8% O_2, 40% O_2 showed higher surface expressions as well as higher levels of matured forms of β and γ ENaC subunits (Husted, Lu et al. 2010). Thus, an O_2 concentration can regulate the ENaC activity of renal epithelial cells (Husted, Lu et al. 2010).

Actin organization of renal epithelial cells of the proximal tubule was found to be affected by ischemia (White, Doctor et al. 2000). In renal epithelial monolayers, chemically induced hypoxia-mimetic condition created by ATP depletion resulted in the disruption of F-actin cytoskeleton organization and tight junctions and endocytosis of Na^+/K^+-ATPase. Spectrin (called fordin in epithelial cells) network connects actin cytoskeletal

to the cellular surface membrane. The dissociation of fordin and ankyrin from actin cytoskeleton causes fordin and ankyrin to become dispersed throughout the cellular cytoplasm (Molitoris, Dahl et al. 1996). Similarly during ischemia, the disruption of the cellular cytoskeleton can lead to the dissociation of Na^+/ K^+-ATPase from fordin and cytoskeleton, and Na^+/ K^+-ATPase becomes free to be distributed to the apical membrane of the proximal tubule (Molitoris, Dahl et al. 1992). The reabsorption of ions and water by proximal tubule cells is normally maintained due to the lipid and protein polarity in the apical and basolateral membranes. An ischemic injury decreases sodium reabsorption by kidney proximal tubular cells due to the apical redistribution of Na^+/ K^+-ATPase from the basolateral side. The loss of membrane polarity due to ischemia can cause disruption of the tight junctions and actin cytoskeleton (Molitoris 1991). *In vitro*, apical redistribution of renal Na^+/ K^+-ATPase was found to transport Na^+ ions from basolateral to apical side (Molitoris 1993).

In the VHL deficient clear cell renal cell carcinoma (CCRCC) cell line, the expression of VHL which is known to promote HIF1α degradation, increased the expression of claudin-1, E-cadherin, and occludin proteins. Immunofluorescence for ZO1 showed intact tight junctions when VHL was present. The application of small interfering RNAs (siRNAs) against HIF-1α was shown to promote ZO1, claudin-1, and occludin based junctional assembly in the VHL deficient renal epithelial cells. The *in vivo* kidney cysts formed due to VHL deficiency showed diminished levels of claudin-1 and occludin proteins. Inactivation of VHL in the kidney epithelium was shown to down-regulate cell–cell adhesion molecules involved in AJs and tight junctions. Similar to HIF-1α-SiRNAs, histone deacetylase inhibitor sodium butyrate, which is known to inhibit HIF activation,

was able to restore ZO1, claudin-1, occludin, and E-cadherin in these VHL- deficient renal epithelial cells (Harten, Shukla et al. 2009).

Thus, HIF-1α or hypoxia can alter renal epithelial tight junctions and active Na^+ transport.

1.8.4.2 Effects of Hypoxia on Alveolar Epithelial Cells

In the human and rat alveolar cells, the active Na^+ transport was found to decrease in response to hypoxia (Mairbäurl, Wodopia et al. 1997; Mairbäurl, Mayer et al. 2002). The decreased numbers of membrane-bound ENaC under hypoxia can cause a decrease in the ENaC activity in alveolar epithelial cells (Wodopia, Ko et al. 2000; Jain and Sznajder 2005). In the alveolar epithelial cells, short-term (1 hour) hypoxia was shown to decrease Na^+/ K^+-ATPase due to the endocytosis of Na^+/ K^+-ATPase. A prolonged hypoxia produces reactive oxygen species (ROS) activating PKC-ζ molecules which cause endocytosis of Na^+/ K^+-ATPase by a process involving phosphorylation of the serine reside at the position 18 of the N-terminus of Na^+/ K^+-ATPase (Dada, Chandel et al. 2003). During the severe hypoxia, not the intracellular Na^+/ K^+-ATPase, but the Na^+/ K^+-ATPase in the plasma membrane of alveolar epithelial cells were found to decrease around 50% within 2 hours in order to minimize oxygen consumption (Jain and Sznajder 2005). Thus, hypoxia was shown affect the expression or activity of apical ENaC and basolateral Na^+/ K^+-ATPase, causing a decrease in the active Na^+ transport and resulting in reduced ability of alveolar epithelium to clear alveolar edema fluid (Vivona, Matthay et al. 2001; Planès, Blot-Chabaud et al. 2002; Dada, Chandel et al. 2003).

Hypoxia was also found to decrease ZO1 and occludin protein levels, affect the organization of actin cytoskeleton, and cause mislocalization of occludin from tight junctions to the cell interior in alveolar epithelial cells. Consistent with the effects on

cellular junctions, hypoxia was found to increase transepithelial electrical conductance in the alveolar epithelial monolayers (Bouvry, Planes et al. 2006; Caraballo, Yshii et al. 2011).

Thus, in alveolar epithelial cellular monolayers, hypoxia affects the active Na^+ transport and epithelial tight junctions.

1.8.4.3 Effects of Hypoxia or HIF-stabilization on Endothelial Cells

Hypoxia was shown to alter tight junctions and permeability of other cell types, such as brain microvessel endothelial cells and intestinal epithelial cells (Xu, Lu et al. 1999; Yamagata, Tagami et al. 2004; Engelhardt, Al-Ahmad et al. 2014). The stabilization of HIF-1α by hypoxia or chemically using $CoCl_2$, DFX or DMOG was shown to disrupt the barrier function of brain microvessel endothelial cells due to alterations of tight junctions caused by the delocalization and elevated levels of tyrosine phosphorylation of tight junction proteins. The application of a HIF-1α inhibitor was shown to restore the barrier function in endothelial cells under hypoxia. In the endothelial cells, under hypoxia with 1% O_2, ZO1 protein levels were found to decrease significantly after 48 hours (Engelhardt, Al-Ahmad et al. 2014). HIF-1 is known to bind to a HRE in the 5' flanking region of the VEGF gene and stimulates the transcription of VEGF (Forsythe, Jiang et al. 1996). The tight junction proteins ZO1 and occludin are known to be phosphorylated by VEGF in endothelial cells (Antonetti, Barber et al. 1999). The elevated level of VEGF was shown to decrease the expression of occludin and induce dissociation of ZO1 and occludin from tight junctions in the endothelial monolayers (Wang, Dentler et al. 2001). Thus, hypoxia or HIF stabilization can alter tight junctions of endothelial cells.

In summary, HIF stabilization or hypoxia can affect tight junctions, and thereby may affect the paracellular transport in endothelial and epithelial cells. The active or

transcellular transport in renal and alveolar epithelia was also shown to be modified by hypoxia or HIF.

1.9 Research Hypothesis and Significance

As described above, hypoxia or HIF-stabilization can affect active transport of renal and alveolar epithelial cells and passive transport of epithelial and endothelial cells. Cyst expansion, stagnant fluid accumulation, and inadequate vascular supply can result in localized chronic ischemia-hypoxia in cysts and as well as in normal epithelia adjacent to a cyst as discussed previously. HIF-1α is known to be a major regulator of cellular response to hypoxia. Active Cl^- secretion by kidney cystic epithelia was shown to be affected by HIF-1α as mentioned earlier. Normal epithelia near a cyst encounter the ischemic-hypoxic environment created by cysts, and we aim to understand whether this ischemic-hypoxic condition or HIF-stabilization may act as a major contributor in PKD progression by affecting the transport properties of normal renal epithelial cells (Nag and Resnick 2018).

We hypothesize that in normal renal epithelia near a cyst, the stabilization of HIF-1α can alter active and passive transport of normal epithelia, transforming the normal absorptive epithelial phenotype to a secretory cyst-like and paracellularly leaky phenotype, and may contribute to cyst expansion (Nag and Resnick 2018).

The findings of this study can be broadly applicable to other kidney diseases or pathologies related to ischemia-hypoxia, e.g., AKIs and CKDs.

In addition, renal cilia are believed to have an important role in PKD progression and ciliary flow-sensing is known to regulate active Na^+ transport in renal epithelial monolayers as discussed before. Renal ciliary lengths and biomechanical property were shown to be affected due to HIF-stabilization as mentioned earlier. In this current study,

we have not investigated the specific contribution of cilia to the effect of HIF-stabilization on renal transepithelial transport. Future studies, involving comparisons among transepithelial transports in ciliated and deciliated epithelial monolayers with or without HIF-stabilization, can help to understand the role of cilia and ciliary flow-sensing in this context.

CHAPTER II

MATERIALS & METHODS

2.1 Cell Culture

Experiments were performed using two cell lines, a mouse cell line (Kolb, Woost et al. 2004) developed by microdissection from the cortical collecting duct (mCCD 1296 (d)) of a heterozygous offspring mouse carrying a transgene, temperature-sensitive SV40 large T antigen under the control of an interferon-γ response element (Nag and Resnick 2017), and another cell line, a commonly used MDCK epithelial cell line (ATCC CRL 2935). Both cell types were grown onto collagen-coated and suspended membrane cell culture inserts. The cultures of mCCD cell line maintain the major phenotypic features, such as contact inhibition, tight junction formation, cell polarity, and directed salt and water transport, similar to the characteristics of primary cortical collecting duct cultures (Nag and Resnick 2017). Most of the experiments were performed using these mCCD cells.

2.1.1 mCCD Cell Culture

mCCD cells were allowed to grow until confluence under the incubation conditions of 33°C and 5% CO_2. The growth medium was formulated by adding the following media constituents at final concentrations: Dulbecco's Modified Eagle Medium (DMEM) without glucose and Ham's F12 at a ratio of 1:1, 5 mg/ml transferrin, 5 mg/ml insulin, 10 mg/ml

epidermal growth factor (EGF), 4 mg/ml dexamethasone, 15 mM 4-(2-hydroxyethyl)- 1-piperazineethanesulfonic acid (HEPES), 0.06 w/v% $NaHCO_3$, 2 mM L-glutamine, 10 ng/ml mouse interferon-γ, 50 μM ascorbic acid 2- phosphate, 20 nM selenium, 1 nM 3,3′,5-triiodo-L-thyronine (T3), and 5% fetal bovine serum (FBS). The fully grown cellular monolayers were incubated in an incubation condition of 39°C and 5% CO_2 to promote differentiation. For cells to differentiate, FBS and growth factors (insulin, EGF, and interferon-γ) were withdrawn from the apical differential media (APDM) and only growth factors were withdrawn from the basolateral differentiation media (BLDM) (Nag and Resnick 2017). Antibiotics, Penicillin-streptomycin (stock concentration of 10 mg/ml, 100X) and gentamycin (stock concentration of 50 mg/ml, 1000X) were added to cell culture media with final concentrations of 1X.

Cells were first grown onto collagen-coated suspended membrane cell culture inserts having 30 mm diameter (Millipore PICM03050, area= 4.71 cm^2), inside a 6-well cell culture plate (Falcon# 35116). When sufficient cellular numbers (> 80% confluence) were achieved, cells were then passaged at a dilution of 1:3 onto suspended membrane cell culture inserts having 12 mm diameter (Millipore PICM 01250, area= 1.13 cm^2), within a 24-well cell culture plate (Falcon# 353047). Next, the cells were grown to confluence and were allowed to differentiate resulting in a ciliated functional epithelial monolayer that maintained a directed salt and water transport (Nag and Resnick 2017).

2.1.2 MDCK Cell Culture

MDCK epithelial cells were cultured in a growth medium containing DMEM and Ham's F-12 in a 1:1 ratio, 15 mM HEPES, 0.06 w/v% $NaHCO_3$, 2 mM L-glutamine, and 10% FBS. Upon confluence, FBS was reduced to 1% to promote differentiation and

ciliogenesis. Penicillin-streptomycin and gentamycin were added to MDCK cell culture media as described previously. During both growth and differentiation, MDCK cells were maintained in an incubator at 37°C and 5% $CO_{2.}$ MDCK cells were first grown onto 60 mm tissue culture dishes (Celltreat# 229660) and after reaching confluence, cells were passaged onto collagen coated small cell culture inserts (area= 1.13 cm^2) inside a 24-well plate as discussed above. These MDCK cells were first grown and then the monolayers were differentiated for at least 3 days prior to performing permeability studies. MDCK monolayers do not display directed salt and water transport as mCCD monolayers, but MDCK monolayers do express a functional cilium early, after 3 days of serum starvation (Resnick 2016).

2.1.3 Cell Culture Experimental Designs

Figures 13 and 14 show schematic timelines of the cell culture experiments. Day 0 is defined as the starting point, when confluent monolayers are switched to differentiation conditions. Upon entering differentiation culture conditions, over time mCCD monolayers develop functional characteristics, such as the development of a directed Na^+ transport and the emergence of functional primary cilia, after approximately 5 days. As shown in figure 13, mCCD monolayers are considered fully differentiated after 7-10 days having stable electrophysiological properties and remain viable for an additional 24 days (Nag and Resnick 2017). By contrast, MDCK cells express primary cilia after 3 days in differentiation conditions and are only viable for an additional 7 days as shown in figure 14. Throughout the experiment, the apical media volume was restricted (100 µl) so that the thin fluid layer could allow adequate diffusion of O_2 and maintain a normoxic culture condition (Resnick 2011; Nag and Resnick 2017).

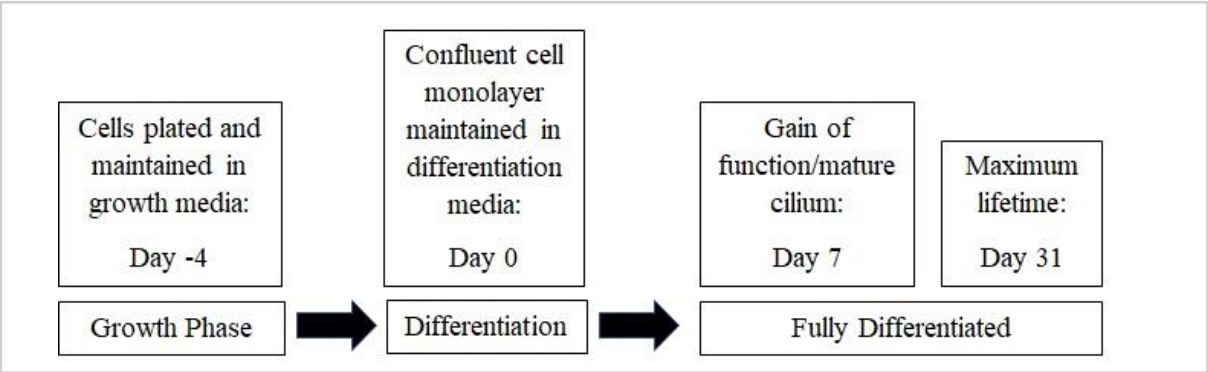

Figure 13: mCCD cell culture time line (Nag and Resnick 2017).

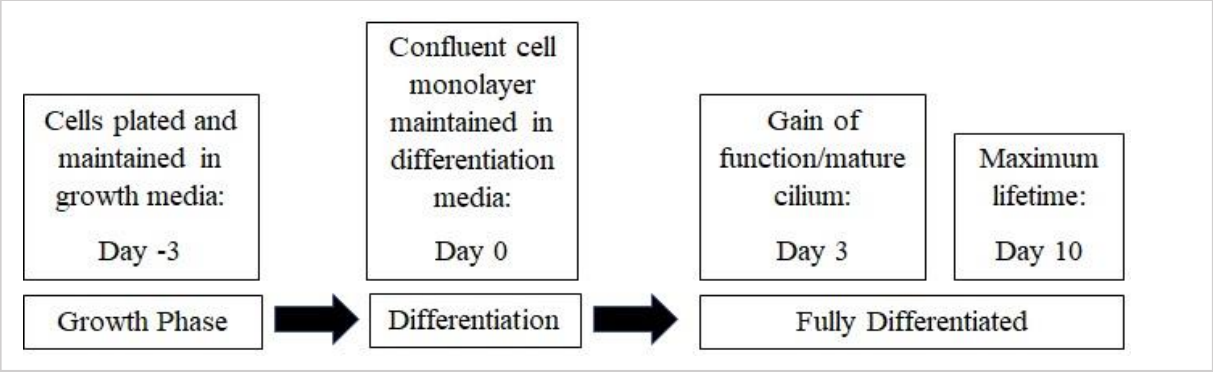

Figure 14: MDCK cell culture time line.

2.1.4 Application of fluid flow

The presence of fluid flow was shown to alter active Na^+ transport in mCCD monolayers (Resnick and Hopfer 2007; Resnick 2011). Fluid flow in mCCD cell cultures was generated by placing the cell culture plates onto an orbital plate shaker **(**IKA MS3 digital) and operating the shaker at 4.2 Hz (~250 RPM) (Nag and Resnick 2017).

2.2 $CoCl_2$ Treatment

$CoCl_2$ hexahydrate (S93179 from Fisher Scientific) was dissolved in a sterile 1X Phosphate Buffer Saline (PBS) to prepare 100 mmol/L $CoCl_2$ stock solution, which was diluted in APDM or BLDM or MDCK differentiation media to obtain the final desired concentration of 100 µmol/L. Experiments were carried out with $CoCl_2$ added to APDM,

BLDM, or to both APDM and BLDM (Nag and Resnick 2017). $CoCl_2$ was used in order to stabilize or prevent degradation of HIF1α in mCCD and MDCK monolayers (Verghese, Zhuang et al. 2011) (Nag and Resnick 2017).

A preliminary experiment was performed to study the effect 30 µmol/L of HIF-1α inhibitor, methyl 3-[[2-[4-(2-adamantyl) phenoxy] acetyl] amino]-4-hydroxybenzoate from San Cruz Biotechnology (Catalog no. sc-205346) on FITC-dextran permeability in MDCK monolayers in which HIF1α was stabilized using $CoCl_2$.

2.3 Fluorescein isothiocyanate (FITC)-dextran Permeability Assay

Anionic FITC-dextran molecules with two different molecular weights (3 kDa and 70 kDa), D 3305 and D 1823 (Molecular Probes, Life Technologies) in Hanks' Balanced Salt Solution (HBSS), 1X (21-023-CM, Cellgro, Mediatech) were used to measure the transepithelial permeability. According to the manufacturer (Molecular Probes), the specific lots consist of 1 mole of FITC per mole of 3 kDa dextran (Lot# 1709577 and 1485224) and 7 moles of FITC per mole of 70 kDa dextran (Lot # 1583589) (Nag and Resnick 2017).

2.3.1 Generation of Calibration Graphs

The stock concentration of 120 µmol/L of both 3 kDa and 70 kDa dextran was serially diluted in 1X HBSS buffer to formulate eight different concentrations, ranging from 120 µmol/L to (120×10^{-8}) µmol/L to create a calibration graph of FITC-dextran concentrations versus fluorescence intensities. Each concentration was prepared in four replicates, and then 100 µL solutions of each replicate at different concentrations were added into a 96-well plate, and fluorescence values were detected using a fluorescence plate reader (Perker Elmer Life Sciences/ Wallac Victor Multilabel Counter and Wallac

1420 Manager software) at 490 nm excitation and 530 nm emission. These calibration graphs were used to determine the unknown FITC-dextran concentrations from the fluorescence intensity values in renal epithelial permeability experiments (Nag and Resnick 2017).

2.3.2 Experimental Procedure and Sample Collection

In the FITC-dextran permeability experiments, the cell culture inserts with cellular monolayers were first transferred into a 12-well plate for easier manipulation. These cell culture inserts were gently washed with an HBSS buffer (HyClone, Catalog No. SH30268.02) three times to remove any residual media. Then, as shown in figure 10, 100 µl of FITC-dextran in the HBSS buffer was added to the apical side and 1 ml of the HBSS buffer was added to the basolateral side of the cell culture inserts. The 12-well plate with the cell culture inserts were placed inside a cell culture incubator maintained at 37°C and 5% CO_2. A volume of 100 µl of buffer sample was collected from the basolateral side every 10 minutes, for a total of 70 minutes, to detect FITC-dextran transport from the apical to basolateral side as shown in figure 15. Each of the collected sample from the 12-well plate was deposited onto a 96-well plate. The fluorescence intensity value of the sample was measured using the plate reader with the same settings as described previously, and then the sample was added back to the basolateral side of the cell culture insert to maintain a constant fluid volume as shown in figure 15. After finishing up the transport experiment with 3 kDa FITC-dextran, the cell culture inserts were washed with HBSS buffer thrice, and the 70 kDa FITC-dextran transport was performed in the same way. In the beginning of each experiment, the concentration of initial stock solutions of 3 kDa and 70 kDa FITC-dextran molecules were determined from the calibration graphs. Each replicate of the

sample was individually plotted to calculate the permeability value. The average permeability of 3-5 replicates was calculated and shown in the results (Nag and Resnick 2017).

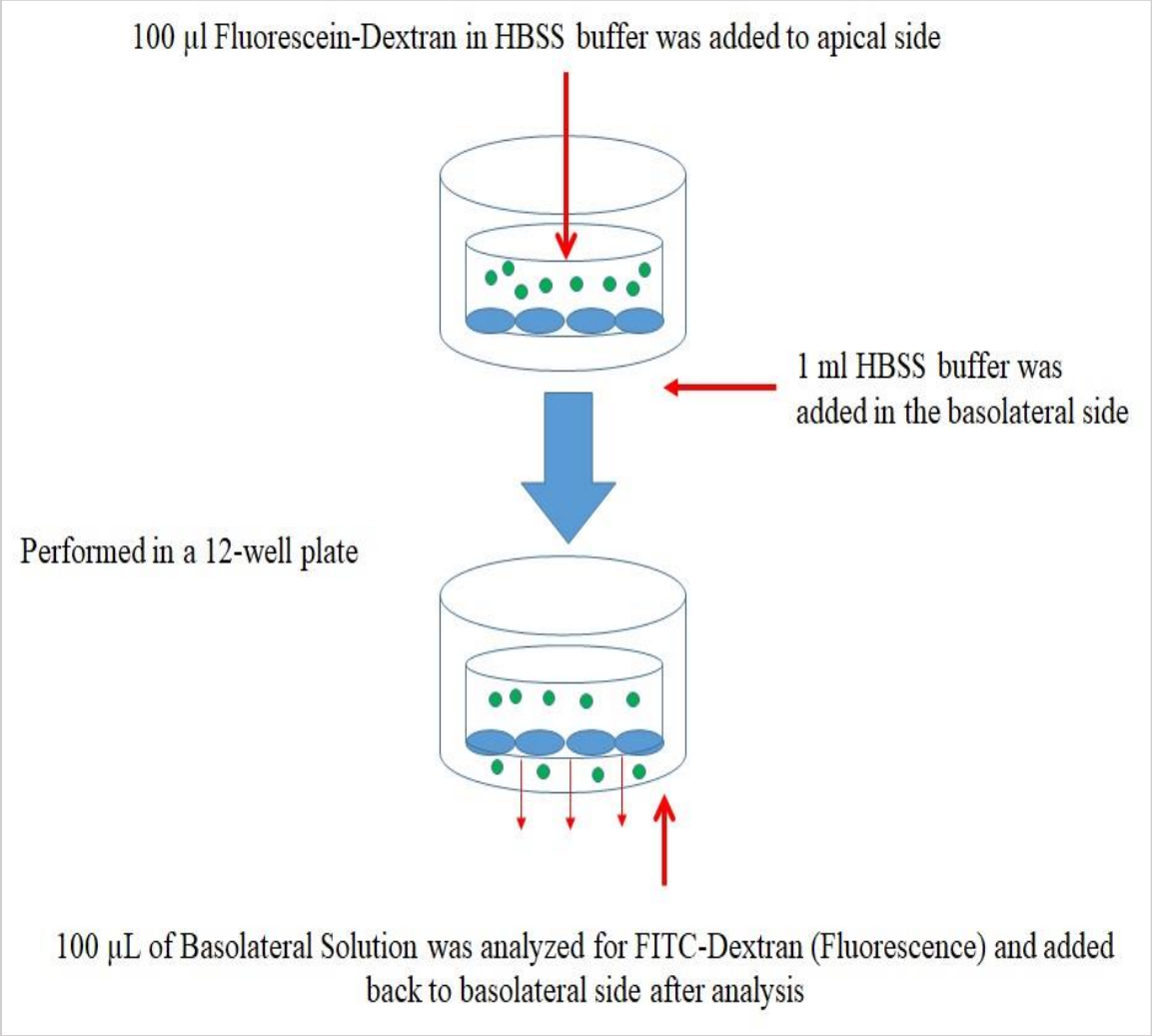

Figure 15: Experimental procedure of FITC-dextran permeability assay.

2.3.3 Quantification of Epithelial Monolayer Permeability

There are various published methods that are used to determine transepithelial permeability (Siflinger-Birnboim, del Vecchio et al. 1987; Artursson 1990; Abbott, Revest et al. 1997; Gaillard, Voorwinden et al. 2001; Matter and Balda 2003; Balda and Matter 2007; Yuan and Rigor 2010). Our quantification of an epithelial monolayer permeability

is based on the relationship between the time-dependent changes in tracer particles, such as FITC-dextran, and the transepithelial permeability. The derivation used in the quantification is shown below. This derivation considers all the physiological parameters (such as the area of the cellular monolayer and apical and basolateral fluid volumes) relevant to the experimental setup. However, this derivation, like other methods, cannot distinguish between transcellular and paracellular pathways (Nag and Resnick 2017).

Following Fick's first law of diffusion (Fick 1855), the mass flux of a tracer from the apical compartment passing through a semipermeable surface (area = 'A') to the basolateral compartment can be expressed using the equation:

$$\frac{\mathrm{dM}_{bl}}{\mathrm{dt}} = \mathrm{P\ A}\ [\mathrm{C(t)}_{ap} - \mathrm{C(t)}_{bl}] \tag{1}$$

Where 'M_{bl}' is the total mass of tracer particles in the basolateral side, 'P' is the permeability with units of length/time, '$C(t)_{ap}$' is the time-dependent concentration of tracer particles in the apical compartment, and '$C(t)_{bl}$' is the time-dependent concentration of tracer particles in the basolateral compartment (Nag and Resnick 2017).

With our experimental design, we can assume that the fluid volumes in the apical and basolateral sides stayed constant, and any possible changes were negligible during the time of the experiment (~ 80 minutes). Thus, as the apical and basolateral fluid volumes remain constant, dividing by the basolateral fluid volume 'V_{bl}' and using the equation of conservation of mass $M_0 = C(t)_{ap}V_{ap} + C(t)_{bl}V_{bl}$, we obtain

$$\frac{\mathrm{dC}_{bl}}{\mathrm{dt}} = \frac{\mathrm{P\ A}}{V_{bl}}\left[\frac{M_0}{V_{ap}} - \mathrm{C(t)}_{bl}\frac{V_{ap} + V_{bl}}{V_{bl}}\right] \tag{2}$$

In the beginning of the experiment, when the tracer (FITC-dextran) was just added to the apical side (i.e., at time t = 0 second), the basolateral concentration of the tracer was $C_{bl}(0) = 0$. Now, we can use this initial experimental condition to find the solution of this equation.

$$\mathrm{C(t)}_{bl} = \mathrm{C}_0 \left[1 - \mathrm{Exp}\left[-PA\left(\frac{1}{V_{bl}} + \frac{1}{V_{ap}}\right)t\right]\right] \tag{3}$$

where 'C_0' is the initial tracer concentration and $C_0 = M_0/(V_{ap}+V_{bl})$. For convenience, we combine all the constant parameters as a single constant and denote it as the constant B = A $(1/V_{bl} + 1/V_{ap})$ and reorganize the equation to solve for the permeability:

$$\mathrm{P\,t} = -\frac{ln(1 - C(t)_{bl}/C_0)}{B} \tag{4}$$

Thus, from the measurements of the basolateral concentrations of FITC-dextran '$C(t)_{bl}$' as a function of elapsed time 't' (unit: seconds), we calculate the permeability 'P' as the slope of a best-fit line. The values of the parameters used in the calculation of permeability values are shown in table 2 (Nag and Resnick 2017).

Table II: FITC-dextran permeability calculation parameters.

Parameter	Value
Initial FITC-dextran concentration= C_0	Variable
Area of semipermeable filter= A	1.13 cm^2
Volume of fluid in apical chamber= V_{ap}	100 µL
Volume of fluid in basolateral chamber= V_{bl}	1 mL
'B' (see equation 4) = constant= A $(1/V_{bl} + 1/V_{ap})$	12.43 cm^{-1}

2.4 Renal Epithelial Electrophysiology

The measurements of transepithelial voltage and resistance values were carried out using Endohm chambers (ENDOHM-24SNAP or ENDOHM-12) from World Precision Instruments (WPI) connected to a Millicell-ERS voltmeter from Millipore or EVOM2 epithelial voltmeter from WPI. Both voltmeters were calibrated using a test resistor of 1 kΩ from WPI to ensure accurate resistance read outs. The resistance values were recorded using the voltmeter in a current-clamp mode. The Endohm chamber was first cleaned with 70% ethanol for 10 minutes, followed by rinsing in distilled water. The chamber was then exposed to UV within our laminar cell culture hood for an hour. A volume of basolateral differentiation media sufficient to connect both sets of Ag/AgCl electrodes was added to the chamber, and electrodes immersed in the media were allowed to equilibrate for at least three to eight hours, until the voltage readings became stabilized.

As discussed previously, epithelial monolayers were created on permeable membrane cell culture inserts, and then the cells were differentiated so that the cells maintain primary cilia and show functional electrophysiological properties. Once the Endohm-voltmeter measurement system was equilibrated and ready to use, the cell culture inserts with differentiated epithelial monolayers were transferred one by one onto the Endohm chamber to record cellular electrophysiological properties. This Endohm chamber has two sets of concentric electrodes: one for voltage measurement and another for current as shown in figure 16. The electrodes are made of Ag/AgCl and are considered to be safe for biological applications since Ag is known to dissolve slowly and is known to be non-toxic (Nadeau 2017).

The electrical read outs are acquired from the voltmeter as resistance and voltage values. The TER values are presented with a unit of Ω-cm^2 or kΩ-cm^2 by multiplying raw resistance values with the area (1.13 cm^2) of the cell culture insert. The short circuit equivalent current (I_{eq}) was calculated from voltage and resistance read outs using Ohm's law, I= V/R. I_{eq} values were expressed as μA/ cm^2 by dividing obtained I_{eq} values by the area (1.13 cm^2) of the filter. The values of I_{eq} relative to the control group are presented. Greater than 95% of the I_{eq} in mCCD monolayers was inhibited by the apical application of 10 μmol/L amiloride. Thus, the I_{eq} value in mCCD monolayers is considered proportional to ENaC activity or active Na^+ transport (Resnick and Hopfer 2007; Resnick 2011; Nag and Resnick 2017). The monolayers of MDCK cells did not produce any detectable voltage values, and hence MDCK cells were not used to study I_{eq} or active ion transport. To exclude samples that lost confluence or may have otherwise been damaged, any mCCD culture possessing a TER value below a resistance threshold of 1000 Ω-cm^2 was discarded. Similarly, any MDCK culture with a TER value below a resistance threshold of 150 Ω-cm^2 was also omitted from the studies. Before collecting electrophysiological read outs, 100 μl of APDM was gently added to cell culture inserts in addition to the 100 μl of APDM already present to ensure electrical contact between the upper electrodes and apical fluid (Nag and Resnick 2017). Thus, electrophysiological analyses were performed.

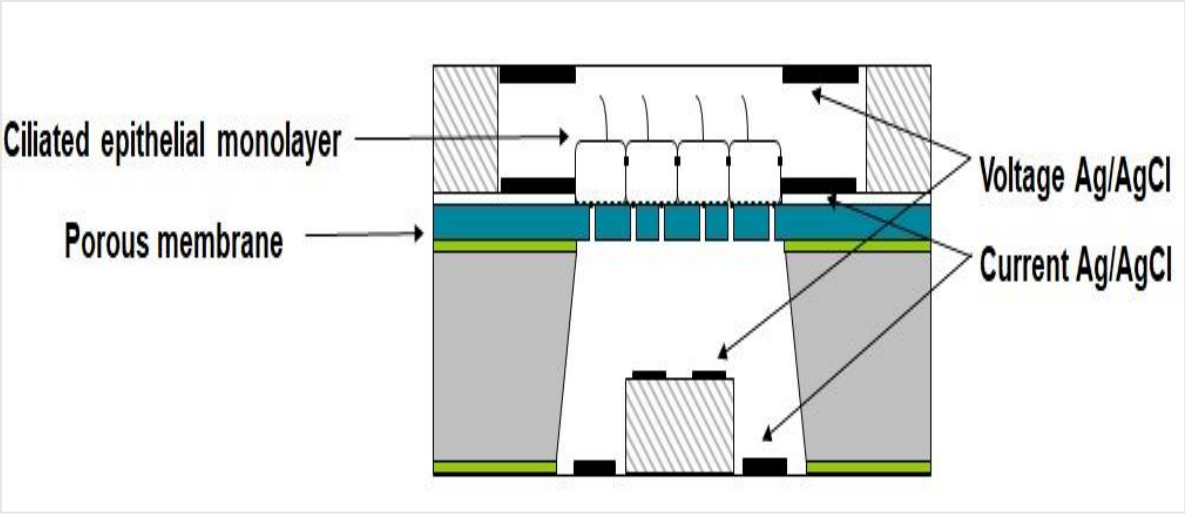

Figure: 16: Electrophysiological Endohm chamber was used in the measurement of transepithelial transport (Image credit: Dr. Andrew Resnick). Ciliated epithelial monolayers were grown and differentiated onto permeable membrane and these monolayers were transferred to Endohm chamber to obtain I_{eq} and TER values.

2.5 Western Blot

2.5.1 Cell Lysate Preparation

Whole cell lysates were prepared using RIPA 1X cell lysis buffer. The original stock of 10X RIPA buffer from Cell Signaling Technology (Product no. 9806) was first diluted in molecular biology grade protease-free water (Fisher Scientific, Product no. BP 2819) to prepare 1X buffer. The Halt Protease Inhibitor Cocktail from Thermo Scientific (Product no. 78430) was added at a final concentration of 1X. The RIPA buffer cell lysis protocol from Cell Signaling Technology was followed to prepare whole cell lysates (Nag and Resnick 2017). The protein levels of EPO, ZO1, and Na^+/K^+-ATPase α1 subunit were compared in the whole cell lysates.

Nuclear extracts were prepared using NE-PER Nuclear and Cytoplasmic Extraction Reagents from Thermo Scientific (Product no. 78833). The cells were treated with trypsin to detach and then centrifuged to form cellular pellets and the pellets were washed with

PBS buffer twice. For a confluent mCCD monolayer on a large cell culture insert (area= 4.71 cm^2) 56 µL Cytoplasmic Extraction Reagent I (CER I), 3 µL Cytoplasmic Extraction Reagent II (CER II), and 28 µL Nuclear Extraction Reagent (NER) were used. The Halt Protease Inhibitor Cocktail was added to the CER I and NER as instructed by the manufacturer. The protocol from Thermo Scientific was followed to separate cytoplasmic components to obtain nuclear extracts. During the cell lysate or nuclear extract preparation, samples were maintained on ice or at 4°C to minimize any possible protein degradation. The HIF-1α protein levels were compared in the nuclear extracts.

The protein concentration in each sample was determined using Bradford assay using Coomassie Plus Protein Assay Reagent from Thermo Scientific (Product No. 1856210). Before loading the samples in the wells of the polyacrylamide gels, sample buffer was added and samples were heated for 6 minutes at 95°C (Nag and Resnick 2017).

2.5.2 Sodium Dodecyl Sulfate (SDS) Polyacrylamide Gel Electrophoresis (SDS-PAGE)

Twelve percent acrylamide-bisacrylamide gels and 4% stacking gels were used. In each well of the gel, same amount (30 µg) of proteins were loaded. The samples were run in a 1X running buffer containing SDS, glycine, and Tris Base for 2.5 hours at 100 volts. The gels were put onto methanol preactivated polyvinylidene difluoride (PVDF) membranes. Using a wet transfer method, the transfer was performed for 2 hours at 100 volts in a cold transfer buffer containing 20% methanol. The membrane was blocked for 1-2 hours in 6% non-fat dry milk in 1X Tris-buffered Saline-Tween 20 (TBST) buffer at room temperature. The concentrations of primary and secondary antibodies were formulated in 6% non-fat dry milk in TBST. The following antibody concentrations were

used: mouse monoclonal beta-actin (Novus Biologicals# NB600-501) at a concentration of 1:10,000, mouse monoclonal HIF-1α (Santa Cruz Biotechnology# sc-13515) at a concentration of 1:200, mouse monoclonal EPO (Santa Cruz Biotechnology# sc-80995) at a concentration of 1:200, mouse monoclonal Glyceraldehyde 3-phosphate dehydrogenase (GAPDH) (Santa Cruz Biotechnology# sc-166545) at a concentration of 1:1000, rat monoclonal ZO1 (Developmental Studies Hybridoma Bank at University of Iowa# R26.4C) at a concentration of 1:100, mouse monoclonal Na^+/ K^+-ATPase α1 subunit (Developmental Studies Hybridoma Bank at University of Iowa# a6F) at concentration of 1:600. Secondary HRP-conjugated anti-mouse and anti-rat antibodies were used at a concentration of 1:2000. The membranes were kept in primary antibody at 4°C overnight on a shaker and after washing steps these membranes were incubated with secondary antibody for 2 hours at the room temperature on a shaker. After incubation in primary or secondary antibodies, the membranes were washed with 1X TBST buffer for every 10 minutes for a total of 40 minutes and during the washing steps the membranes were kept on the shaker. A chemiluminescence detection kit (Amersham ECL Prime Western Blotting Detection Reagent) from GE Healthcare (Catalog no. RPN 2232) was used. The luminol and peroxide solutions were mixed in a ratio of 1:1 and the mixture was evenly spread onto the membrane. The membranes were read using an Odyssey FC Imaging System from LI-COR Biosciences using Image Studio Software version 2.1. The following membrane exposure times were found to be optimum to detect different proteins: membranes probed for ZO1 and Na^+/ K^+-ATPase α1 subunit with 5 minutes' exposure, the membranes probed for HIF-1α and EPO with 10 minutes' exposure, membranes probed

for beta-actin with 1-minute exposure, and membranes probed for GAPDH with 2 minutes' exposure.

To compare beta-actin levels in the membrane which was first analyzed for EPO levels, a stripping buffer, Restore Plus Western Blot Stripping Buffer from Thermo scientific (Product no. 46430), was used. Antibodies were stripped from the membrane for 10 minutes, followed by washing with 1X TBS and 1X TBST buffers, and the membrane was blocked again before the addition of the primary antibody, i.e. monoclonal beta-actin antibody. As described above, the membrane was treated in the same way with a secondary antibody and the detection reagents to find beta-actin protein levels (Nag and Resnick 2017).

2.5.3 Densiometric Analysis

The LI-COR Image Studio Software was used to measure band intensities in order to perform densiometric analysis (Nag and Resnick 2017). In the same membrane, the ratio of the band intensity of protein of interest obtained from a sample and the band intensity of beta-actin or GAPDH of the same sample was first calculated for a control sample (i.e., the lysate prepared from cells without $CoCl_2$ treatment). Similarly, the ratio was calculated for a $CoCl_2$-treated sample. The fold increase or decrease of the treated sample ratio was calculated by dividing the treated sample ratio with the control sample ratio. The control sample ratio after dividing by the same sample ratio is assigned a value of 1, and the results as folds of increase or decrease of treated samples as compared to the control samples are shown. Average values of densitometric fold changes with standard errors for 3-6 replicates are presented.

2.6 Cellular Metabolic Activity Assay

The yellow colored tetrazolium salt, 3-(4,5-dimethythiazol2-yl)-2,5-diphenyl tetrazolium bromide (MTT), is known to be reduced by the mitochondrial succinate dehydrogenase enzyme of viable cells to produce purple colored formazan crystals (Mosmann 1983). A Cell Titer 96 Non-Radioactive Cell Proliferation Assay (MTT) G4000 (Promega) kit was used to check if cellular metabolic activity was affected by the addition of $CoCl_2$. In brief, BLDM was removed and APDM was replaced with 150 µl of fresh APDM to which 20 µl of MTT dye solution was added and the culture was incubated for four hours. Next, 150 µl of MTT solubilization/stop (acidic isopropanol) solution was added to the apical compartment and the culture was incubated for an additional 4 hours. Vigorously pipetted formazan crystals, formed by viable cells, were dissolved into the solution, and 200 µl of the homogenized solution was then transferred into a 96-well plate. Sample absorbance values were detected at 570 nm using an absorbance plate reader (Perker Elmer Life Sciences/ Wallac Victor Multilabel Counter and Wallac 1420 Manager Software). The average absorbance of 4 replicates are shown in the graph. Using trypan blue dye and a hemocytometer, cell enumeration was performed and a calibration graph was generated from cell seeding densities and absorbance values (Nag and Resnick 2017). MTT assay compares cellular metabolic activities and can be an indirect indicator of cellular viability (Jover, Ponsoda et al. 1994).

2.7 Statistical Analysis

Microsoft Excel 2016 was used to calculate values of mean or average and standard deviation. Standard error of mean (SEM) was calculated from standard deviation (σ) as $SEM = \frac{\sigma}{\sqrt{n}}$ where, n = number of replicates. Values of SEM are shown in all the graphs.

A type three (i.e., two-sample unequal variance and heteroscedastic) and a two-tailed Student's t-test was performed using Microsoft Excel to compare level of any significant difference between two groups, and IBM-SPSS software was used to perform a One-way ANOVA with post-hoc Tukey to compare among more than two groups (Nag and Resnick 2017). The Pearson's linear correlation analysis was also carried out using the SPSS software.

CHAPTER

III. RESULTS & DISCUSSION

3.1 Results

3.1.1 $CoCl_2$ Stabilizes HIF1α in the Nucleus of Renal Epithelial Cells

Western blots were performed to show that the addition of 100 μmol/L $CoCl_2$ to our culture media increased nuclear HIF-1α in mCCD cells (Figures 17A & 17B) and MDCK cells (Figures 18A and 18B). Nuclear stabilization of HIF1α was found to cause a slight increase of HIF-1α effector molecule EPO levels in the whole cell extracts prepared from mCCD cells (Figures 19A and 19B) (Nag and Resnick 2018) and MDCK cells (Figures 20A and 20B). These findings are in agreement with previous studies (FISHER and Langston 1967; Fandrey, Frede et al. 1997; Verghese, Zhuang et al. 2011). According to densiometric analysis we found a significant increase in HIF-1α in the nuclear extracts of both mCCD and MDCK cells (Figures 17B and 18B). However, the slight increase of EPO levels was not statistically significant in mCCD or MDCK cells (Figures 19B and 20B). We did not notice any effect of fluid flow on EPO levels of mCCD cells along with $CoCl_2$ (Figures 19A and 19B)

GAPDH gene has a HRE and its level can be elevated by nuclear stabilization of HIF-1α (Graven, Yu et al. 1999; Lu, Gu et al. 2002). The beta-actin mRNA level was found to be elevated by hypoxia (Zhong and Simons 1999). Thus, increased level of HIF1α by $CoCl_2$ may increase the protein levels of our loading controls: GAPDH and beta-actin, and the densitometric analysis of our western blots may underestimate the effect of the application of 100 µmol/L $CoCl_2$ on HIF1α and EPO protein levels to some extent.

3.1.1.1 $CoCl_2$ Stabilizes HIF-1α in the Nucleus of mCCD Cells

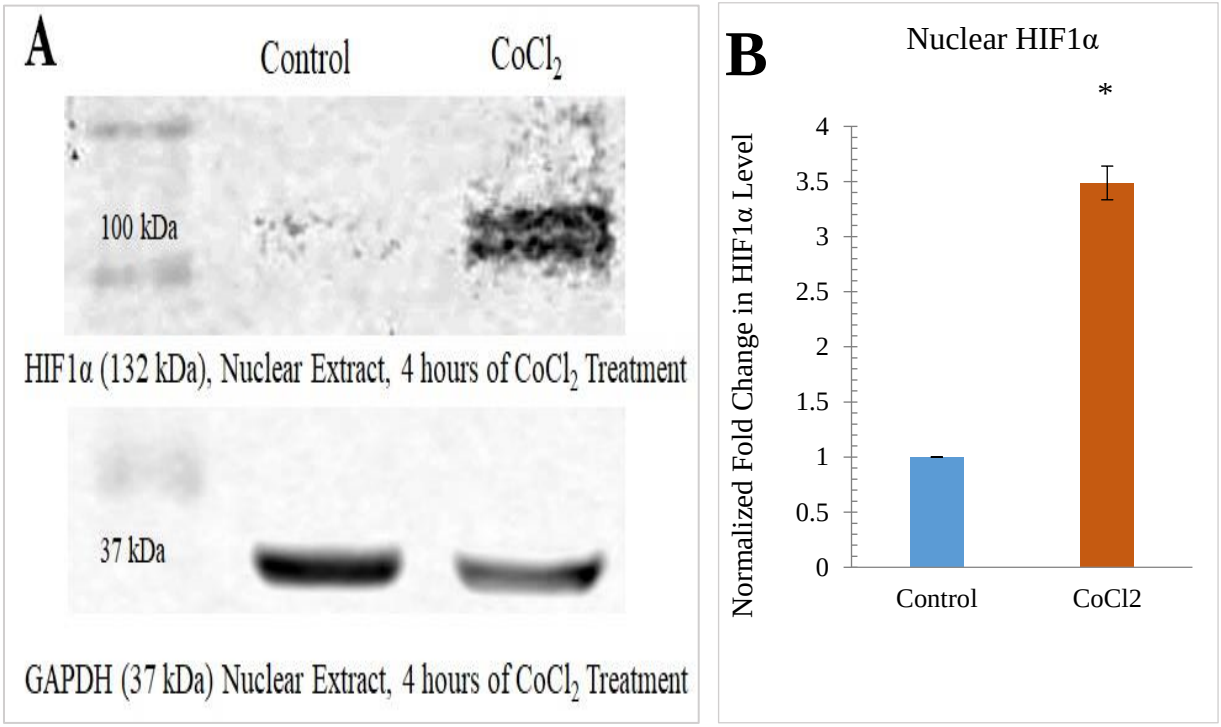

Figure 17: HIF-1α was stabilized in the nucleus of mCCD cells by 100 µmol/ L $CoCl_2$. (A) Shows the western blots for HIF1α and GAPDH (loading control) in the nuclear extracts prepared from cells treated with $CoCl_2$ or without $CoCl_2$ (Control) for 4 hours. (B) Shows the densiometric analysis of the HIF-1α bands, Student's t-test, P= 0.004, N= 3.

3.1.1.2 $CoCl_2$ Stabilizes HIF-1α in the Nucleus of MDCK Cells

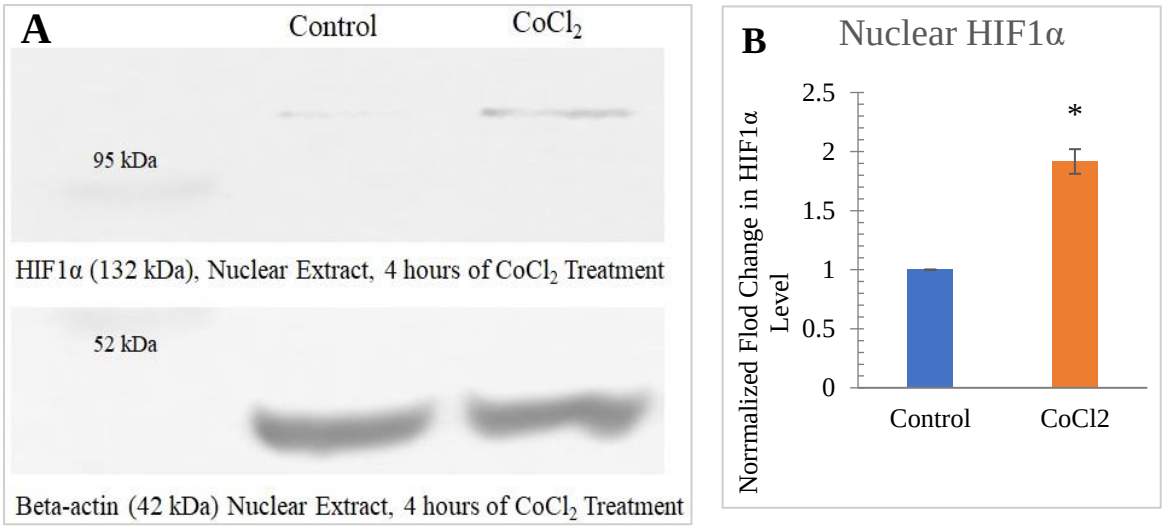

Figure 18: HIF-1α was stabilized in the nucleus of MDCK cells by 100 µmol/ L $CoCl_2$. (A) Shows the western blots for HIF-1α and beta-actin (loading control) in the nuclear extracts prepared from cells treated with $CoCl_2$ or without $CoCl_2$ (Control) for 4 hours. (B) Shows the densiometric analysis of the HIF1α bands, Student's t-test, P = 0.01, N= 3.

3.1.1.3 $CoCl_2$ Slightly Increases EPO Production in mCCD Cells

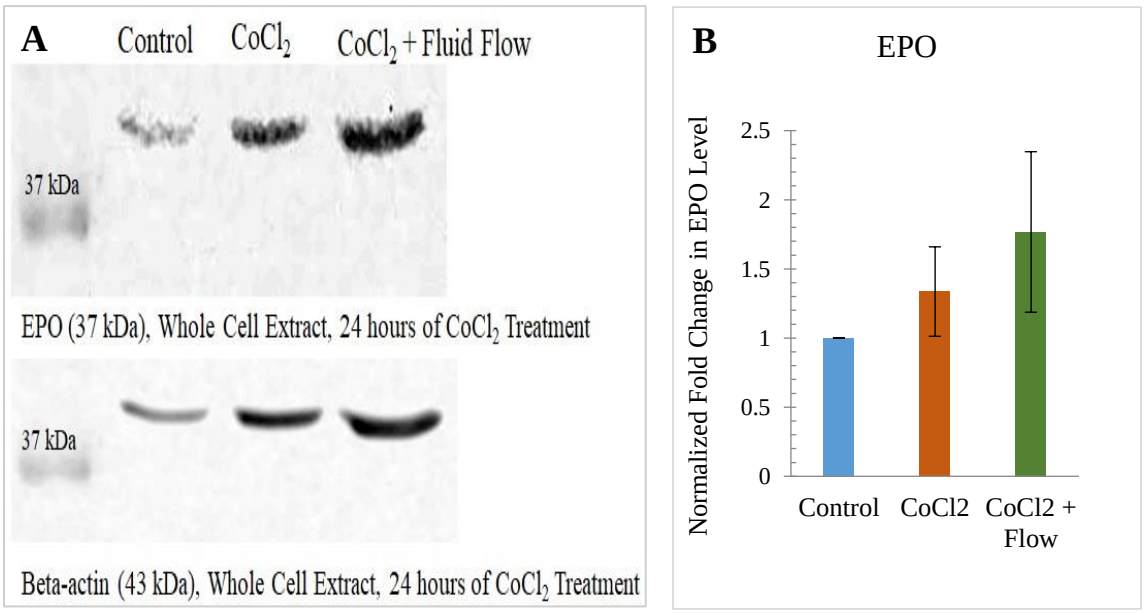

Figure 19: EPO protein level was slightly increased in mCCD cells by 100 µmol/ L $CoCl_2$. (A) Shows the western blots for EPO and beta-actin (loading control) in the whole cell extracts prepared from cells treated without $CoCl_2$ (Control), with $CoCl_2$, and $CoCl_2$ with fluid flow for 24 hours. (B) Shows the densiometric analysis of the EPO bands, One-way ANOVA, P > 0.05, N= 3.

3.1.1.4 CoCl2 Slightly Increases EPO Production in MDCK Cells

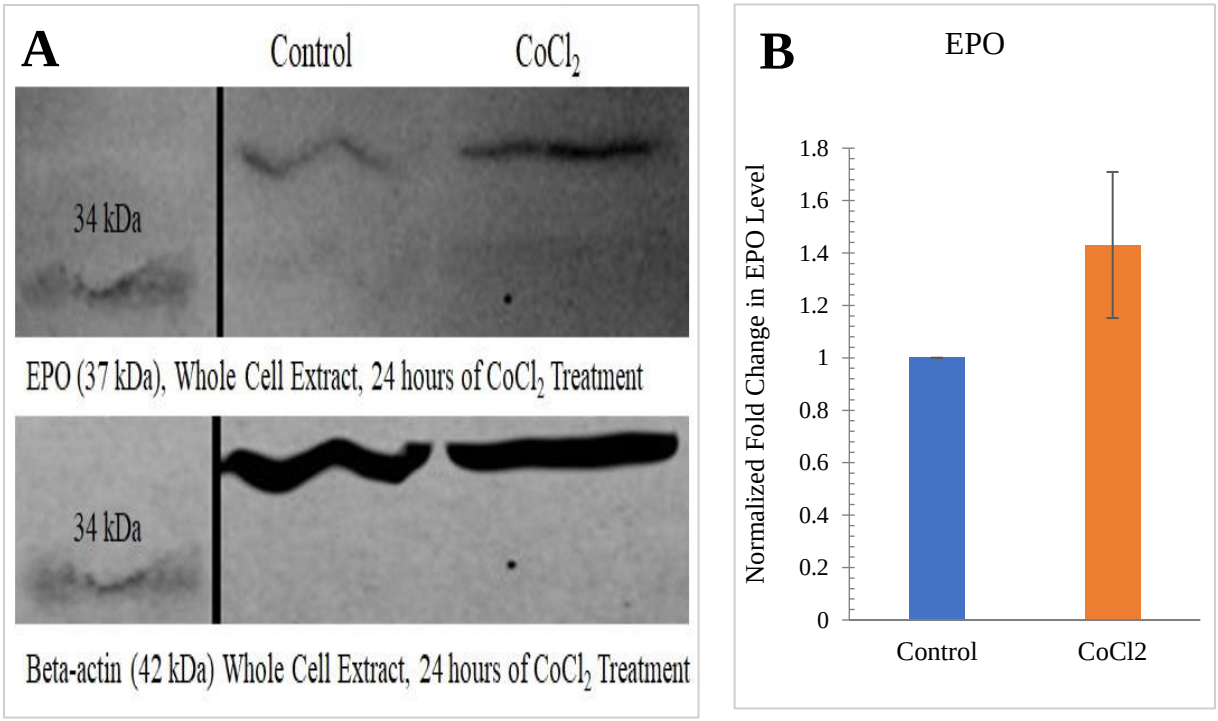

Figure 20: EPO protein level was slightly increased in MDCK cells by 100 µmol/ L $CoCl_2$. (A) Shows the western blots for EPO and beta-actin (loading control) in the whole cell extracts prepared from cells treated without $CoCl_2$ (Control), with $CoCl_2$, and $CoCl_2$ with fluid flow for 24 hours. The lanes between the ladder and the bands are spliced out (following American Journal of Physiology Guidelines) to show the bands or samples of interest. (B) shows the densiometric analysis of the EPO bands, Student's t-test, $P > 0.05$, N= 3.

3.1.2 Cellular Metabolic Activity: MTT Assay

3.1.2.1 MTT Calibration Graphs

Cells were seeded onto cell culture inserts with an area of 1.13 cm^2 at different mCCD cell seeding densities ranging from 10^4 to 7×10^5 cells per insert. MTT assay was performed in mCCD cells in growth condition (figure 21A) and in mCCD cells in fully differentiated condition (figure 21B). The calibration graphs showed that MTT absorbance values increase with initial cell seeding density. A logarithmic trend line was used to fit the scatter plot of cell seeding density versus MTT absorbance values. Our calibration graphs

show that we can detect changes in cellular metabolic activities and we may detect cellular cytotoxicity due to the addition of $CoCl_2$.

These mCCD cells express thermolabile the simian virus 40 (SV40) large tumor (T) antigen (TAg) under the control of major histocompatibility complex H-2Kb promoter, which is induced by interferon γ (IFN γ). In the permissive temperature of 33 °C and in a growth medium containing of IFN γ, cells continuously proliferate. Under non-permissive temperature around 39°C and in a differentiation medium without IFN γ, mCCD cells stop proliferating and start to differentiate (Jat, Noble et al. 1991; Whitehead, VanEeden et al. 1993; Resnick and Hopfer 2007). At high cell seeding densities, we do not notice any difference of MTT absorbance values, most likely due to the equal level of cellular confluence achieved by high cell seeding densities.

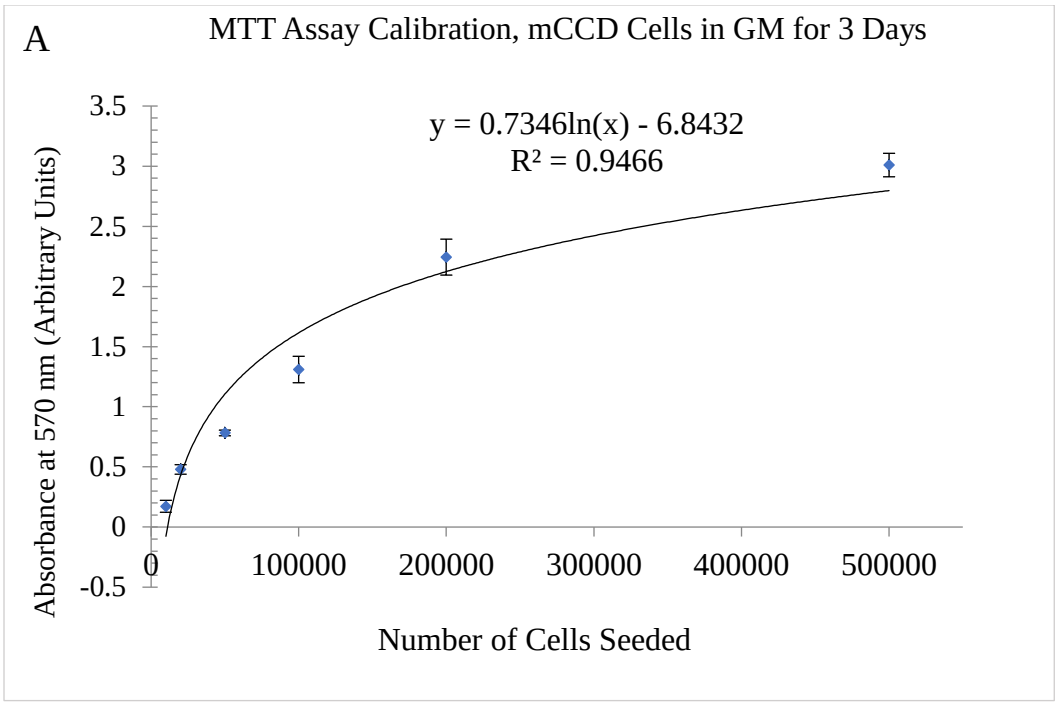

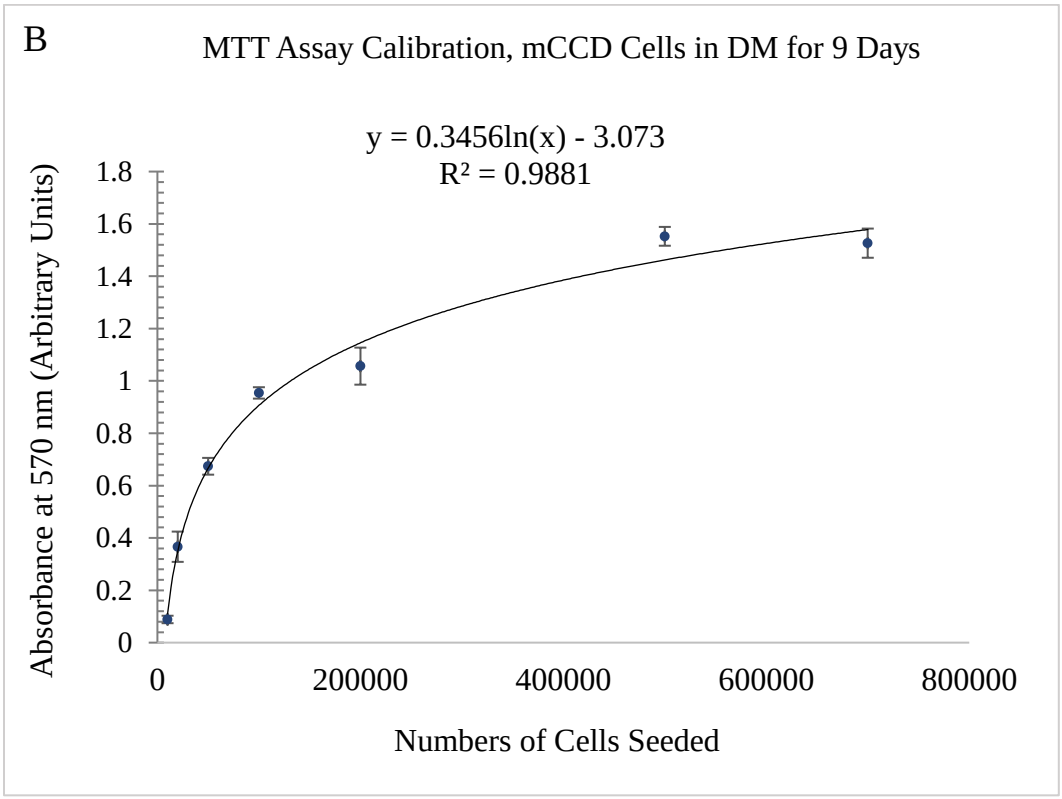

Figure 21: Cell seeding number versus MTT absorbance calibrations, N= 3-4. (A) Shows mCCD cells with specific cell seeding numbers after 3 days in growth media (GM) (B) Shows mCCD cells with specific cell seeding numbers in 3 days in growth media and 9 days in differentiation media (DM).

3.1.2.2 Effect of 100 µmol/L of $CoCl_2$ on Cellular Metabolic Activity

An MTT assay determines cellular metabolic activity and can indirectly reflect the number of viable cells present (Mosmann 1983; van Meerloo, Kaspers et al. 2011). MTT absorbance values showed that there were no significant differences between control and $CoCl_2$ treatment groups both in the presence or absence of fluid flow after 3 days (figure 22A). MTT results indicate that the addition of 100 µmol/L $CoCl_2$ to our culture media did not have any effect on cellular metabolic activities and can indicate equivalent cellular viability (Nag and Resnick 2018) or no significant cytotoxic effect up to 4 days of treatment (figures 22A and 22B). After 9 days of $CoCl_2$ treatment, cellular metabolic activity was found to decrease and indicated decrease in cellular viability or cytotoxic effects (figure 22C). It is to be emphasized that all our epithelial transport analyses were performed within 3 days of $CoCl_2$ treatment and the cytotoxic effect of 9 days of $CoCl_2$ treatment is not applicable to our study.

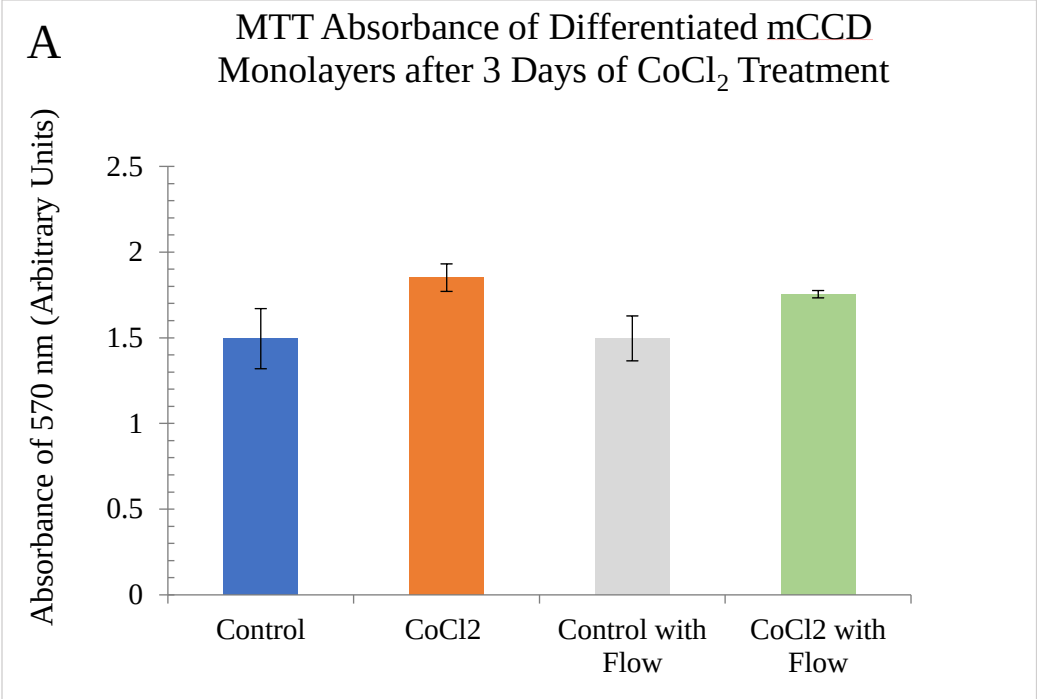

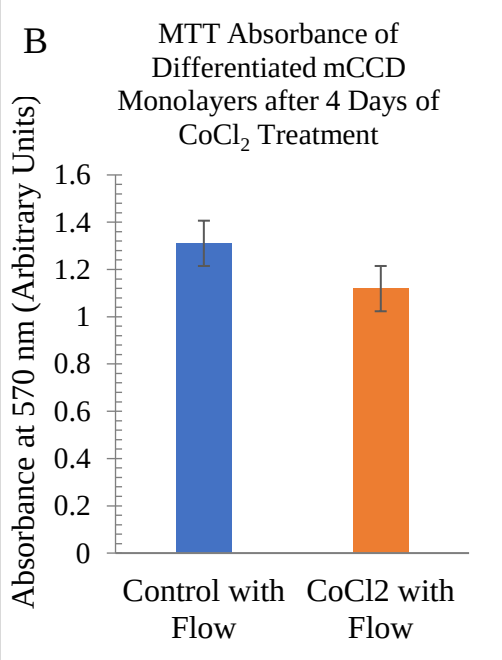

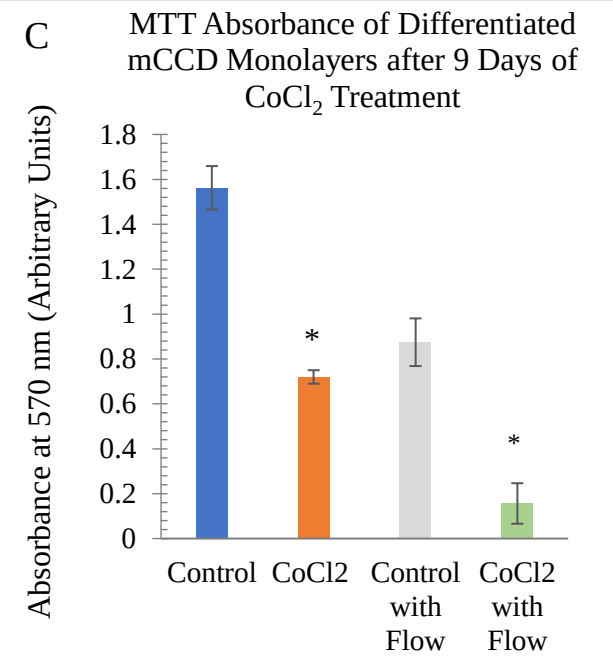

Figure 22: Effect of $CoCl_2$ on cellular metabolic activity of mCCD cells. (A) and (B) show that MTT absorbance values do not significantly change with the addition of 100 µmol/L $CoCl_2$ up to 3-4 days, indicating cell viability may have remained unchanged during 4 days of treatment, either in the presence or absence of fluid flow, One-way ANOVA, $P > 0.05$, N= 3-5. (C) Shows that the treatment of cells with 100 µmol/L $CoCl_2$ for 9 days causes significant decrease in the MTT absorbance i.e., cellular metabolic activity. One-way ANOVA, $P < 0.0001$, N= 3-4.

3.1.3 FITC-dextran Permeability

3.1.3.1 Calibration Graphs and Permeability Calculation

Figures 23 and 24 show calibration graphs of fluorescence intensities versus different concentrations of 3 kDa and 70 kDa FITC-dextran molecules. As shown in figure 23, fitting a power-law curve to the 3 kDa FITC-dextran data obtains the equation $y = 5.67*10^4 x^{0.767}$. Similarly, 70 kDa FITC-dextran data yields a power law fit $y = 6.13*10^5 x^{0.813}$ as shown in figure 24. Power law curve fitting was chosen because at low concentrations, the proportional change of fluorescence intensity is related to the proportional change of FITC concentration (Ohannesian and Streeter 2001).

To calculate permeability value for each sample, a graph was generated for that sample by plotting ln [1- (C_t- C_0)] versus time t in seconds as shown in figure 25. Here, C_t represents FITC-dextran concentration at time t (0- 4200) seconds for measurements obtained at intervals of every 600 seconds. C_0 is the initial concentration in the apical side. The concentration (C_0 and C_t) values of 3 kDa FITC-dextran were obtained from the equation of figure 23. The permeability value was calculated for a specific sample using the specific graph. For example, as shown in figure 25, permeability value was calculated from slope of the linear trend line. The slope of the line is 4×10^{-7} sec^{-1} and dividing this slope by the constant B = 12.43 cm^{-1}, we can calculate the permeability value for this specific sample. Thus, we obtain a 3 kDa FITC-dextran permeability value of 3.22×10^{-8} cm/sec.

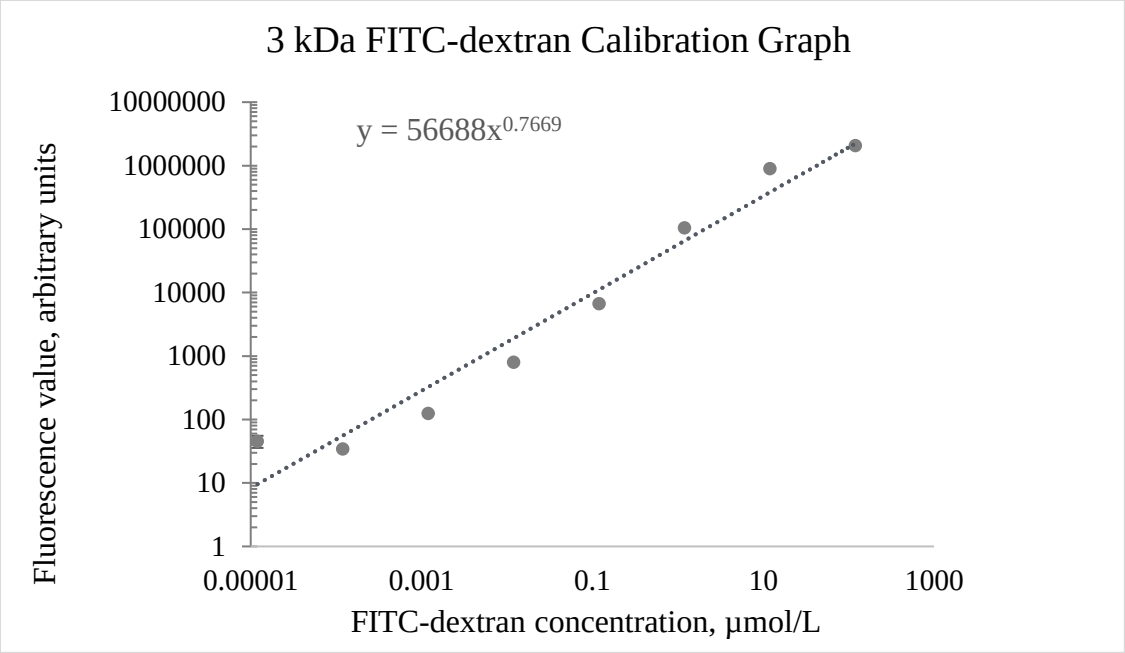

Figure 23: Concentration vs florescence intensity calibration graph of FITC-dextran, 3 kDa (N= 4). Using the equation of this graph, we can determine FITC-dextran (3 kDa) concentration from a fluorescence intensity value.

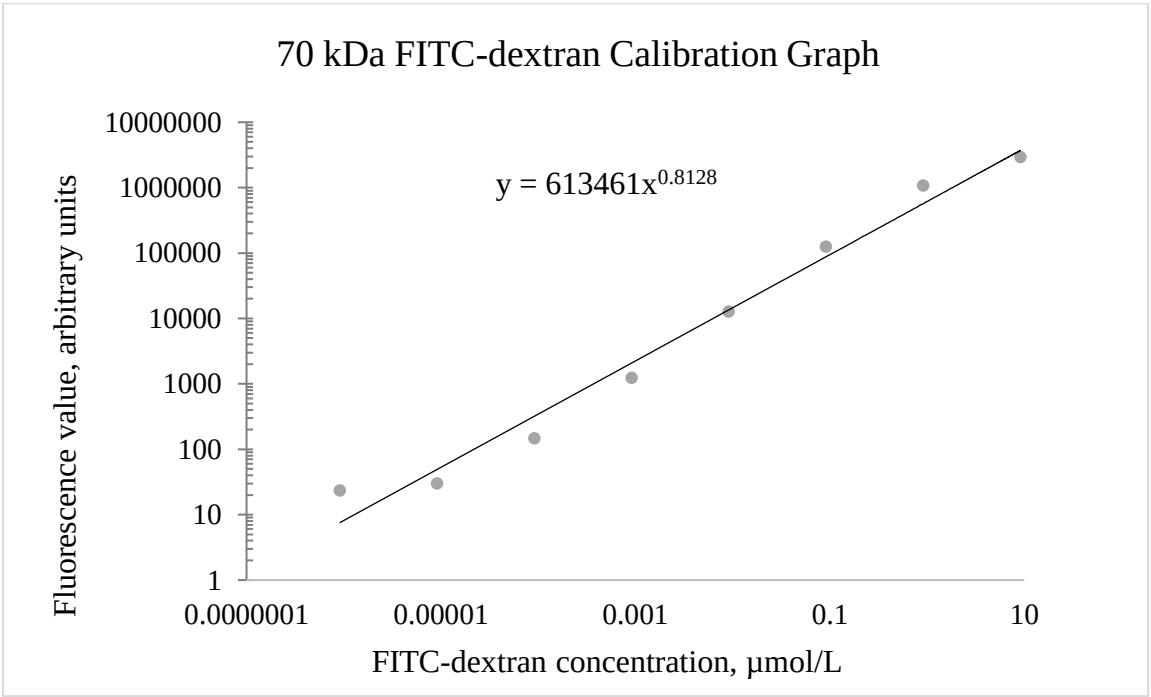

Figure 24: Concentration vs florescence intensity calibration graph of FITC-dextran, 70 kDa (N= 4). Using the equation of this graph, we can determine FITC-dextran (70 kDa) concentration from a fluorescence intensity value.

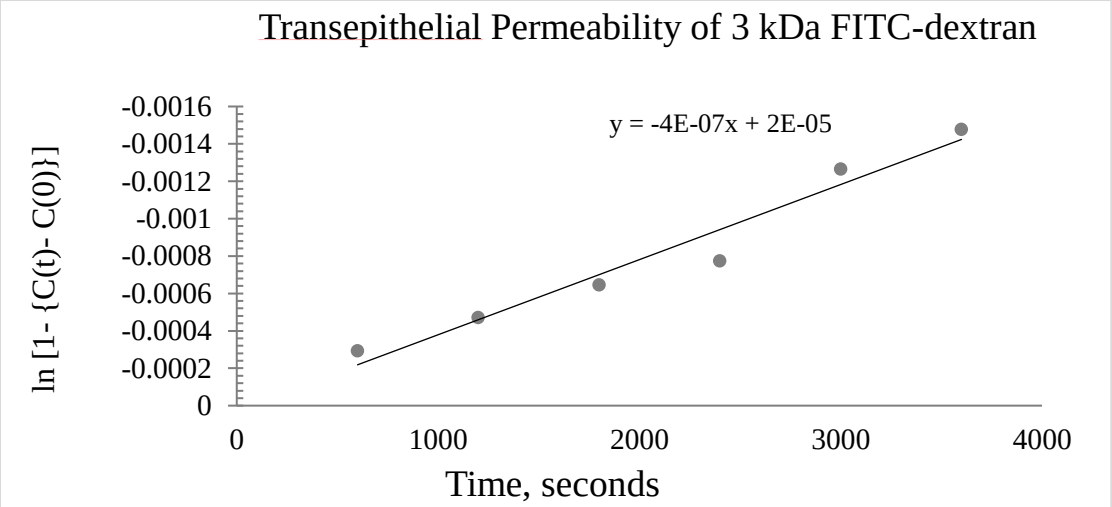

Figure 25: 3 kDa FITC-dextran transepithelial permeability acquired from fluorescence intensity measurements. Slope= 4×10^{-7} sec^{-1}, corresponding to Permeability = 3.22×10^{-8} cm/sec.

3.1.3.2 FITC-dextran Permeability in mCCD and MDCK Epithelial Monolayers

Using the approach shown in figure 25, the permeability of a cell-free collagen-coated cell culture insert was found to be $(1.21 \pm 0.46) \times 10^{-5}$ cm/s (3 kDa) and $(1.01 \pm 0.40) \times 10^{-6}$ cm/s (70 kDa) as shown in figure 26.

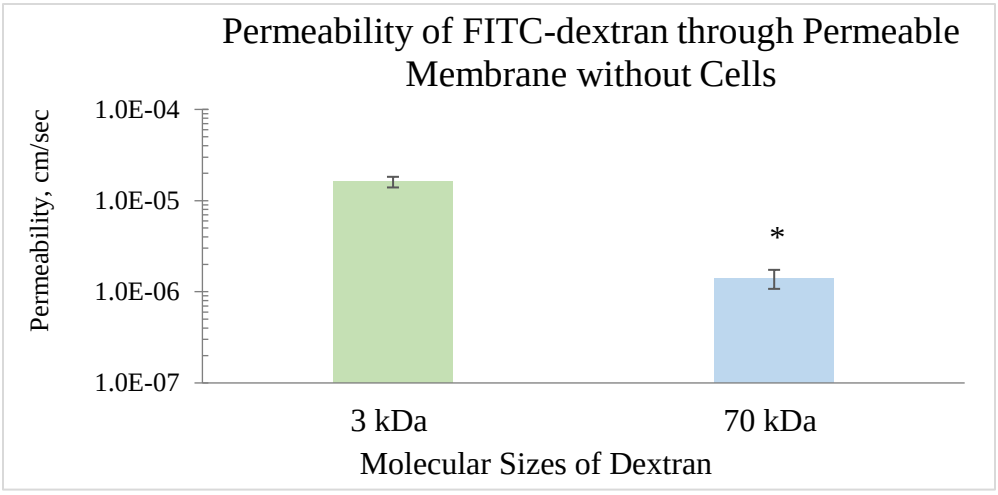

Figure 26: Permeability of FITC-dextran through empty cell culture inserts without cells, Student's t-test, $P < 0.0001$, N= 8.

As mCCD epithelial cells differentiate, they undergo ciliogenesis, and the cells start to form tight junctions and gain functional properties, such as directed transport of salt and water. Figure 27 presents the data on transepithelial permeability of mCCD monolayers during this differentiation phase. As per our expectation, 3 kDa FITC-dextran permeability at day 1 (i.e., 24 hours after the onset of differentiation) was found to be significantly higher (8 times) as compared to a fully differentiated mCCD monolayer after 10 days of differentiation as shown in figure 27A. This finding provides some evidence that the principal path of 3 kDa FITC-dextran diffusion in mCCD monolayers is through paracellular pathway, as tight junctions may form early during the differentiation process (Koizumi, Kojima et al. 2007). By contrast, the permeability of 70 kDa FITC-Dextran showed no changes during differentiation (Figure 27B) (Nag and Resnick 2017).

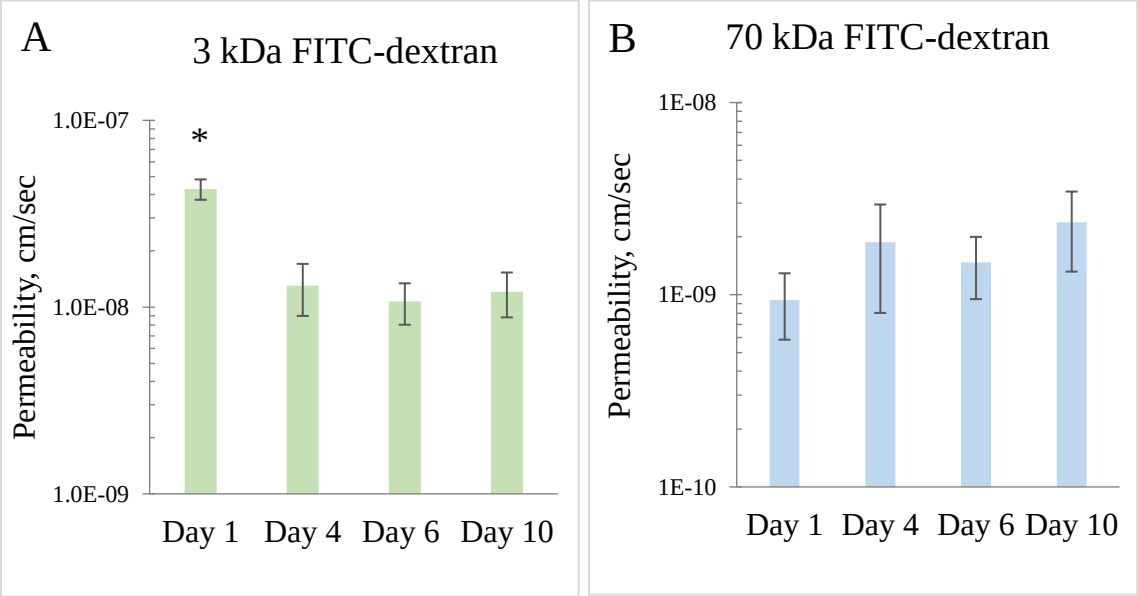

Figure 27: Transepithelial permeability of FITC-dextran molecules in mCCD monolayers under differentiation. (A) Shows that 3 kDa FITC-dextran transepithelial permeability at the onset of differentiation (day 1) is significantly higher as compared to fully differentiated mCCD monolayers (day 10), One-way ANOVA, $P < 0.05$, N=3-6. (B) Shows that the permeability of 70 kDa FITC-dextran does not change significantly during differentiation, One-way ANOVA, $P > 0.05$, N= 3-6.

Fully differentiated mCCD monolayers showed 3 kDa FITC-dextran permeability of (5.36 ± 1.67) × 10^{-9} cm/s and 70 kDa FITC-dextran permeability of (1.56 ± 0.89) × 10^{-9} cm/s as shown in figure 28. Permeability values of 3 kDa and 70 kDa FITC-dextran molecules in the differentiated mCCD monolayers are significantly decreased when compared to the cell-free insert (figures 26 and 28), demonstrating the importance of cellular tight junctions in regulating the transport through paracellular pathways (Nag and Resnick 2017). The monolayer permeability values of differentiated mCCD cells remained stable.

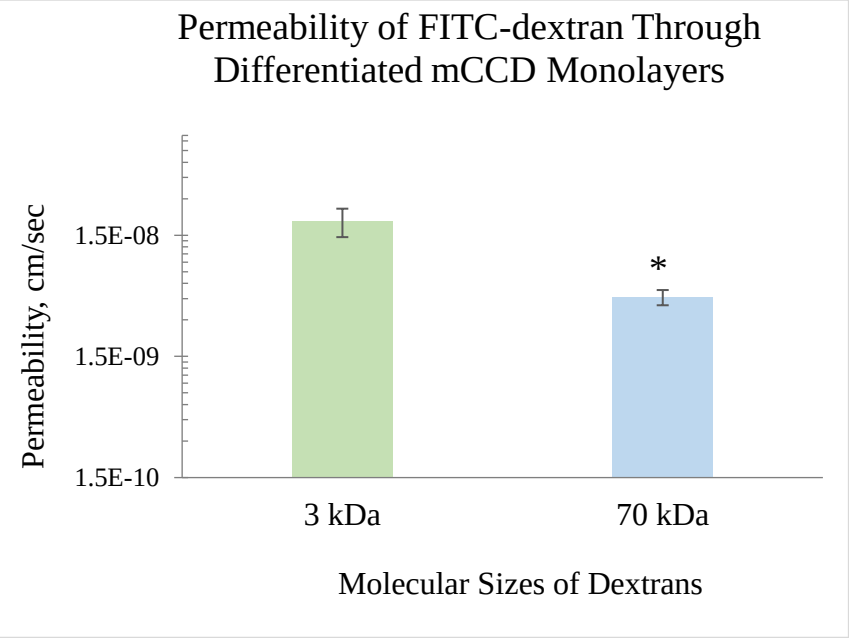

Figure 28: Transepithelial permeability of fully differentiated mCCD monolayers, Student's t-test, $p < 0.02$, N= 8.

As shown in figure 29, once cells are fully differentiated, MDCK monolayers showed 3 kDa permeability of (2.64 ± 1.11) × 10^{-8} cm/s and 70 kDa permeability of (5.75 ± 2.15) × 10^{-10} cm/s and these monolayer permeability values of MDCK cells remained stable.

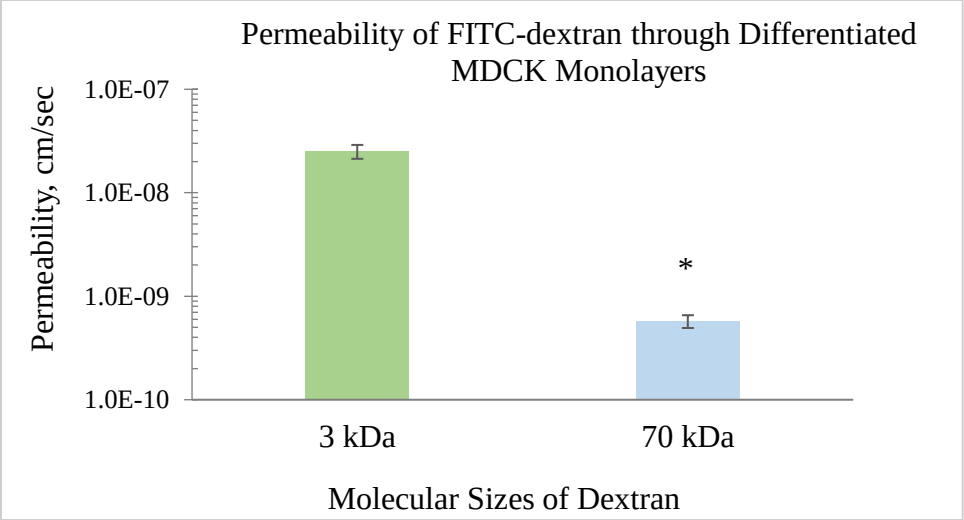

Figure 29: Transepithelial permeability of fully differentiated MDCK monolayers, Student's t-test, $P < 0.001$, N= 7-8.

3.1.3.3 HIF-stabilization by CoCl2 Increases Transepithelial Permeability

We studied the effect of HIF-stabilization by $CoCl_2$ on monolayer permeability. $CoCl_2$ was found to alter the transepithelial permeability of FITC-dextran molecules through fully differentiated mCCD monolayers. An addition of 100 µmol/L of $CoCl_2$ for 48 hours increased 3 kDa FITC-dextran permeability to $(4.02 \pm 3.15) \times 10^{-7}$ cm/s and the addition of 100 µmol/L $CoCl_2$ for 72 hours increased the transepithelial permeability further to $(9.05 \pm 8.13) \times 10^{-7}$ cm/s as shown in figure 30A. The treatment of $CoCl_2$ increased the transepithelial permeability of 70 kDa FITC-dextran to $(1.99 \pm 2.13) \times 10^{-8}$ cm/s at 48 hours and $(7.24 \pm 6.47) \times 10^{-8}$ cm/s at 72 hours as shown in figure 30B. The treatment with $CoCl_2$ increased 3 kDa FITC-dextran permeability more than 100-fold and 70 kDa FITC-dextran nearly 40-fold after 72 hours. Thus, HIF-stabilization by $CoCl_2$ significantly affected permeability of 3 kDa and 70 kDa FITC-dextran molecules in differentiated mCCD monolayers (Nag and Resnick 2017).

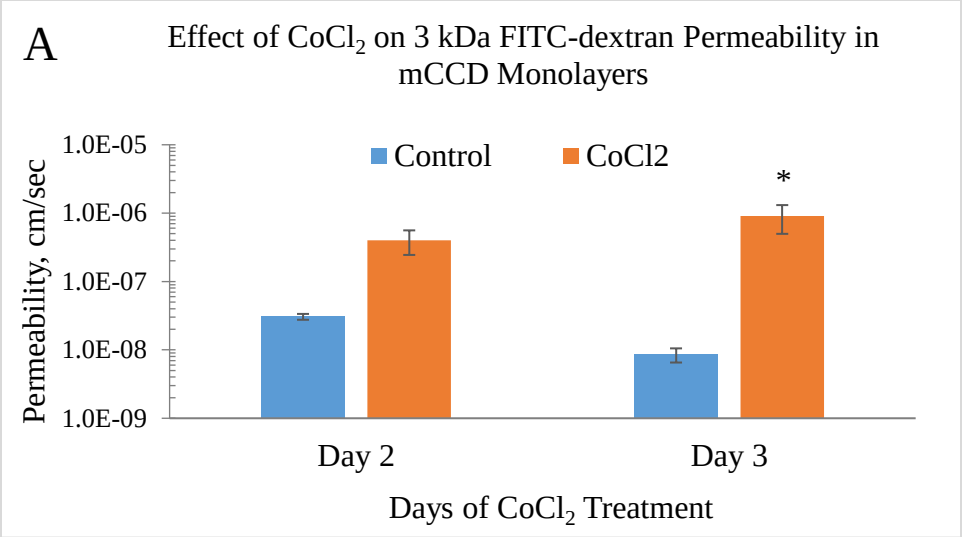

Figure 30 A: Effect of $CoCl_2$ on permeability of 3 kDa FITC-dextran in differentiated mCCD monolayers. $CoCl_2$ was added on day 0. Data shows that $CoCl_2$ treatment for 48 hours (Day 2) and 72 hours (Day 3) increased the permeability of differentiated mCCD monolayers. $CoCl_2$ treatment significantly (One-way ANOVA, P = 0.02, N= 4-5) increased monolayer permeability on day 3. No statistically significant difference was found between control groups.

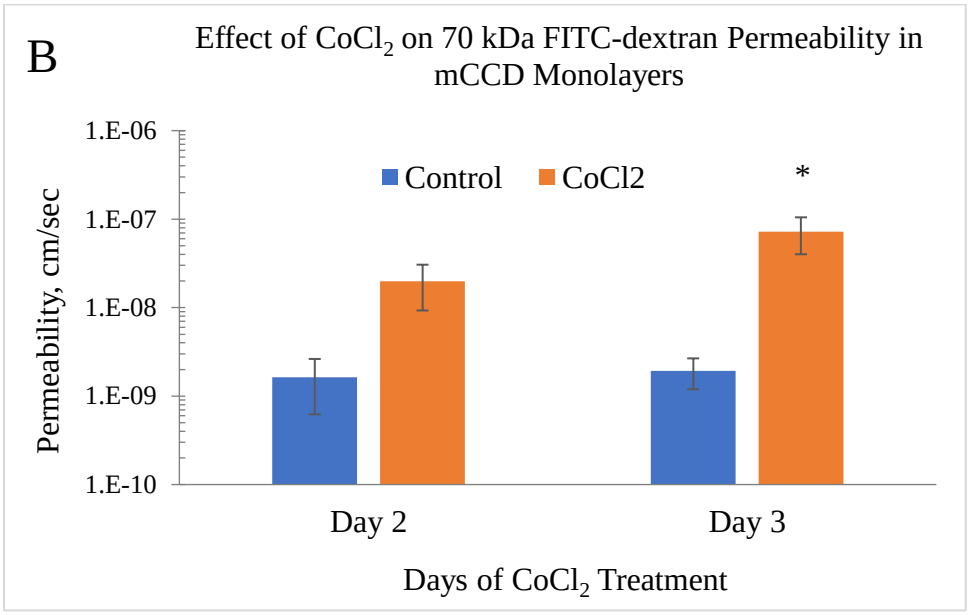

Figure 30 B: Effect of $CoCl_2$ on permeability of 70 kDa FITC-dextran in differentiated mCCD monolayers. $CoCl_2$ was added on day 0. Data shows that $CoCl_2$ treatment for 48 hours (Day 2) and 72 hours (Day 3) increased the permeability of differentiated mCCD monolayers. $CoCl_2$ treatment significantly (One-way ANOVA, P = 0.02, N= 4-5) increased monolayer permeability on day 3. No statistically significant difference was found between control groups.

Similarly, we investigated the effect of HIF-stabilization by 100 µmol/L $CoCl_2$ in MDCK monolayers. Figure 31A shows 3 kDa FITC-dextran permeability increased for MDCK monolayers: $(3.65 \pm 0.96) \times 10^{-8}$ cm/sec after 48 hours of incubation and $(3.62 \pm 0.46) \times 10^{-8}$ cm/sec after 72 hours of incubation. Treatment with $CoCl_2$ for 72 hours significantly increased 70 kDa FITC-dextran permeability as well, to $(1.61 \pm 0.0) \times 10^{-9}$ cm/sec as shown in figure 31B. The treatment with $CoCl_2$ increased the permeability of 3 kDa and 70 kDa dextran molecules in MDCK monolayers around 2-3 folds. The effect of HIF-stabilization by $CoCl_2$ on the transepithelial permeability of MDCK monolayer was statistically significant, but the fold changes were much less in MDCK monolayers as compared to mCCD monolayers.

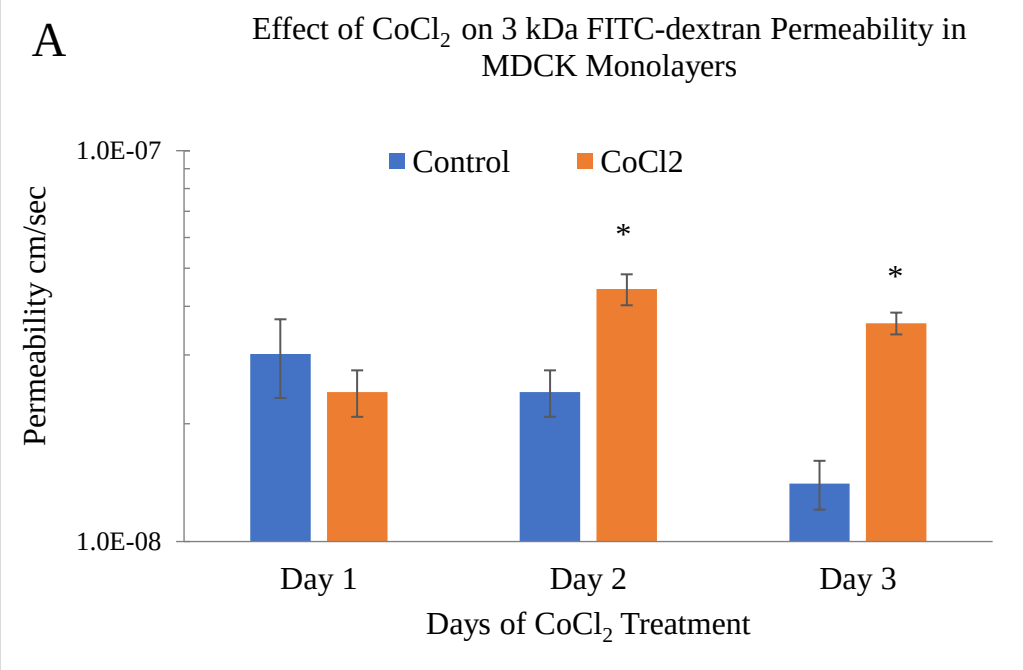

Figure 31 A: Effect of $CoCl_2$ on permeability of 3 kDa FITC-dextran in differentiated MDCK monolayers. $CoCl_2$ was added on day 0. Data shows that $CoCl_2$ treatment for 48 hours (Day 2) and 72 hours (Day 3) significantly (One-way ANOVA, $P < 0.0001$, N= 4-12) increased the permeability of differentiated MDCK monolayers. No statistically significant differences were found among control groups.

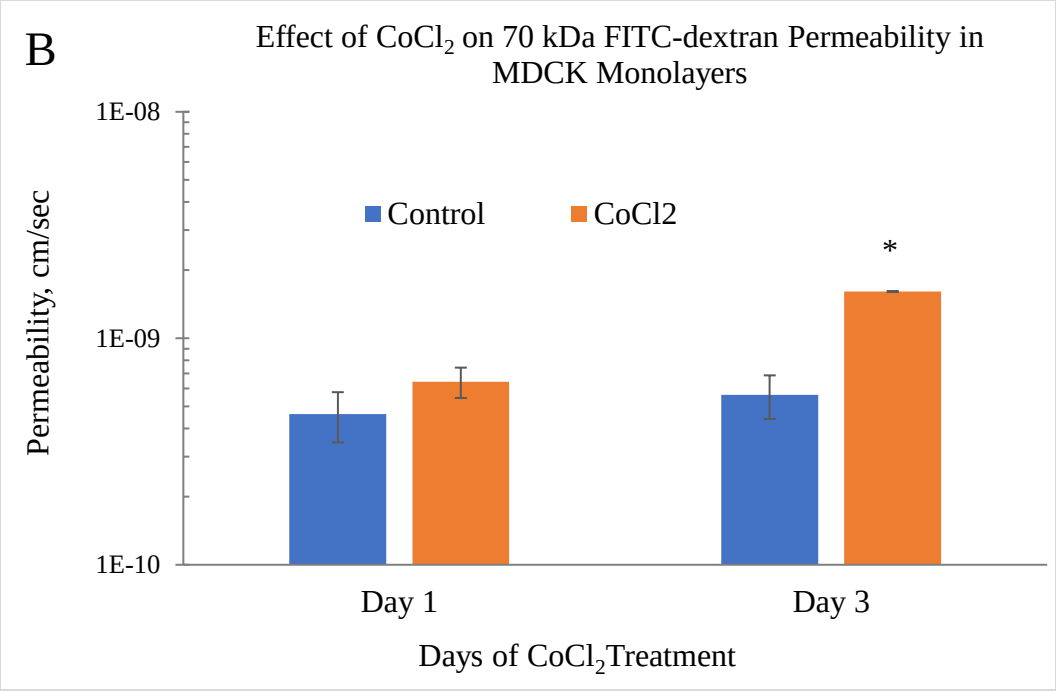

Figure 31 B: Effect of $CoCl_2$ on permeability of 70 kDa FITC-dextran in differentiated MDCK monolayers. $CoCl_2$ added on day 0. Data shows that $CoCl_2$ treatment for 72 hours (Day 3) significantly (One-way ANOVA, $P < 0.025$, N= 3-4) increased the permeability of differentiated MDCK monolayers. No statistically significant difference was found between control groups.

The table below summarizes our permeability measurements:

Table III: Summary of 3 kDa and 70 kDa FITC-dextran permeability values.

	3 kDa, P (cm/sec)	**70 kDa, P (cm/sec)**
Cell-free insert	$(1.61 \pm 0.61) \times 10^{-5}$	$(1.41 \pm 0.94) \times 10^{-6}$
mCCD w/o $CoCl_2$ (control)	$(8.53 \pm 4.46) \times 10^{-9}$	$(1.93 \pm 1.65) \times 10^{-9}$
mCCD w/ 48h $CoCl_2$	$(4.02 \pm 3.15) \times 10^{-7}$	$(1.99 \pm 2.13) \times 10^{-8}$
mCCD w/ 72h $CoCl_2$	$(9.05 \pm 8.13) \times 10^{-7}$	$(7.24 \pm 6.47) \times 10^{-8}$
MDCK w/o $CoCl_2$ (control)	$(1.41 \pm 0.40) \times 10^{-8}$	$(5.63 \pm 0.21) \times 10^{-10}$
MDCK w/ 48h $CoCl_2$	$(3.65 \pm 0.96) \times 10^{-8}$	Did not measure
MDCK w/ 72h $CoCl_2$	$(3.62 \pm 0.46) \times 10^{-8}$	$(1.61 \pm 0.0) \times 10^{-9}$

3.1.3.4 Effect of HIF-1α Inhibitor Along with $CoCl_2$

A preliminary experiment was performed in MDCK monolayers to see if an inhibitor of HIF-1α can affect the cellular permeability along with $CoCl_2$. In this experiment, an HIF-1α inhibitor was applied at a concentration 30 µmol/L as suggested by the supplier (Santa Cruz Biotechnology). We would like to emphasize that the HIF-1α inhibitor was not sequentially added; rather the inhibitor was added at the same time when $CoCl_2$ was added. The HIF-1α inhibitor alone did not show any significant effect in altering 3 kDa and 70 kDa FITC-dextran permeability on day 3 as shown in figures 32A and 32B. HIF-1α is known to be degraded under normoxic conditions, and, therefore, an HIF-1α inhibitor under normoxia does not show any effects on transepithelial permeability as expected. However, we made an interesting observation that the permeability of 3 kDa FITC-dextran increased more than 40-fold when monolayers were incubated with $CoCl_2$ and HIF-1α inhibitor for 72 hours (figure 32A). The treatment with $CoCl_2$ alone was found to increase 3 kDa FITC-dextran permeability only around 3-fold. Therefore, it is tempting to speculate that the application of an HIF-1α inhibitor along with the stabilization of HIF1α by $CoCl_2$ creates a chaotic cellular condition which may drastically affect tight junctions and shows a drastic increase in 3 kDa FITC-dextran permeability. However, we did not notice such an effect with 70 kDa FITC-dextran permeability (figure 32B). Application of the HIF-1α inhibitor is further discussed under the section of future directions.

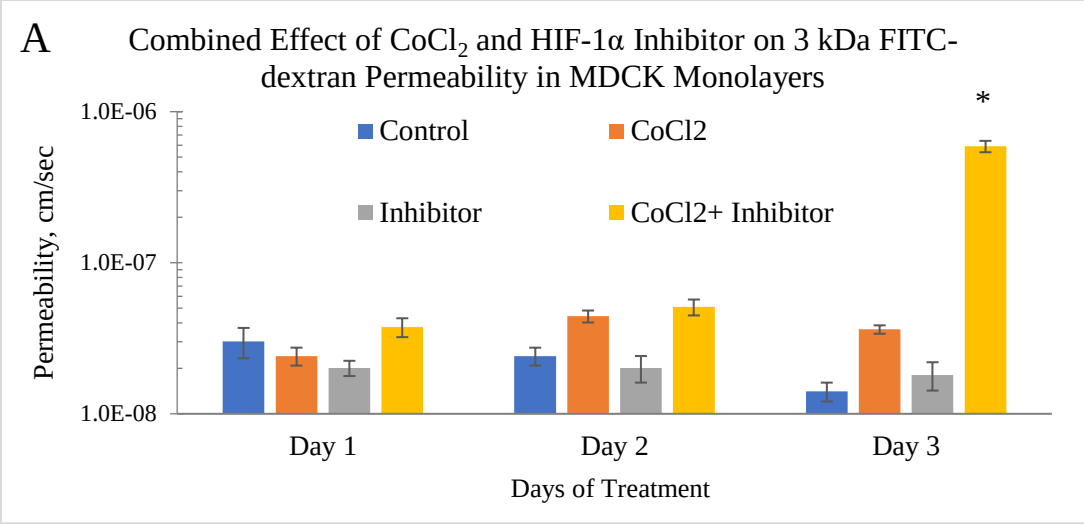

Figure 32 A: Effect of HIF-1α inhibitor along with $CoCl_2$ on 3 kDa FITC-dextran permeability in differentiated MDCK monolayers. Treatment started on Day 0. Combined application of 100 µmol/L of $CoCl_2$ and 30 µmol/L of HIF1α inhibitor for 72 hours (Day 3) drastically increased (40 folds) 3 kDa FITC-dextran permeability and this increase was statistically significant (One-way ANOVA, $P < 0.0001$, N=3-4). The application of $CoCl_2$ alone for 72 hours increased the permeability around 3 folds. The application of HIF-1α inhibitor alone did not have any significant effect.

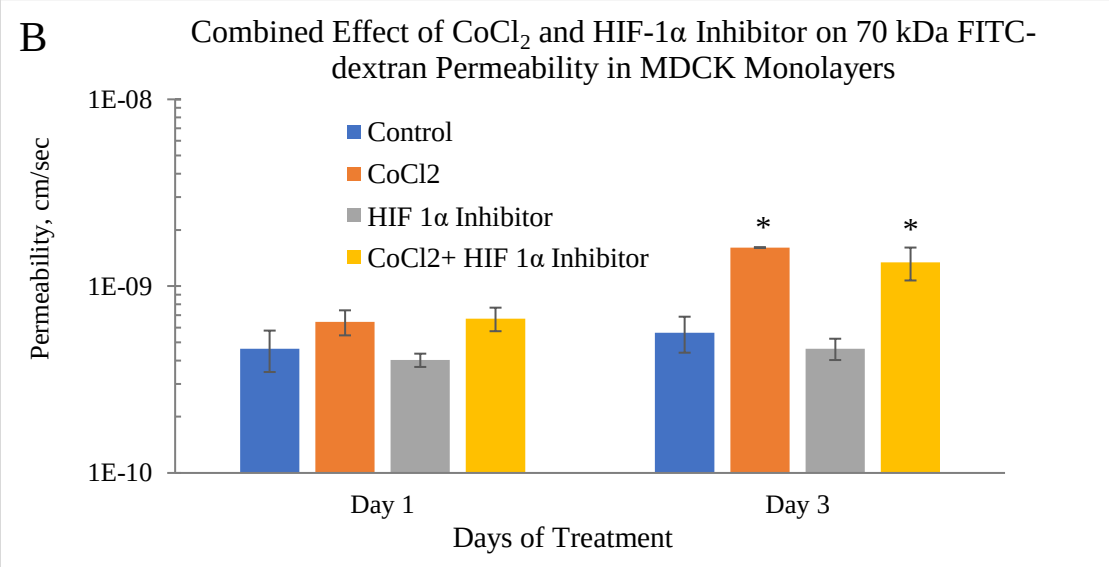

Figure 32 B: Effect of HIF-1α inhibitor along with $CoCl_2$ on 70 kDa FITC-dextran permeability in differentiated MDCK monolayers. Treatment started on Day 0. Combined application of 100 µmol/L of $CoCl_2$ and 30 µmol/L of HIF1α inhibitor for 72 hours (Day 3) increased 70 kDa permeability around 2 folds and the application of $CoCl_2$ alone for 72 hours (Day 3) increased 70 kDa FITC-dextran permeability around 3 folds (One-way ANOVA, $P < 0.0001$, N= 3-4). The application of HIF-1α inhibitor alone did not have any significant effect.

3.1.4 HIF-stabilization by $CoCl_2$ Decreases ZO1 Protein Level

ZO1 protein is known to link tight junction strand proteins to the actin cytoskeleton, and thereby ZO1 maintains the integrity of tight junctions and controls transport through paracellular routes (Denker and Sabath 2011). In mCCD cells, HIF-stabilization by $CoCl_2$ decreased ZO1 protein levels as seen in the western blot (figure 33 A). The densiometric analysis demonstrates significant reductions in ZO1 protein levels due $CoCl_2$ treatment as shown in figure 30B. Fluid flow along with $CoCl_2$ did not seem to have any additional effect. Decreased level of ZO1 due to HIF-stabilization by $CoCl_2$ is consistent with the increased permeability of FITC-dextran molecules through mCCD monolayers (Nag and Resnick 2017).

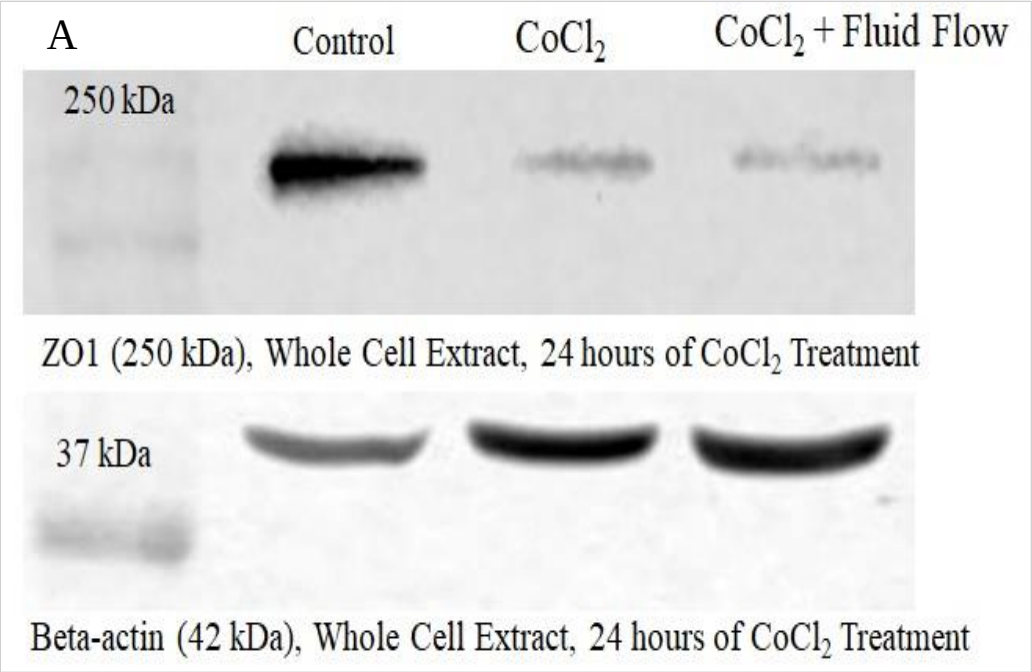

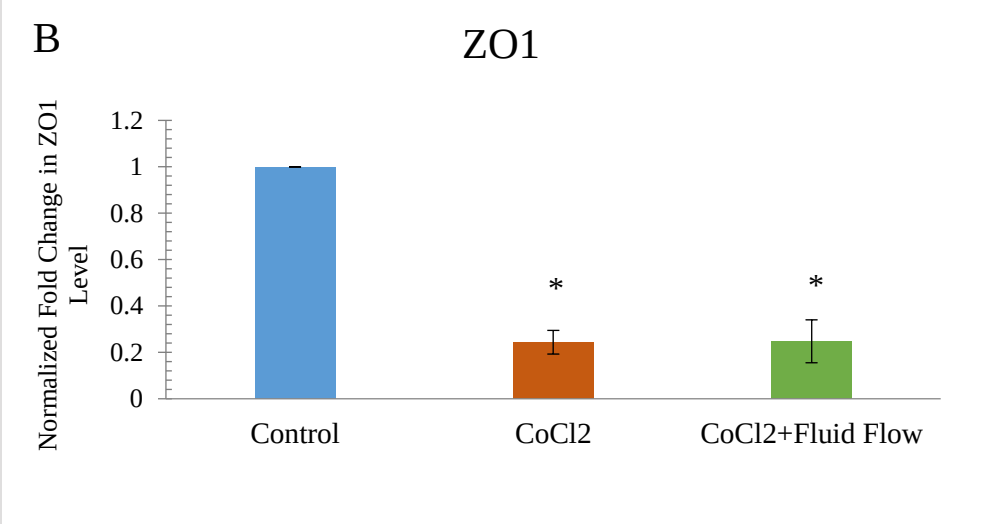

Figure 33: ZO1 protein level in mCCD cells was decreased due to treatment with 100 µmol/ L $CoCl_2$. (A) Shows the western blots for ZO1 and beta-actin (loading control) in the whole cell extracts prepared from cells treated without $CoCl_2$ (Control), with $CoCl_2$, and $CoCl_2$ with fluid flow for 24 hours. (B) Shows the densiometric analysis of the ZO1 bands, One-way ANOVA, $P < 0.0001$, N= 4.

3.1.5 Transepithelial Electrophysiology Results

3.1.5.1 TER Results

I. Development of TER During Cellular Growth

As shown in figure 31, TER values start to develop from the growth phase in mCCD cells. Increases in the TER value corresponds to the increment of transcellular resistance due to increase in cellular numbers during the growth phase as well as contributed by the cellular junctions.

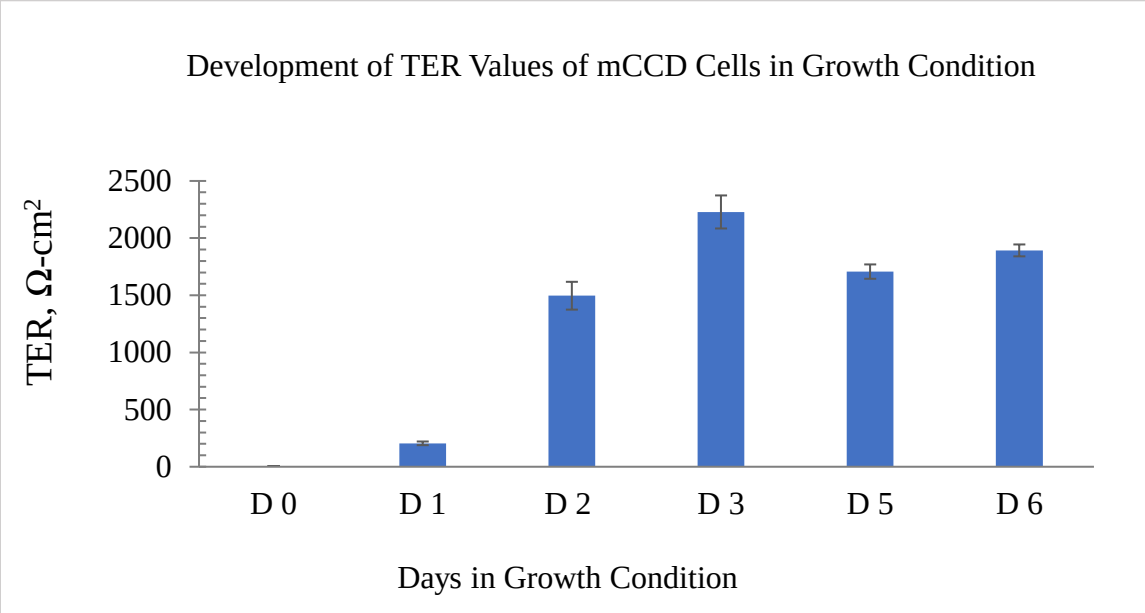

Figure 34: Development of TER values in growth condition of mCCD cells, N= 3-48.

II. Effect of Fluid Flow on TER of mCCD Monolayers

Fluid flow was applied during differentiation of mCCD monolayers. As shown in Figure 35, the presence of fluid flow did not seem to have any permanent effect on differentiating (up to day 8 i.e., D8) and in differentiated mCCD monolayers (e.g., day 8 or D8 and onwards). Figure 35 also shows the variability and possible range of TER values.

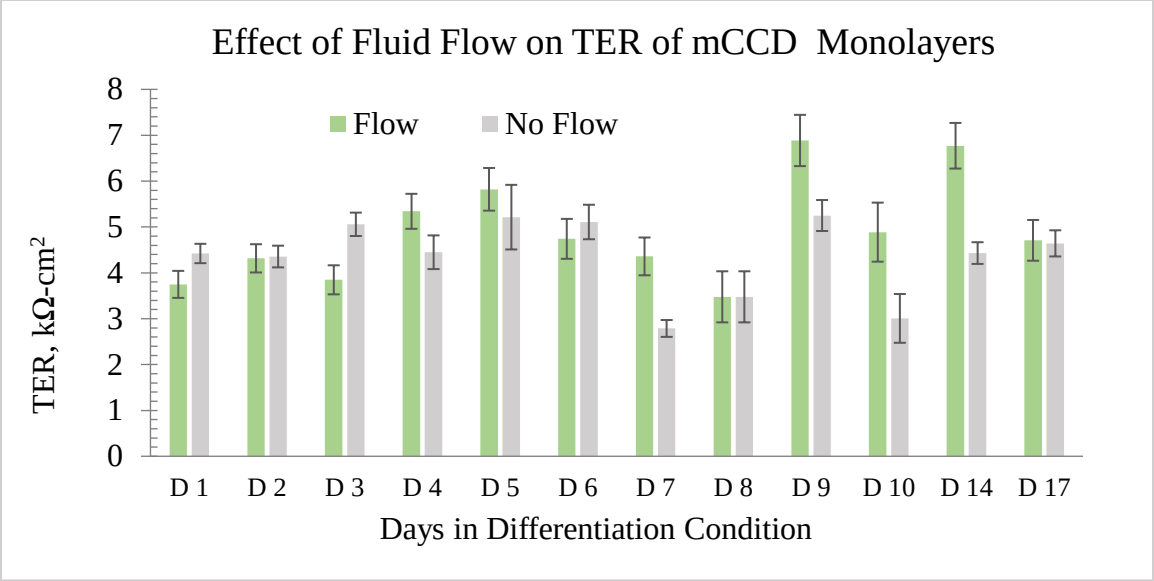

Figure 35: Effect of fluid flow on TER of differentiating or differentiated mCCD monolayers. Differentiation up to day 7-8 (D7 or D8) and differentiated on day 8 onwards, N= 7-46.

III. Effect of HIF-stabilization by $CoCl_2$ on TER of Renal Epithelial Monolayers

Due to the integrity of tight junctions, an untreated confluent and fully differentiated mCCD monolayer maintains a TER value around 3 kΩ-cm^2. As shown in figure 36A and 36B, extended application of $CoCl_2$ results in a significant decrease in TER value at day 2 and 3. This decrease in TER value due to $CoCl_2$ treatment is consistent with the decreased level of ZO1 and increased permeability of FITC-dextran molecules. HIF-stabilization by $CoCl_2$ in mCCD monolayers cultured without fluid flow (figure 36A**)** showed an average TER value reduction after 30 hours, whereas in HIF-stabilized monolayers cultured with fluid flow (figure 36B), the average TER value was found to decrease after 48 hours. The TER of mCCD monolayers was found to decrease 4-fold in the absence of fluid flow and 3-fold in the presence of fluid flow due to HIF-stabilization by $CoCl_2$. Statistical analysis suggests that the effect of HIF-stabilization in lowering TER values was favored when fluid flow was absent (Nag and Resnick 2017).

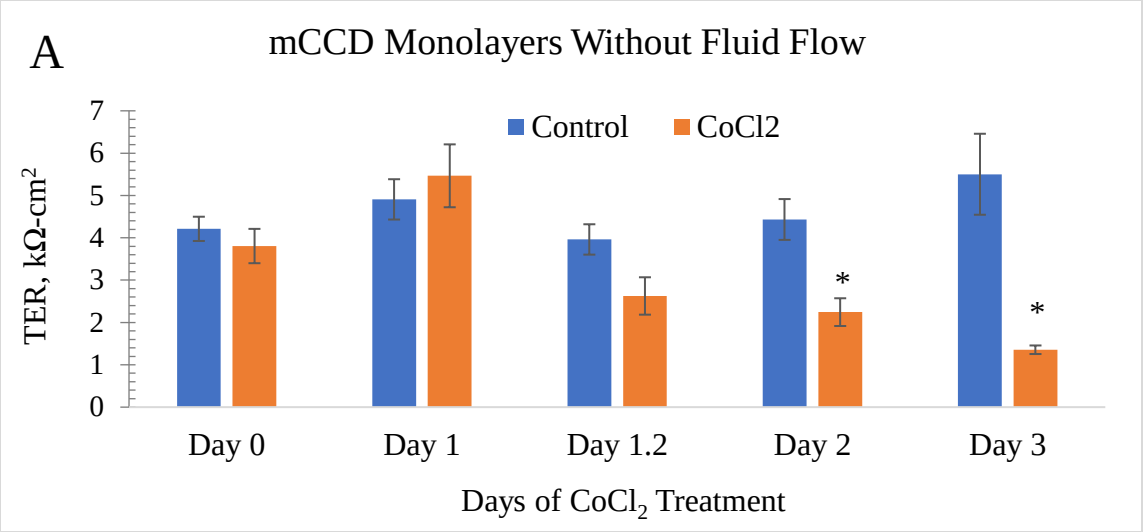

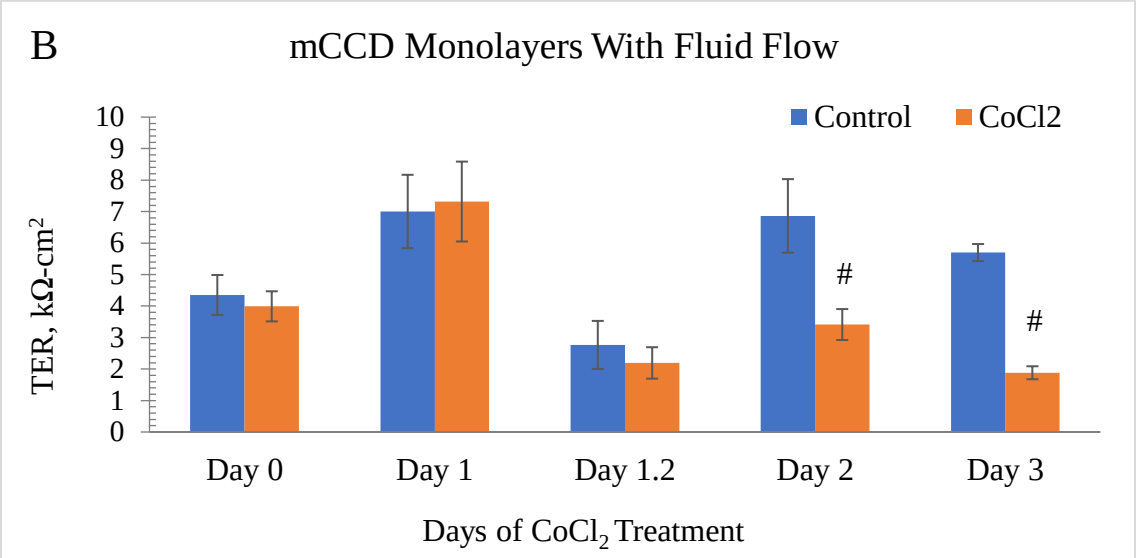

Figure 36: Effect of $CoCl_2$ on TER of differentiated mCCD monolayers. $CoCl_2$ was added on day 0 in the absence (A) or presence (B) of chronic steady fluid flow, N= 4-16, One-way ANOVA. * denotes significant change ($p < 0.05$) between a control and $CoCl_2$ treatment at a specific time-point. # denotes $CoCl_2$ treatment causes significant change ($p < 0.05$) between $CoCl_2$ treated sample at a specific time point with control or $CoCl_2$ treated sample at a different time point. One-way ANOVA shows no significant ($P > 0.05$) TER changes among control groups in (A) or (B). Data in (A) shows that application of 100 µmol/L $CoCl_2$ significantly decreased TER values of differentiated mCCD monolayers after 48 hours (2 days) and 72 hours (3 days) without fluid flow. In figure (B) with fluid flow, at a specific time points of Day 2 and Day 3, statistical significance ($P > 0.05$) was not detected between control and $CoCl_2$. However, we noticed $CoCl_2$ treatment group value was significantly ($P < 0.05$, denoted by #) decreased as compared to control value at a different time point. TER on Day 3 of $CoCl_2$ treated group was significantly decreased as compared to Day 2 control. Similarly, TER on Day 2 of $CoCl_2$ treated group was significantly decreased as compared to Day 1 control.

In contrast to mCCD monolayers, a confluent and fully differentiated monolayer of MDCK cells has a TER value around 200-400 Ω-cm^2. Figure 37 demonstrates that the TER values of MDCK monolayers increase due to HIF-stabilization by $CoCl_2$ treatment.

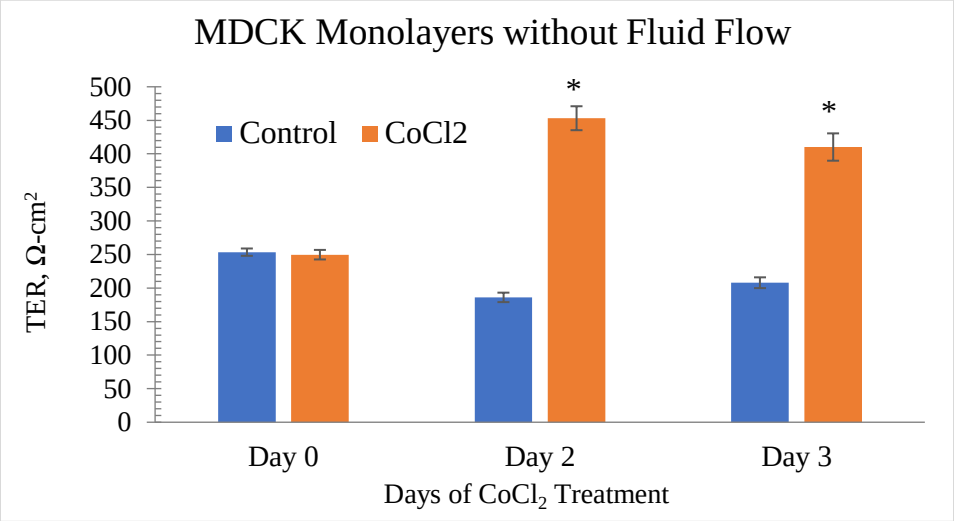

Figure 37: Effect of $CoCl_2$ on differentiated MDCK monolayers without fluid flow. $CoCl_2$ was added on day 0 in the absence of fluid flow. TER values increased significantly at Day 2 and Day 3 of $CoCl_2$ treatment (One-way ANOVA, $P < 0.0001$, N= 3-9). No statistically significant differences were found among control groups.

The Table below summarizes our TER measurements:

Table IV: Summary of TER values.

	TER w/o flow [Ω-cm^2]	**TER w/ flow** [Ω-cm^2]
mCCD w/o $CoCl_2$	5502 ± 2870	5699 ± 665
mCCD w/ $CoCl_2$, 72 h	1356 ± 202	1881 ± 506
MDCK w/o $CoCl_2$	208 ± 14	Did not measure
MDCK w/ $CoCl_2$, 72 h	410 ± 35	Did not measure

HIF-stabilization in MDCK monolayers increased FITC-dextran permeability but also increased TER value instead of decreasing it. We further investigated this finding by statistical analysis. We combined all the data of 3 kDa FITC-dextran and 70 kDa FITC-

dextran permeability and TER values of fully differentiated and untreated mCCD and MDCK monolayers. We analyzed the data to find correlation between TER and permeability. The summary of the correlation shown in the table below:

Table V: Pearson's correlation between TER values and 3 kDa or 70 kDa FITC-dextran permeability in mCCD and MDCK monolayers.

Cell Type	TER versus 3 kDa Dextran Permeability: Pearson's Linear Correlation Coefficient, r	Statistical Significance of 3 kDa Dextran vs TER Correlation	TER versus 3 kDa Dextran Permeability: Pearson's Linear Correlation Coefficient, r	Statistical Significance of 70 kDa Dextran vs TER Correlation
mCCD	-0.5	$P < 0.0001$, N = 56	-0.54	$P < 0.0001$, N = 56
MDCK	0.21	P = 0.32, N = 24	-0.36	P = 0.3, N =13

TER is known to maintain an inverse relation with permeability. In mCCD monolayers, Pearson's correlation coefficient (r) values were -0.5 and -0.54 for 3 kDa and 70 kDa dextran, respectively (table 5). These values suggest fair or moderate correlation between FITC-dextran permeability and TER values in mCCD monolayers. The permeability and TER correlation was statistically significant in mCCD cells. In the case of MDCK monolayers, the 3 kDa FITC-dextran and TER showed a positive r value, indicating that the inverse correlation was not maintained (table 5). TER and 70 kDa FITC-dextran showed a weak correlation. Moreover, in the MDCK monolayer, the correlation was not statistically significant as shown in table 5. Thus, the TER values of mCCD monolayers can be an indicator of FITC-dextran permeability, but not for MDCK monolayers (Nag and Resnick 2018).

3.1.5.2 Ieq Results

I. Effect of Fluid Flow on Ieq of mCCD Monolayers

The presence of fluid flow was found to decrease I_{eq} values. The effect of fluid flow in lowering I_{eq} values was consistent both in differentiating and differentiated mCCD cellular monolayers as shown in figure 38. This finding agrees with previous reports (Resnick and Hopfer 2007; Resnick 2011). Active Na^+ transport is mainly responsible for I_{eq} in mCCD monolayers and active Na^+ transport can be regulated by functional cilia and fluid flow.

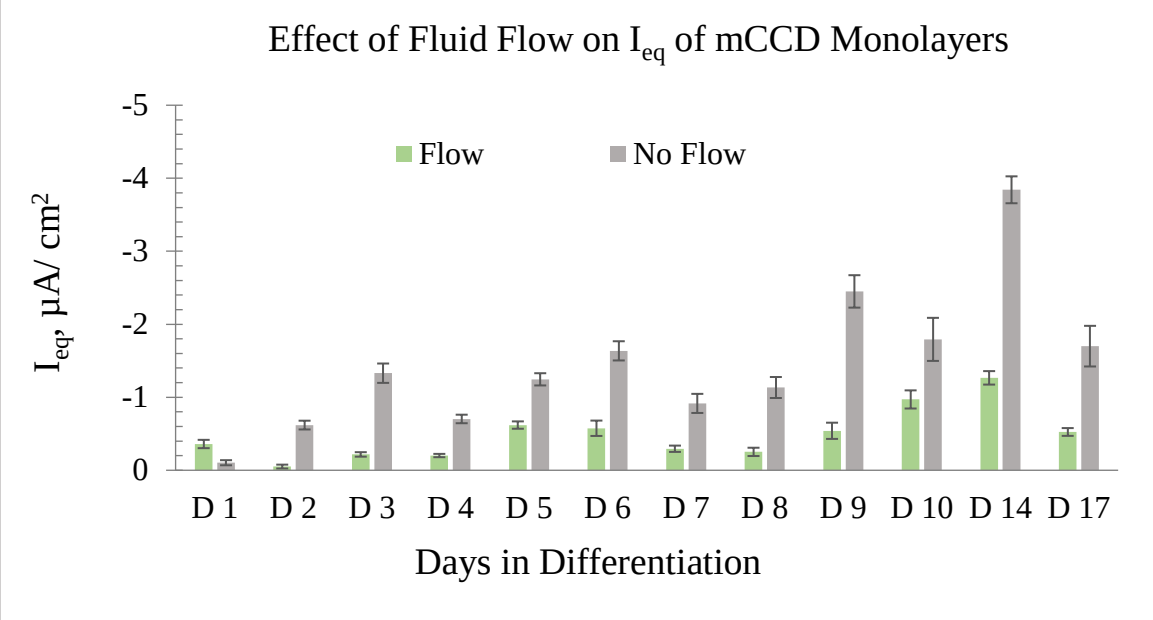

Figure 38: Effect of fluid flow on I_{eq} of differentiating or differentiated mCCD monolayers, Differentiation up to day 7-8 (D7 or D8) and differentiated on day 8 onwards, N= 7-46.

II. HIF-stabilization by $CoCl_2$ Alters I_{eq} of mCCD Monolayers

The effect of HIF-stabilization by $CoCl_2$ on I_{eq} was found to be more prominent in mCCD monolayers cultured in the absence fluid flow (Figure 39A) as compared to monolayers cultured in the presence of fluid flow (Figure 39B). Treatment with $CoCl_2$ in the absence of fluid flow showed a significant decrease of normalized I_{eq} values after 30

hours or 1.2 days (Figure 39A). Due to $CoCl_2$ treatment for 3 days in monolayers not exposed to fluid flow, I_{eq} values showed a significant change and, very interestingly, a positive mean I_{eq} value of 0.9 µA/ cm^2 was detected. Movement of positively charged Na^+ from the apical to basolateral side results in a negative value of I_{eq}. Thus, a positive I_{eq} value suggests that the net active ion transport may be occurring in the opposite direction, and the monolayer may have become secretory. It is tempting to interpret this finding as a confirmation of our hypothesis that the stabilization of HIF-1α for an extended period can transform a normally absorptive renal epithelial monolayer into a secretory monolayer.

Analysis of normalized I_{eq} values of mCCD monolayers cultured with chronic fluid flow showed that the normalized I_{eq} values were significantly reduced at day 2 in response to $CoCl_2$ treatment as shown in figure 39B. Control samples had a mean I_{eq} value of -2.6 µA/ cm^2, whereas $CoCl_2$ treated samples showed mean I_{eq} values of 0.1 µA/ cm^2 and 0.2 µA/ cm^2 after 2 and 3 days, respectively.

When figures 39A and 39B are compared, it is to be noted that HIF-stabilization by $CoCl_2$ significantly altered I_{eq} values in the monolayers without fluid flow after 30 hours, whereas in the monolayers cultured with fluid flow, significant changes occurred after 48 hours. In monolayers without fluid flow, $CoCl_2$ treatment for 72 hours showed a more prominent change. Therefore, it can be inferred that the lack of fluid flow may have intensified the effect of HIF-stabilization (Nag and Resnick 2017). However, with our EPO western blots, we were unable to find any direct contribution of fluid flow in HIF-stabilization.

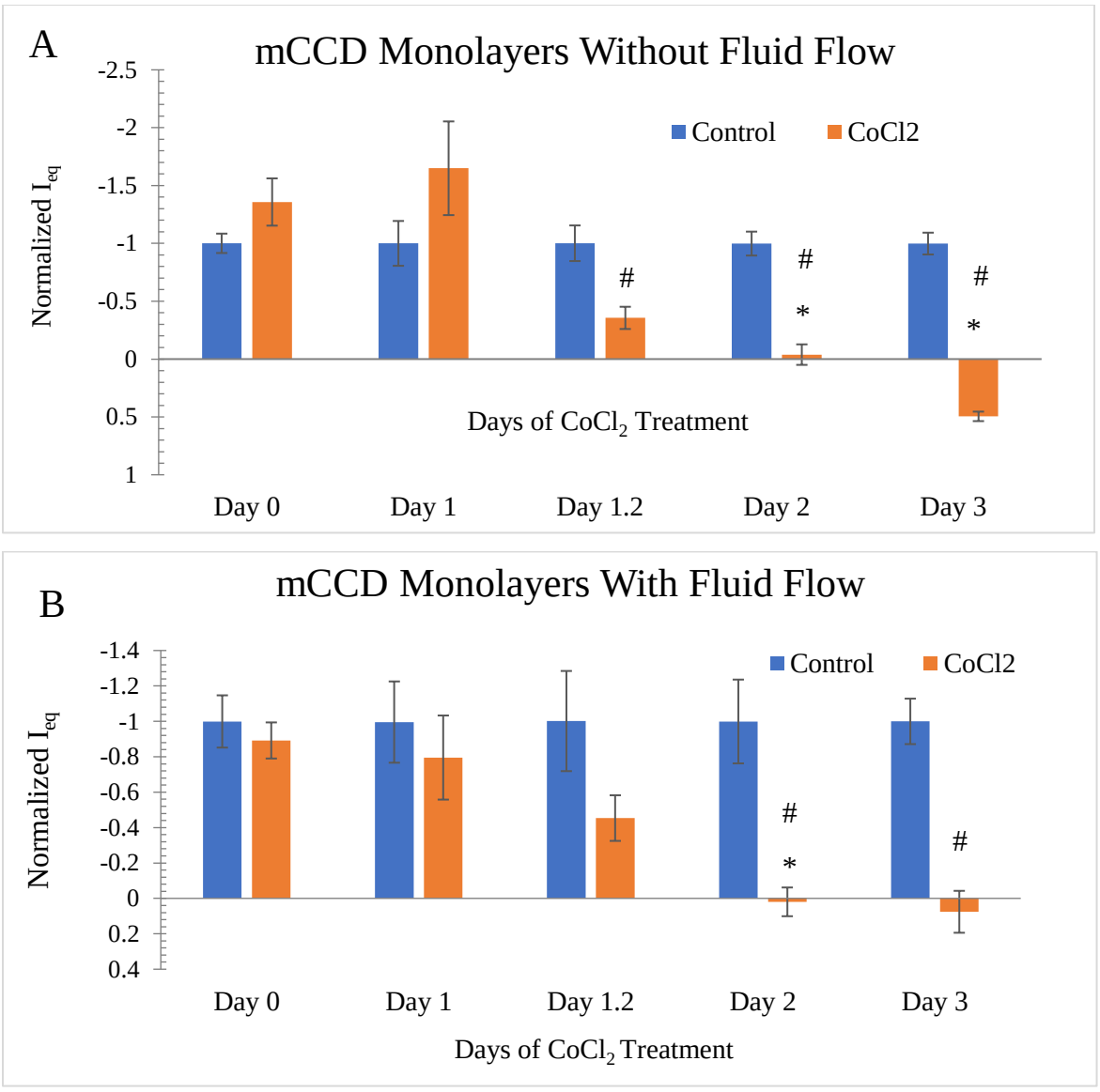

Figure 39: Effect of $CoCl_2$ on I_{eq} of differentiated mCCD monolayers. (A) Without fluid flow. (B) With chronic steady fluid flow. $CoCl_2$ was added on day 0. Data shows that application of 100 µmol/L $CoCl_2$ significantly decreased I_{eq} values of differentiated mCCD monolayers after 48 hours (2 days) in both (A) and (B). Interestingly, after 3 days of treatment, I_{eq} value switched to the positive direction. Current values are plotted as normalized I_{eq} (i.e., relative to average control I_{eq} values) as discussed in methods, N = 4-16, One-way ANOVA. * denotes significant change ($P < 0.05$) between a control and $CoCl_2$ treatment at a specific time-point. # denotes significant change ($P < 0.05$) between a $CoCl_2$ treated sample at a specific time point with a control or $CoCl_2$ treated sample at a different time point. In figure (A) and (B), $CoCl_2$ treatment shows a gradual decrease of negative I_{eq}. Some of these gradual decreases of I_{eq} are statistically significant (e.g., figure (A) Day 1 $CoCl_2$ vs Day 1.2 $CoCl_2$; figure (A) Day 1.2 $CoCl_2$ vs Day 2 $CoCl_2$; figure (B) Day 1 $CoCl_2$ vs Day 2 $CoCl_2$) and were denoted by #. In figure (B) Day 3 $CoCl_2$ shows a statistically significant decrease as compared to Day 2 Control (denoted by #).

3.1.5.3 $CoCl_2$ Acts on Basolateral Side of mCCD Cells

In our mCCD cells, the transporter responsible for Co^{2+} uptake has not been clearly identified. In mammalian cells, the divalent metal cation transporters Slc11a1 and Sla11a2 are believed to be responsible for Co^{2+} uptake (Gunshin, Mackenzie et al. 1997; Forbes and Gros 2003). We found that mCCD monolayers cultured in the presence of fluid flow exposed to apical $CoCl_2$ treatment showed an initial, transient, increase in TER values but no chronic change to TER values as shown in Figure 40A. Apical treatment with $CoCl_2$, did not have any effect on I_{eq} values of mCCD monolayers (figure 40B). However, when $CoCl_2$ was withdrawn from the apical media and added to the basolateral media, we noted significant dose-dependent decreases in both TER and I_{eq} values, as shown in figure 41A and 41B. Basolateral treatment with 100 µmol/L $CoCl_2$ showed significant decreases in TER and I_{eq} values after 2 days of treatment as shown in figure 41A and 41B. The effect of $CoCl_2$ on cellular electrophysiology (TER and I_{eq}) when added to basolateral media was similar as the effect of $CoCl_2$ when added to both apical and basolateral media. Thus, it is interesting to find that $CoCl_2$ affects the electrophysiological properties of our monolayers only when it is added in the basolateral media, potentially identifying the site of Co^{2+} uptake (Nag and Resnick 2017).

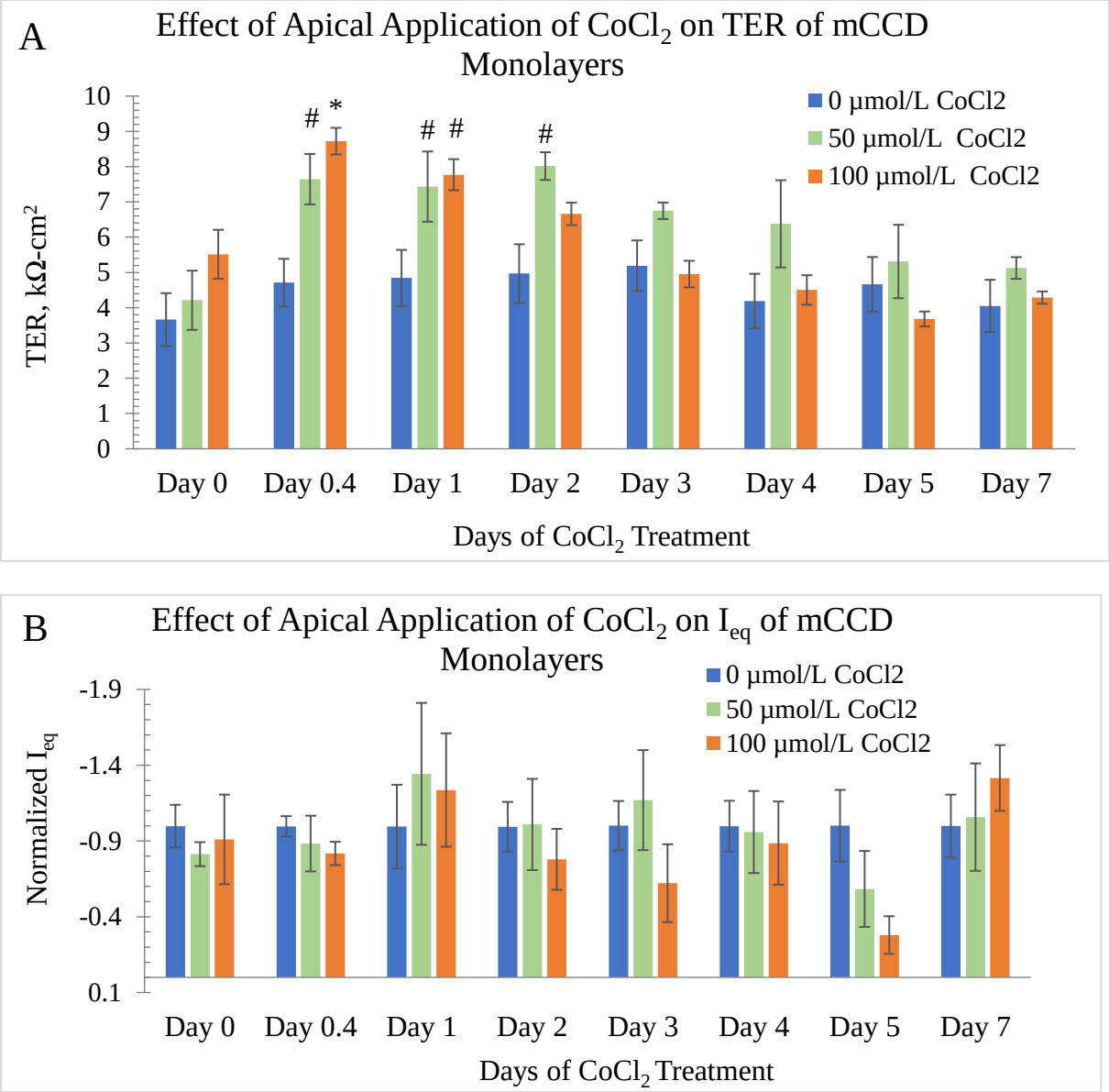

Figure 40: Effect of $CoCl_2$ added to apical media of differentiated mCCD monolayers cultured in the presence of chronic steady fluid flow. (A) TER and (B) I_{eq} measurements. Data shows that application of $CoCl_2$ in apical media does not cause any chronic changes in TER values (A) or I_{eq} values (B) of differentiated mCCD monolayers, One-way ANOVA, N = 5-8. In the TER and I_{eq} data, One-way ANOVA shows no significant ($P > 0.05$) TER and I_{eq} changes among any control groups. In the TER plot (A), * denotes a significant change ($P < 0.05$) between 0 µmol/L $CoCl_2$ and 100 µmol/L $CoCl_2$ treatment at Day 0.4 (6 hours). # denotes a significant difference ($P < 0.05$) between a $CoCl_2$ treated sample at a specific time point and a $CoCl_2$ treated or control (0 µmol/L $CoCl_2$) sample at a different time point. # are marked onto any noticeable significant changes due to $CoCl_2$ treatment. There is no significant effect ($P > 0.05$) of apical application of 0, 50, or 100 µm $CoCl_2$ on I_{eq} of mCCD monolayers.

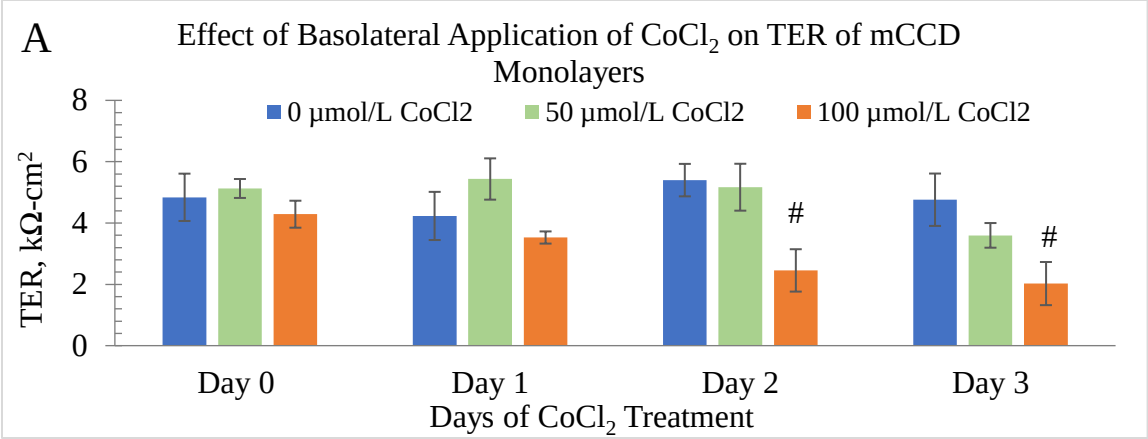

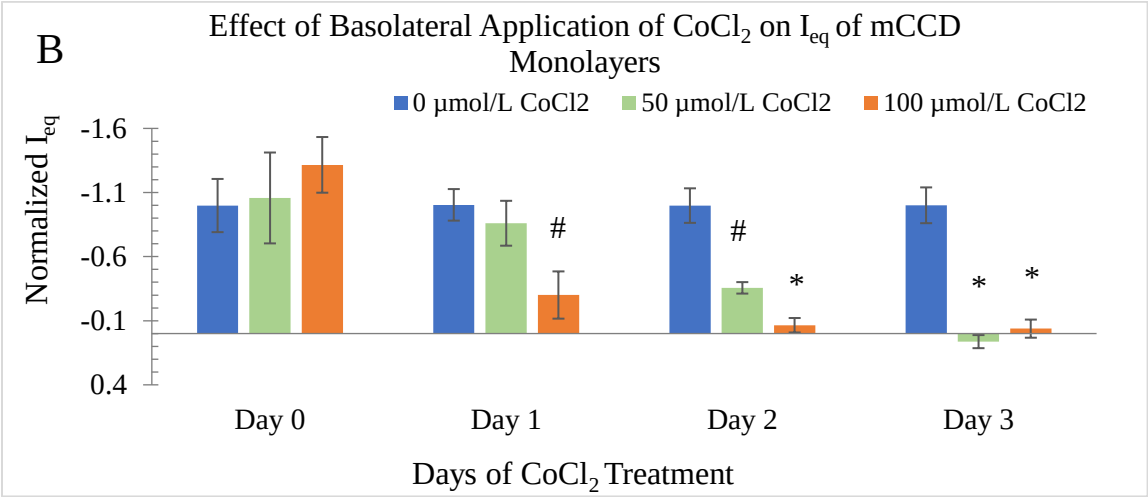

Figure 41: Effect of $CoCl_2$ when withdrawn from apical media and added to basolateral media of differentiated mCCD monolayers in the presence of chronic steady fluid flow. (A) TER and (B) I_{eq} measurements. Data shows that application of 100 µmol/L of $CoCl_2$ to basolateral media significantly decreased TER values (A) and I_{eq} values (B) of mCCD monolayers in a dose-dependent manner after 2 days of treatment (N = 5-6). In the TER and I_{eq} data, One-way ANOVA shows no significant ($p > 0.05$) TER and I_{eq} changes among control groups**.** * denotes significant change ($p < 0.05$) among 0, 50, and 100 µmol/L $CoCl_2$ treatment at a specific time-point. # denotes $CoCl_2$ treatment causes significant change ($p < 0.05$) between $CoCl_2$ treated sample at a specific time point and $CoCl_2$ treated or control sample at a different time point. In figure (A) we do not see statistically significant decrease of TER, * ($p < 0.05$) on day 2 or day 3 by 50 or 100 µmol/L $CoCl_2$ as compared to control (0 µmol/L $CoCl_2$) on that specific day. However, we notice some significant decrease of TER as compared to control at a different time point. For example, on day 3, 100 µmol/L $CoCl_2$ causes a significant decrease in the TER value when compared to 0 µM $CoCl_2$ TER value on day 2, denoted by #. In figure (B) we notice significant loss of I_{eq} with 100 µmol/L $CoCl_2$ treatment on day 2 and significant loss of I_{eq} with both 50 and 100 µM $CoCl_2$ treatment on day 3. Any noticeable significant changes due to $CoCl_2$ treatment are denoted by #.

3.1.6. HIF-stabilization by $CoCl_2$ Decreases Na^+/ K^+- ATPase α1 Subunit Protein Level

The catalytic subunit α of Na^+/ K^+-ATPase is known to be mainly responsible for active transport of Na^+. Using western blot, we notice that HIF-stabilization by $CoCl_2$ decreases Na^+/ K^+-ATPase α1 subunit level in our mCCD cells as shown in figure 42A. Densiometric analysis confirms the significant decrease of Na^+/ K^+-ATPase α1 due to HIF-stabilization (figure 42B). The presence or absence of fluid flow along with HIF-stabilization did not seem to have any additional effect on Na^+/ K^+-ATPase α1 level (figures 42A and 42B) (Nag and Resnick 2017). The decrease of Na^+/ K^+-ATPase α1 subunit level due to HIF-stabilization is consistent with the loss of I_{eq} i.e., decreased active Na^+ transport from apical to basolateral side in mCCD monolayers.

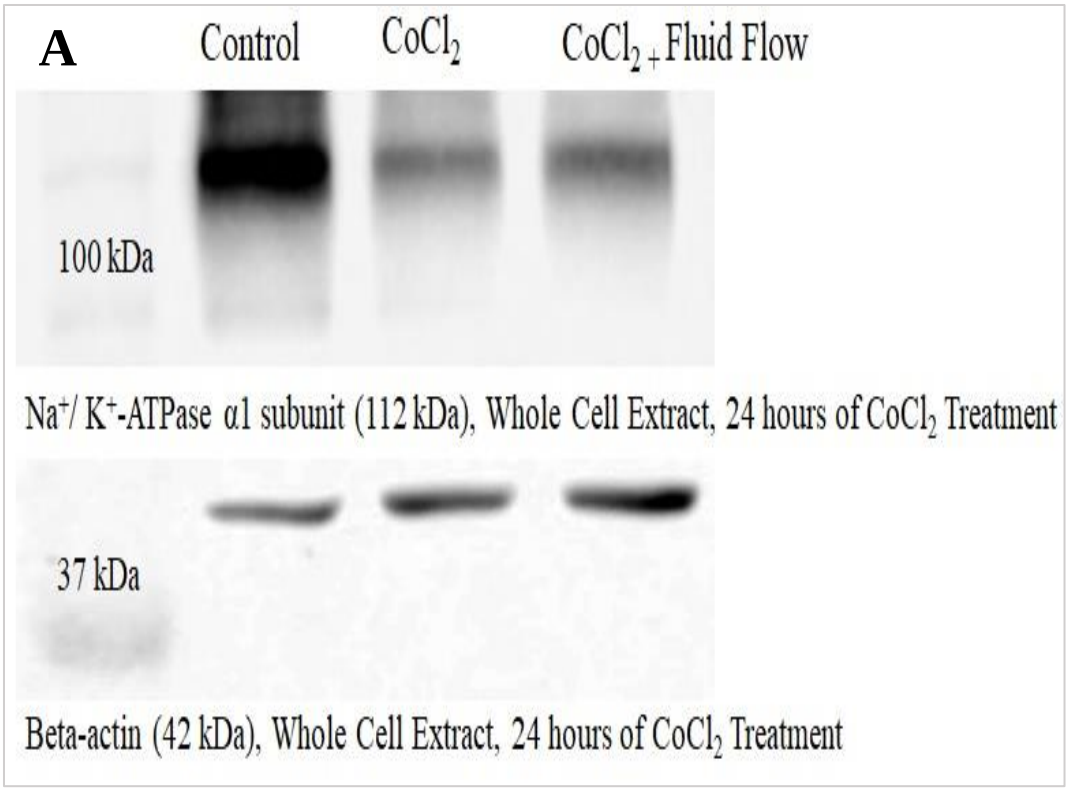

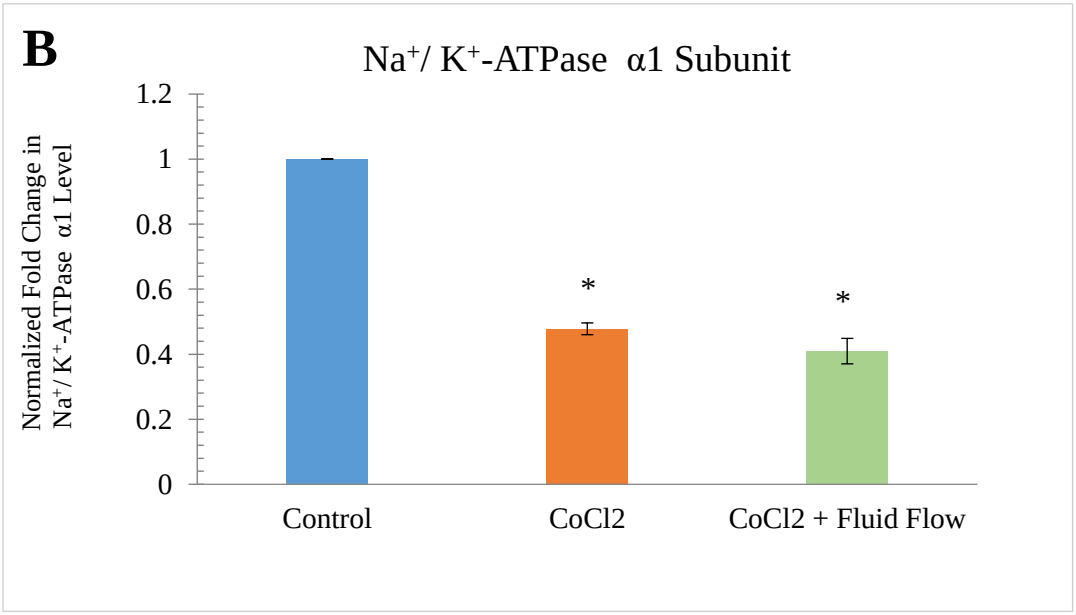

Figure 42: Na^+/ K^+-ATPase α1 subunit protein level in mCCD cells was decreased due to treatment with 100 µmol/ L $CoCl_2$. (A) Shows the western blots for Na^+/ K^+-ATPase α1 subunit and beta-actin (loading control) in the whole cell extracts prepared from cells treated without $CoCl_2$ (Control), with $CoCl_2$, and $CoCl_2$ with fluid flow for 24 hours. (B) Shows the densiometric analysis of the ZO1 bands, One-way ANOVA, P = 0.001, N= 3.

3.2 Discussion

3.2.1 100 µmol/L $CoCl_2$ Stabilizes HIF-1α without Any Detectable Cellular Cytotoxic Effects until 4 Days

In our mCCD and MDCK monolayers 100 µmol/L $CoCl_2$ was found to stabilize HIF-1α in the nucleus and also resulted in a slightly increased production of EPO. We detected EPO by western blot in the cell lysates. We think that the EPO was mostly released in the cell culture media and since we did not analyze EPO levels in cell culture media, we may have underestimated the effect of HIF-stabilization by $CoCl_2$ in increasing EPO production by mCCD and MDCK cells. A concentration of 100 µmol/L $CoCl_2$ was previously reported to stabilize HIF-1α in the nucleus of MDCK cells (Verghese, Zhuang et al. 2011). Other studies showed cobalt can increase EPO production (FISHER and Langston 1967; Fandrey, Frede et al. 1997). $CoCl_2$ was previously shown to prevent cellular growth of mouse embryonic fibroblasts at a concentration of 100 µmol/L. However, MTT assay showed 100 µmol/L $CoCl_2$ did not have any significant cytotoxic effect on fibroblasts after 72 hours (Vengellur and LaPres 2004). Similarly, using an MTT assay we did not notice any effect on the cellular metabolic activity of mCCD cells by 100 µmol/L $CoCl_2$ up to 4 days of $CoCl_2$ treatment. All our epithelial transport experiments were carried out within 3 days of $CoCl_2$ treatment, and during this time $CoCl_2$ did not seem to have any cytotoxic effect. MTT assay may show a delayed response to indicate cytotoxic effects or may be unable to detect small variation in cellular viability (Page, Bejaoui et al. 1988; Sieuwerts, Klijn et al. 1995). In this context, it is important to point out that we ensured that all our mCCD monolayers maintained a threshold TER value of 1 kΩ- cm^2 during epithelial transport experiments. Any small gap due to loss of cells (0.4 % loss of

cellular coverage) would cause 80% decrease in TER value (ávan der Meer, JungáKim et al. 2015). We did not notice such a drastic change of TER values in our monolayers due to $CoCl_2$ treatment up to 3 days, supporting our MTT assay results that $CoCl_2$ treatment may not have affected number of viable cells at least up to 3-4 days.

As discussed previously, in kidney cystic epithelia of rats and humans, protein levels of HIF-1α and mRNA levels of HIF-α target genes, such as EPO, Glut-1, and VEGF were found to be elevated (Bernhardt, Wiesener et al. 2007). Using $CoCl_2$, we prevented degradation of HIF-1α in monolayers of mCCD and MDCK epithelial cells to understand the role of hypoxia or HIF-stabilized environment as experienced by normal renal epithelial cells in a hypoxic environment created by cysts in PKD (Nag and Resnick 2017).

In our study, we considered that the cell culture in a regular incubator with 5% CO_2 as cells under normoxia. The normal atmospheric O_2 is around 20%. In a normal cell culture incubator, the percent of O_2 is similarly around 20%. The alveolar cells normally encounter around 20% O_2 and arterial blood has O_2% around 10-13% and O_2% is other organs is around 1-8%. *In vivo* kidney medulla was reported to encounter around 1% O_2 (Lübbers and Baumgärtl 1997). Therefore, renal epithelial cell culture maintained in a CO_2 incubator may experience a hyperoxic environment, rather than a normoxic environment (Wenger, Kurtcuoglu et al. 2015). Future work can address this limitation using an O_2 controlling chamber or incubator.

3.2.2 Effect of Fluid Flow with HIF-stabilization

Chronic fluid flow alone did not seem to have any effect on TER values of mCCD monolayers, but the presence of flow showed consistently decreased I_{eq} value, i.e, decreased Na^+ transport, and this finding is consistent with previous reports (Resnick and

Hopfer 2007; Resnick 2011). Our results of electrophysiological analysis suggest that the presence of chronic fluid flow may blunt HIF-stabilized altered transepithelial transport. TER and normalized I_{eq} values decreased more rapidly in the absence of fluid flow as compared to monolayers cultured in the presence of fluid flow. It is tempting to suggest that monolayers cultured in the absence of fluid flow may be hypoxic to some extent and may already have increased HIF-1α to some extent. However, we maintained a thin apical fluid thickness that ensures adequate O_2 availability to the monolayer. Our western blots did not show any additional effect of the presence or absence of fluid flow along with $CoCl_2$ on protein levels of EPO, ZO1, and Na^+/ K^+-ATPase. Therefore, renal epithelial response to fluid flow seems to be independent of HIF-1α (Nag and Resnick 2017).

3.2.3 HIF-stabilization by $CoCl_2$ Alters Transcellular and Paracellular Transport

We presented our method of quantification of FITC-dextran permeability and showed permeability as a stable function of mCCD and MDCK epithelial monolayers. In MDCK C-7 epithelial cell monolayers with TER value of around 4000 Ω-cm^2, 4 kDa FITC-dextran apparent permeability (P_{app}) value was reported to be around 2×10^{-9} cm/sec (Gekle, Wünsch et al. 1994; Kaiser, Pereira et al. 2015). In our mCCD monolayers with TER value around 3000 Ω-cm^2, 3 kDa permeability value was found to be $(8.53 \pm 4.46) \times 10^{-9}$ cm/sec. Thus, our calculated permeability values agree with previous reports. Using 3 kDa and 70 kDa FITC-dextran molecules, we were able to identify that the size selectivity was maintained in both mCCD and MDCK epithelial monolayers. 3 kDa FITC-dextran can be transported through epithelial monolayers either by fluid-phase transcytosis or by paracellular transport, whereas large 70 kDa dextran molecules are known to be transported

only through the paracellular pathway (Matter and Balda 2003). Thus, changes in 70 kDa FITC-dextran transport through mCCD and MDCK monolayers due to HIF-stabilization represent changes in the paracellular pathway. Increased permeability of anionic FITC-dextran from apical to basolateral side suggests increased paracellular transport which can also be indicative of increased water permeability.

In the mammalian kidney, paracellular permeability is known to decrease from the proximal tubule to the collecting duct due to the expression of different claudins and higher levels of occludin and ZO1 proteins (Gonzalez-Mariscal, Namorado et al. 2000; Denker and Sabath 2011). Paracellular transport through epithelial tight junctions is known to be driven by the ion gradient created by transcellular active transport. Proximal tubule is a leaky epithelial monolayer with a high paracellular permeability and low TER. The proximal tubule is known to be more than 100 fold more permeable than the collecting duct (Denker and Sabath 2011). In our mCCD monolayers HIF-stabilization for 72 hours with $CoCl_2$ resulted in a 100-fold increase of 3 kDa FITC-dextran permeability and 40-fold increase of 70 kDa FITC-dextran permeability. Therefore, HIF-stabilized collecting duct epithelial monolayers appear to behave as monolayers from a more permeable region of the kidney, such as proximal tubule.

The cortical collecting duct is responsible for 0.5% salt reabsorption and helps in fine-tuning water and salt balance in the body. In mCCD monolayers, I_{eq} primarily shows the active Na^+ transport through ENaC channels since more than 95% of I_{eq} is known to be blocked by 10 µmol/L of Na^+ channel blocker amiloride (Resnick and Hopfer 2007; Resnick 2011). We noticed that HIF-stabilization by $CoCl_2$ caused a loss of I_{eq} values after 48 hours, indicating diminished active Na^+ transport. The decreased protein level of Na^+/

K^+-ATPase α1 subunit was consistent with the loss of active Na^+ transport. Similar observations were previously reported in kidney collecting duct epithelial monolayers, in which hypoxia was shown to decrease ENaC activity and thereby decreased I_{eq} of the monolayers (Husted, Lu et al. 2010). Moreover, in the HIF-stabilized mCCD monolayers without fluid flow, we noticed a switch in the direction of the current after 72 hours, suggesting that the direction of net ion transport was opposite as compared to the normal. Thus, we noticed our absorptive mCCD monolayer transformed to a secretory monolayer due to HIF-stabilization.

In renal epithelial monolayers, hypoxia mimetic condition, created by depletion of ATP, caused disruption of actin cytoskeleton organization and tight junctions and endocytosis of Na^+/ K^+-ATPase (Molitoris, Dahl et al. 1996). Similarly, we found that the Na^+/ K^+-ATPase catalytic subunit α1 level decreased in our mCCD cells, supporting the loss of active Na^+ transport as observed by the loss of negative I_{eq} value in our mCCD monolayers. We also noticed that permeability increased and ZO1 protein level decreased in our mCCD monolayers, indicating alteration of tight junctions. In renal carcinoma cells, HIF-1α was shown to regulate tight junctions by altering normal protein levels of claudin-1 and occludin and normal localization of ZO1, claudin-1, and occludin (Harten, Shukla et al. 2009).

Ischemic injury was shown to decrease sodium reabsorption by kidney proximal tubule due to apical redistribution of Na^+/ K^+-ATPase α-subunit from basolateral side (Molitoris 1991; Molitoris, Dahl et al. 1992). *In vitro* apical redistribution of Na^+/ K^+-ATPase was shown to be functional in switching Na^+ transport from the basolateral to apical side (Molitoris 1993). In our mCCD monolayers, HIF-α stabilization in the absence

of fluid flow showed a positive I_{eq} value which indicated that ions, most likely Na^+, are actively transported in the opposite direction. This switch in the direction of active ion transport could be due to the similar redistribution of Na^+/ K^+-ATPase to the apical side in our mCCD cells.

Previous studies in alveolar epithelial cells reported similar observations as our results in renal epithelial cells (Mairbäurl, Mayer et al. 2002). Hypoxia was shown to decrease active Na^+ transport in rat alveolar epithelial monolayers and also decrease TER of monolayers, increasing monolayer permeability of 4 kDa FITC-dextran (Mairbäurl, Mayer et al. 2002; Bouvry, Planes et al. 2006). We noticed that HIF-stabilization by $CoCl_2$ increased permeability of 3 kDa and 70 kDa FITC-dextran permeability both in our mCCD and MDCK monolayers. We also noticed that TER values of mCCD monolayers also decreased due to HIF-stabilization. In contrast, in MDCK monolayers, TER and FITC-dextran permeability both increased due to HIF stabilization. As mentioned previously, in MDCK monolayers, TER did not seem to be a good indicator of FITC-dextran permeability (Nag and Resnick 2018). MDCK monolayers were reported to show increased TER values as well as increased permeability of 3, 4 and 40 kDa FITC-dextran permeability in different studies (Balda, Whitney et al. 1996; McCarthy, Francis et al. 2000; Van Itallie, Fanning et al. 2009).

Hypoxia was shown to affect the expression or activity of apical ENaC and basolateral Na^+/ K^+-ATPase causing decrease in active Na^+ transport of alveolar epithelia (Vivona, Matthay et al. 2001; Planès, Blot-Chabaud et al. 2002; Dada, Chandel et al. 2003). Alveolar Na^+/ K^+-ATPase activity is known to be decreased in response to hypoxia by endocytosis, which involves phosphorylation and ubiquitination of α1 subunit (Dada,

Chandel et al. 2003). The phosphorylation of Na^+/K^+-ATPase is known to be mainly driven by PKC (Feschenko, Stevenson et al. 2000; Dada, Welch et al. 2007).

Hypoxia was also reported to alter tight junctions and thereby showed increased permeability of monolayers of brain microvessel endothelial cells and intestinal epithelial cells (Xu, Lu et al. 1999; Yamagata, Tagami et al. 2004; Engelhardt, Al-Ahmad et al. 2014), further supporting our findings that HIF-stabilization can decrease monolayer resistance and can increase FITC-dextran permeability.

Hypoxia was found to decrease ZO1 protein levels in the monolayers of alveolar epithelial cells (Bouvry, Planes et al. 2006). ZO1 protein level was shown to decrease in brain microvascular endothelial cells through HIF-1α (Engelhardt, Al-Ahmad et al. 2014). Similarly, we also noticed decreased level of ZO1 protein in our mCCD cells due to stabilization of HIF-1α. Hypoxia can affect the actin cytoskeleton organization and can result in occludin mislocalization from tight junctions to the cellular interior in alveolar epithelial cells (Bouvry, Planes et al. 2006). Stabilization of HIF-1α was shown to affect the integrity of tight junctions of brain microvascular endothelial cells due to the mislocalization and tyrosine phosphorylation of tight junction complex proteins, such as ZO1 and occludin (Engelhardt, Al-Ahmad et al. 2014).

Thus, our results demonstrating altered transepithelial permeability are relevant and are supported by other findings demonstrating that epithelial tight junction morphology is regulated by HIF, with claudins (Saeedi, Kao et al. 2015), occludins (Caraballo, Yshii et al. 2011), and ZO1 (Engelhardt, Al-Ahmad et al. 2014) being specific targets. Similarly, our electrophysiological results are in agreement with previous reports (Husted, Lu et al. 2010; Caraballo, Yshii et al. 2011).

We think VEGF may be a key player in altering renal epithelial tight junctions due to HIF-stabilization as seen in alveolar epithelial cells (Song, Kim et al. 2017). VEGF is known to be expressed in the renal tubules. VEGF-A mRNA was detected in the epithelial cells of glomerulus, distal tubules, and collecting ducts of humans and rodents (Bacic, Edwards et al. 1995; Tufro, Norwood et al. 1999; Karihaloo, Karumanchi et al. 2005). VEGF has a HRE and is elevated in response to HIF (Forsythe, Jiang et al. 1996). Cystic epithelial cells were found to be hypoxic and showed higher protein levels of VEGF (Bernhardt, Wiesener et al. 2007). Occludin, ZO1, and claudins are known to maintain integrity of tight junctions. Hypoxia was shown to decrease levels of occludin in endothelial cells (Brown and Davis 2005) and ZO1 in alveolar epithelial cells (Bouvry, Planes et al. 2006) and endothelial cells (Engelhardt, Al-Ahmad et al. 2014). VEGF is known to cause phosphorylation of multiple serine and threonine residues of occludin involving activation of PKC (Antonetti, Barber et al. 1999; Harhaj, Felinski et al. 2006). Such a phosphorylation of occludin is known to modulate ubiquitination of occludin (Murakami, Felinski et al. 2009). VEGF is also known to cause tyrosine phosphorylation of ZO1 (Antonetti, Barber et al. 1999). Ischemia was shown to promote tyrosine phosphorylation of occludin in brain endothelial cells (Kago, Takagi et al. 2006). Tyrosine phosphorylation of occludin was shown to disrupt tight junctions due to the decreased interaction with ZO proteins (Kale, Naren et al. 2003). Phosphorylation of ZO1 and occludin correlated to increased permeability of endothelial cells (Antonetti, Barber et al. 1999). Therefore, we think that in our mCCD cells, HIF-stabilization may have increased VEGF level causing alterations of renal epithelial tight junctions and increasing paracellular permeability through similar mechanisms.

By introducing point mutations and replacing serine and threonine residues of occludin and tyrosine residues of ZO1 with alanine residues if we can block the effect of HIF-stabilization by $CoCl_2$, we can investigate if the phosphorylation of tight junction proteins are directly involved in the effect of HIF-stabilization on altered epithelial transport. We suspect that the loss and mislocalization of tight junction proteins may cause mislocalization and apical distribution of Na^+/ K^+-ATPase to the apical membrane and may cause movement Na^+ in the opposite direction. If by blocking the effect of HIF on tight junction proteins, the effect of HIF-stabilization on Na^+/ K^+-ATPase can be blocked, then we can confirm whether the HIF-stabilization affects Na^+/ K^+-ATPase directly or indirectly. By inhibiting the action of VEGF, if the effect of HIF-stabilization can be blocked, we can confirm the direct effect of HIF-stabilization on tight junction protein. We suspect that the decreased level and loss of Na^+/ K^+-ATPase is also directly contributed by phosphorylation and ubiquitination of Na^+/ K^+-ATPase α1 subunit. By introducing point mutations of amino acid at the phosphorylation site of Na^+/ K^+-ATPase α1 subunit, if we can prevent the loss of Na^+/ K^+-ATPase due to HIF-stabilization by $CoCl_2$, the direct effect of HIF-stabilization on Na^+/ K^+-ATPase α1 subunit can be verified.

3.3 Conclusion

In summary, in mCCD monolayers, we noted that HIF-stabilization by $CoCl_2$ caused a loss of negative I_{eq} and showed a positive I_{eq} value in the absence of fluid flow, indicating that there was a switch in the direction of net Na^+ movement through active transport. Thus, our absorptive mCCD epithelial monolayer may have transformed into a secretory monolayer. The loss of I_{eq} was consistent with decreased level of Na^+/ K^+-ATPase α1. We suspect that the apical redistribution of Na^+/ K^+-ATPase α1 may be

responsible for the switch in the direction of active ion transport. In mCCD monolayers, HIF-stabilization showed a significant decrease of the TER values and increase in 70 kDa paracellular permeability. Decreased level ZO1 was consistent with increased paracellular permeability and decreased TER in mCCD monolayers. In MDCK monolayers, HIF-stabilization also showed significant increase of 70 kDa paracellular permeability. Thus, HIF stabilization seems to affect both the transcellular and paracellular pathways of kidney epithelial monolayers. Increased FITC-dextran permeability through cellular monolayers of mCCD and MDCK indicated altered selective epithelial barrier function. Moreover, we identified that Co^{2+} uptake occurs via basolateral side of monolayers. In conclusion, we have provided evidence in support of our hypothesis that HIF-stabilization can reverse net sodium transport and increases permeability of renal epithelial monolayers. Thus, chronic stabilization of HIF, as experienced by normal epithelial cells near to a cyst, can transform normal absorptive phenotype of epithelial cells to a leaky and secretory cyst-like phenotype and may contribute to cyst expansion and PKD progression.

3.4 Future Directions

1. Using immunocytochemistry, possible Na^+/ K^+-ATPase redistribution from basolateral to apical side due to HIF-stabilization can be checked.
2. If functional Na^+/ K^+-ATPase pumps are redistributed to the apical membrane, apical application of ouabain will be able to block the positive I_{eq} seen due to HIF-stabilization.
3. Occludin protein level can be decreased due to HIF-stabilization as known in the literature. This can be checked by western blots.

4. Under the discussion section, we pointed out that VEGF may be the key player in altering renal epithelial tight junctions due to HIF-stabilization. By checking VEGF level after HIF-stabilization can establish the direction connection between HIF-stabilization and altered tight junctions. We suspect that the redistribution of Na^+/ K^+-ATPase occurs as an indirect response to the alteration of actin cytoskeleton and tight junctions by HIF-stabilization. The direct effect of VEGF on tight junctions and indirect on Na^+/ K^+-ATPase can be better understood by using an anti-VEGF antibody.
5. By introducing point mutations of phosphorylation sites of ZO1 and Occludin, the effect of HIF-stabilization by $CoCl_2$ through VEGF can be confirmed.
6. By causing point mutations of amino acid at the phosphorylation site of Na^+/ K^+-ATPase α1 subunit, the direct effect of HIF-stabilization by $CoCl_2$ on the decreased level of Na^+/ K^+-ATPase can be investigated.
7. Use of a chemical inhibitor against HIF-1α will help to strengthen the connection between HIF-stabilization and altered transepithelial transport. The cellular monolayers will be pretreated with the inhibitor, followed by the treatment with $CoCl_2$. HIF1α inhibitor (Santa Cruz Biotechnology, sc-205346) used in a preliminary study can be used. Other, HIF-inhibitors such as chetomin and echinomycin, can be used depending on the effectiveness.
8. Study using another HIF-stabilizer such as, iron chelator DFX may also further strengthen the connection between HIF-stabilization and altered transepithelial transport.

9. Use of a hypoxic chamber will help to understand the effect low O_2 level on transepithelial transport in our mCCD monolayers. The expected findings of active epithelial transport in a hypoxic chamber may be similar to the study reported previously (Husted, Lu et al. 2010) and somewhat consistent with our current findings.
10. Comparisons among transcellular and paracellular transports in ciliated and deciliated mCCD monolayers with or without HIF-stabilization will help us understand the role of ciliary flow-sensing on altered transepithelial transport due to HIF-stabilization.

Funding Support

This research was supported by the Dr. John Vitullos Pilot and Bridge Funding Program at the Center for Gene Regulation in Health and Disease (GRHD) and NIH DK092716 award to Dr. Andrew Resnick and Cleveland State University Dissertation Research Award to Subhra Nag.

References

Abbott, N., P. Revest, et al. (1997). "Preparation of primary rat brain endothelial cell culture. Modified method of CCW Hughes." Drug transport across the blood-brain barrier: in vitro and in vivo techniques. Harwood Academic Publishers, Amsterdam.

Ahn, K., K. M. Madsen, et al. (1993). "Differential expression and cellular distribution of mRNAs encoding alpha-and beta-isoforms of Na (+)-K (+)-ATPase in rat kidney." American Journal of Physiology-Renal Physiology **265**(6): F792-F801.

Alexandre, M. D., Q. Lu, et al. (2005). "Overexpression of claudin-7 decreases the paracellular Cl–conductance and increases the paracellular Na+ conductance in LLC-PK1 cells." Journal of cell science **118**(12): 2683-2693.

Alton, E. and S. Smith (1995). "Applied cell biology." Cystic Fibrosis. Chapman & Hall, London: 41-73.

Anderson, J. M. (2001). "Molecular structure of tight junctions and their role in epithelial transport." Physiology **16**(3): 126-130.

Anderson, J. M. and C. M. Van Itallie (2009). "Physiology and function of the tight junction." Cold Spring Harbor perspectives in biology **1**(2): a002584.

Andringa, K. K. and A. Agarwal (2014). "Role of hypoxia-inducible factors in acute kidney injury." Nephron Clinical Practice **127**(1-4): 70-74.

Antonetti, D. A., A. J. Barber, et al. (1999). "Vascular endothelial growth factor induces rapid phosphorylation of tight junction proteins occludin and zonula occluden 1 A potential mechanism for vascular permeability in diabetic retinopathy and tumors." Journal of Biological Chemistry **274**(33): 23463-23467.

Aranda, V., T. Haire, et al. (2006). "Par6–aPKC uncouples ErbB2 induced disruption of polarized epithelial organization from proliferation control." Nature cell biology **8**(11): 1235.

Artursson, P. (1990). "Epithelial transport of drugs in cell culture. I: A model for studying the passive diffusion of drugs over intestinal absorbtive (Caco-2) cells." Journal of pharmaceutical sciences **79**(6): 476-482.

ávan der Meer, A. D., H. JungáKim, et al. (2015). "Measuring direct current trans-epithelial electrical resistance in organ-on-a-chip microsystems." Lab on a Chip **15**(3): 745-752.

Avner, E. D., W. E. Sweeney, et al. (1992). "Abnormal sodium pump distribution during renal tubulogenesis in congenital murine polycystic kidney disease." Proceedings of the National Academy of Sciences **89**(16): 7447-7451.

Bacic, M., N. A. Edwards, et al. (1995). "Differential expression of vascular endothelial growth factor (vascular permeabilty factor) forms in rat tissues." Growth Factors **12**(1): 11-15.

Balda, M. S. and K. Matter (2000). "The tight junction protein ZO-1 and an interacting transcription factor regulate ErbB-2 expression." The EMBO journal **19**(9): 2024-2033.

Balda, M. S. and K. Matter (2000). Transmembrane proteins of tight junctions. Seminars in cell & developmental biology, Elsevier.

Balda, M. S. and K. Matter (2007). Size-selective assessment of tight junction paracellular permeability using fluorescently labelled dextrans, bmglabtech Ortenberg, Germany.

Balda, M. S., J. A. Whitney, et al. (1996). "Functional dissociation of paracellular permeability and transepithelial electrical resistance and disruption of the apical-basolateral intramembrane diffusion barrier by expression of a mutant tight junction membrane protein." The Journal of cell biology **134**(4): 1031-1049.

Bamberg, E. and W. Schoner (2012). The sodium pump: structure mechanism, hormonal control and its role in disease, Springer Science & Business Media.

Basile, D. P., M. D. Anderson, et al. (2012). "Pathophysiology of acute kidney injury." Comprehensive Physiology **2**(2): 1303.

Becker, J. U., A. O. Saez, et al. (2010). "The mTOR pathway is activated in human autosomal-recessive polycystic kidney disease." Kidney and Blood Pressure Research **33**(2): 129-138.

Beguin, P., A. T. Beggah, et al. (1994). "Phosphorylation of the Na, K-ATPase alpha-subunit by protein kinase A and C in vitro and in intact cells. Identification of a novel motif for PKC-mediated phosphorylation." Journal of Biological Chemistry **269**(39): 24437-24445.

Belibi, F. A., G. Reif, et al. (2004). "Cyclic AMP promotes growth and secretion in human polycystic kidney epithelial cells1." Kidney international **66**(3): 964-973.

Bello-Reuss, E., K. Holubec, et al. (2001). "Angiogenesis in autosomal-dominant polycystic kidney disease." Kidney international **60**(1): 37-45.

Bellomo, R., J. A. Kellum, et al. (2012). "Acute kidney injury." The lancet **380**(9843): 756-766.

Benson, K., S. Cramer, et al. (2013). "Impedance-based cell monitoring: barrier properties and beyond." Fluids and Barriers of the CNS **10**(1): 5.

Bernhardt, W. M., M. S. Wiesener, et al. (2007). "Involvement of hypoxia-inducible transcription factors in polycystic kidney disease." The American journal of pathology **170**(3): 830-842.

Bertorello, A. M. and A. I. Katz (1993). "Short-term regulation of renal Na-K-ATPase activity: physiological relevance and cellular mechanisms." American Journal of Physiology-Renal Physiology **265**(6): F743-F755.

Bertrand, C., D. Durand, et al. (1998). "System for dynamic measurements of membrane capacitance in intact epithelial monolayers." Biophysical journal **75**(6): 2743-2756.

Besschetnova, T. Y., E. Kolpakova-Hart, et al. (2010). "Identification of signaling pathways regulating primary cilium length and flow-mediated adaptation." Current Biology **20**(2): 182-187.

Beuchat, C. A. (1996). "Structure and concentrating ability of the mammalian kidney: correlations with habitat." American Journal of Physiology-Regulatory, Integrative and Comparative Physiology **271**(1): R157-R179.

Bhalla, V. and K. R. Hallows (2008). "Mechanisms of ENaC regulation and clinical implications." Journal of the american society of nephrology **19**(10): 1845-1854.

Bhunia, A. K., K. Piontek, et al. (2002). "PKD1 induces p21waf1 and regulation of the cell cycle via direct activation of the JAK-STAT signaling pathway in a process requiring PKD2." Cell **109**(2): 157-168.

Blanco, G. and R. W. Mercer (1998). "Isozymes of the Na-K-ATPase: heterogeneity in structure, diversity in function." American Journal of Physiology-Renal Physiology **275**(5): F633-F650.

Blaustein, M. P. (1993). "Physiological effects of endogenous ouabain: control of intracellular Ca2+ stores and cell responsiveness." American Journal of Physiology-Cell Physiology **264**(6): C1367-C1387.

Bonventre, J. V. (2003). "Dedifferentiation and proliferation of surviving epithelial cells in acute renal failure." Journal of the american society of nephrology **14**(suppl 1): S55-S61.

Boron, W. F. and E. L. Boulpaep (1989). "The electrogenic Na/HCO3 cotransporter." Kidney international **36**(3): 392-402.

Bouvry, D., C. Planes, et al. (2006). "Hypoxia-induced cytoskeleton disruption in alveolar epithelial cells." American journal of respiratory cell and molecular biology **35**(5): 519-527.

Breiderhoff, T., N. Himmerkus, et al. (2012). "Deletion of claudin-10 (Cldn10) in the thick ascending limb impairs paracellular sodium permeability and leads to hypermagnesemia and nephrocalcinosis." Proceedings of the National Academy of Sciences **109**(35): 14241-14246.

Brill, S. R., K. E. Ross, et al. (1996). "Immunolocalization of ion transport proteins in human autosomal dominant polycystic kidney epithelial cells." Proceedings of the National Academy of Sciences **93**(19): 10206-10211.

Brown, N. E. and N. S. Murcia (2003). "Delayed cystogenesis and increased ciliogenesis associated with the re-expression of polaris in Tg737 mutant mice." Kidney international **63**(4): 1220-1229.

Brown, R. C. and T. P. Davis (2005). "Hypoxia/aglycemia alters expression of occludin and actin in brain endothelial cells." Biochemical and biophysical research communications **327**(4): 1114-1123.

Bruick, R. K. and S. L. McKnight (2001). "A conserved family of prolyl-4-hydroxylases that modify HIF." Science **294**(5545): 1337-1340.

Buchholz, B., G. Schley, et al. (2013). "Hypoxia-inducible factor-1α causes renal cyst expansion through calcium-activated chloride secretion." Journal of the american society of nephrology: ASN. 2013030209.

Butterworth, M. B. (2010). "Regulation of the epithelial sodium channel (ENaC) by membrane trafficking." Biochimica et Biophysica Acta (BBA)-Molecular Basis of Disease **1802**(12): 1166-1177.

Butterworth, M. B., R. S. Edinger, et al. (2005). "Acute ENaC stimulation by cAMP in a kidney cell line is mediated by exocytic insertion from a recycling channel pool." The Journal of general physiology **125**(1): 81-101.

Calvet, J. P. (2002). "Cilia in PKD—letting it all hang out." Journal of the american society of nephrology **13**(10): 2614-2616.

Canessa, C. M., L. Schild, et al. (1994). "Amiloride-sensitive epithelial Na+ channel is made of three homologous subunits." Nature **367**(6462): 463.

Cano, D. A., N. S. Murcia, et al. (2004). "Orpk mouse model of polycystic kidney disease reveals essential role of primary cilia in pancreatic tissue organization." Development **131**(14): 3457-3467.

Capaldo, C. T. and I. G. Macara (2007). "Depletion of E-cadherin disrupts establishment but not maintenance of cell junctions in Madin-Darby canine kidney epithelial cells." Molecular biology of the cell **18**(1): 189-200.

Caraballo, J. C., C. Yshii, et al. (2011). "Hypoxia increases transepithelial electrical conductance and reduces occludin at the plasma membrane in alveolar epithelial cells via PKC-zeta and PP2A pathway." Am J Physiol Lung Cell Mol Physiol **300**(4): L569-578.

Caraballo, J. C., C. Yshii, et al. (2011). "Hypoxia increases transepithelial electrical conductance and reduces occludin at the plasma membrane in alveolar epithelial

cells via PKC-ζ and PP2A pathway." American Journal of Physiology-Lung Cellular and Molecular Physiology **300**(4): L569-L578.

Carafoli, E. (1994). "Biogenesis: plasma membrane calcium ATPase: 15 years of work on the purified enzyme." The FASEB Journal **8**(13): 993-1002.

Cereijido, M., L. Gonzalez-Mariscal, et al. (1983). "Occluding junctions and paracellular pathways studied in monolayers of MDCK cells." Journal of Experimental Biology **106**(1): 205-215.

Cereijido, M., L. Shoshani, et al. (2000). "Molecular physiology and pathophysiology of tight junctions I. Biogenesis of tight junctions and epithelial polarity." American Journal of Physiology-Gastrointestinal and Liver Physiology **279**(3): G477-G482.

Chang, M. Y., E. Parker, et al. (2006). "Haploinsufficiency of Pkd2 is associated with increased tubular cell proliferation and interstitial fibrosis in two murine Pkd2 models." Nephrology Dialysis Transplantation **21**(8): 2078-2084.

Charron, A. J., S. Nakamura, et al. (2000). "Compromised cytoarchitecture and polarized trafficking in autosomal dominant polycystic kidney disease cells." The Journal of cell biology **149**(1): 111-124.

Chauvet, V., X. Tian, et al. (2004). "Mechanical stimuli induce cleavage and nuclear translocation of the polycystin-1 C terminus." The Journal of clinical investigation **114**(10): 1433-1443.

Chen, J., I. Sgouralis, et al. (2010). "A mathematical model of the myogenic response to systolic pressure in the afferent arteriole." American Journal of Physiology-Renal Physiology **300**(3): F669-F681.

Choi, Y.-J., S. Chakraborty, et al. (2000). "Peritubular capillary loss is associated with chronic tubulointerstitial injury in human kidney: altered expression of vascular endothelial growth factor." Human pathology **31**(12): 1491-1497.

Clarke, L. L. (2009). "A guide to Ussing chamber studies of mouse intestine." American Journal of Physiology-Gastrointestinal and Liver Physiology **296**(6): G1151-G1166.

Coresh, J., E. Selvin, et al. (2007). "Prevalence of chronic kidney disease in the United States." Jama **298**(17): 2038-2047.

Cowley, B. D. (2004). "Recent Advances in Understanding the Pathogenesis of Polycystic Kidney Disease." Drugs **64**(12): 1285-1294.

Dada, L. A., N. S. Chandel, et al. (2003). "Hypoxia-induced endocytosis of Na, K-ATPase in alveolar epithelial cells is mediated by mitochondrial reactive oxygen species and PKC-ζ." The Journal of clinical investigation **111**(7): 1057-1064.

Dada, L. A., L. C. Welch, et al. (2007). "Phosphorylation and ubiquitination are necessary for Na, K-ATPase endocytosis during hypoxia." Cellular signalling **19**(9): 1893-1898.

Deane, J. A. and S. D. Ricardo (2007). "Polycystic kidney disease and the renal cilium." Nephrology **12**(6): 559-564.

Delling, M., A. Indzhykulian, et al. (2016). "Primary cilia are not calcium-responsive mechanosensors." Nature **531**(7596): 656.

Denker, B. M. and E. Sabath (2011). "The biology of epithelial cell tight junctions in the kidney." Journal of the american society of nephrology **22**(4): 622-625.

Devarajan, P. (2006). "Update on mechanisms of ischemic acute kidney injury." Journal of the american society of nephrology **17**(6): 1503-1520.

Devuyst, O., C. R. Burrow, et al. (1996). "Expression of aquaporins-1 and-2 during nephrogenesis and in autosomal dominant polycystic kidney disease." American Journal of Physiology-Renal Physiology **271**(1): F169-F183.

Eakle, K., M. Kabalin, et al. (1994). "The influence of beta subunit structure on the stability of Na+/K (+)-ATPase complexes and interaction with K+." Journal of Biological Chemistry **269**(9): 6550-6557.

Eakle, K. A., R.-M. Lyu, et al. (1995). "The influence of subunit structure on the interaction of Na/K-ATPase complexes with Na. A chimeric β subunit reduces the Na dependence of phosphoenzyme formation from ATP." Journal of Biological Chemistry **270**(23): 13937-13947.

Eckardt, K., M. Möllmann, et al. (1989). "Erythropoietin in polycystic kidneys." The Journal of clinical investigation **84**(4): 1160-1166.

Elliott, J., N. N. Zheleznova, et al. (2011). "c-Src inactivation reduces renal epithelial cell-matrix adhesion, proliferation, and cyst formation." American Journal of Physiology-Cell Physiology **301**(2): C522-C529.

Engel, A., T. Walz, et al. (1994). "The aquaporin family of membrane water channels." Current Opinion in Structural Biology **4**(4): 545-553.

Engelhardt, S., A. J. Al-Ahmad, et al. (2014). "Hypoxia selectively disrupts brain microvascular endothelial tight junction complexes through a Hypoxia-Inducible Factor-1 (HIF-1) dependent mechanism." Journal of cellular physiology **229**(8): 1096-1105.

Epstein, A. C., J. M. Gleadle, et al. (2001). "C. elegans EGL-9 and mammalian homologs define a family of dioxygenases that regulate HIF by prolyl hydroxylation." Cell **107**(1): 43-54.

Fandrey, J., S. Frede, et al. (1997). "Cobalt chloride and desferrioxamine antagonize the inhibition of erythropoietin production by reactive oxygen species." Kidney international **51**(2): 492-496.

Farman, N., I. Corthesy-Theulaz, et al. (1991). "Localization of alpha-isoforms of Na (+)-K (+)-ATPase in rat kidney by in situ hybridization." American Journal of Physiology-Cell Physiology **260**(3): C468-C474.

Farquhar, M. G. and G. E. Palade (1963). "Junctional complexes in various epithelia." The Journal of cell biology **17**(2): 375-412.

Féraille, E. and A. Doucet (2001). "Sodium-potassium-adenosinetriphosphatase-dependent sodium transport in the kidney: hormonal control." Physiological reviews **81**(1): 345-418.

Feschenko, M. S., E. Stevenson, et al. (2000). "Interaction of protein kinase C and cAMP-dependent pathways in the phosphorylation of the Na, K-ATPase." Journal of Biological Chemistry **275**(44): 34693-34700.

Fick, A. (1855). "V. On liquid diffusion." Philosophical Magazine Series 4 **10**(63): 30-39.

FISHER, J. W. and J. Langston (1967). "The influence of hypoxemia and cobalt on erythropoietin production in the isolated perfused dog kidney." Blood **29**(1): 114-125.

Fisone, G., S. Cheng, et al. (1994). "Identification of the phosphorylation site for cAMP-dependent protein kinase on Na+, K (+)-ATPase and effects of site-directed mutagenesis." Journal of Biological Chemistry **269**(12): 9368-9373.

Flannery, R. J., N. K. Kleene, et al. (2015). "A TRPM4-dependent current in murine renal primary cilia." American Journal of Physiology-Renal Physiology **309**(8): F697-F707.

Fong, P. and T. Jentsch (1995). "Molecular basis of epithelial Cl channels." The Journal of membrane biology **144**(3): 189-197.

Forbes, J. R. and P. Gros (2003). "Iron, manganese, and cobalt transport by Nramp1 (Slc11a1) and Nramp2 (Slc11a2) expressed at the plasma membrane." Blood **102**(5): 1884-1892.

Forsythe, J. A., B.-H. Jiang, et al. (1996). "Activation of vascular endothelial growth factor gene transcription by hypoxia-inducible factor 1." Molecular and cellular biology **16**(9): 4604-4613.

Friedman, P. A. and F. A. Gesek (1993). "Calcium transport in renal epithelial cells." American Journal of Physiology-Renal Physiology **264**(2): F181-F198.

Frindt, G., Z. Ergonul, et al. (2008). "Surface expression of epithelial Na channel protein in rat kidney." The Journal of general physiology **131**(6): 617-627.

Fromter, E. and J. Diamond (1972). "Route of passive ion permeation in epithelia." Nat New Biol **235**(53): 9-13.

Fuchs, W., E. H. Larsen, et al. (1977). "Current—voltage curve of sodium channels and concentration dependence of sodium permeability in frog skin." The Journal of physiology **267**(1): 137-166.

Furuse, M., K. Fujita, et al. (1998). "Claudin-1 and-2: novel integral membrane proteins localizing at tight junctions with no sequence similarity to occludin." The Journal of cell biology **141**(7): 1539-1550.

Futrakul, N., V. Vongthavarawat, et al. (2005). "Tubular dysfunction and hemodynamic alteration in normoalbuminuric type 2 diabetes." Clinical hemorheology and microcirculation **32**(1): 59-65.

Gabow, P. A. (1993). "Autosomal dominant polycystic kidney disease." New England Journal of Medicine **329**(5): 332-342.

Gaillard, P. J., L. H. Voorwinden, et al. (2001). "Establishment and functional characterization of an in vitro model of the blood–brain barrier, comprising a co-culture of brain capillary endothelial cells and astrocytes." European journal of pharmaceutical sciences **12**(3): 215-222.

Garty, H. (1994). "Molecular properties of epithelial, amiloride-blockable Na+ channels." The FASEB Journal **8**(8): 522-528.

Gekle, M., S. Wünsch, et al. (1994). "Characterization of two MDCK-cell subtypes as a model system to study principal cell and intercalated cell properties." Pflügers Archiv European Journal of Physiology **428**(2): 157-162.

Gilula, N. B. and P. Satir (1972). "The ciliary necklace: a ciliary membrane specialization." The Journal of cell biology **53**(2): 494-509.

Gluck, S. L., D. M. Underhill, et al. (1996). "Physiology and biochemistry of the kidney vacuolar H+-ATPase." Annual review of physiology **58**(1): 427-445.

Glynn, I. (1985). The Na+, K+-transporting adenosine triphosphatase. The enzymes of biological membranes, Springer**:** 35-114.

Gonzalez-Mariscal, L., B. C. De Ramirez, et al. (1985). "Tight junction formation in cultured epithelial cells (MDCK)." The Journal of membrane biology **86**(2): 113-125.

Gonzalez-Mariscal, L., B. C. De Ramirez, et al. (1989). "Establishment of tight junctions between cells from different animal species and different sealing capacities." The Journal of membrane biology **107**(1): 43-56.

Gonzalez-Mariscal, L., M. C. Namorado, et al. (2000). "Tight junction proteins ZO-1, ZO-2, and occludin along isolated renal tubules1." Kidney international **57**(6): 2386-2402.

Gottschalk, C. W. and M. Mylle (1959). "Micropuncture study of the mammalian urinary concentrating mechanism: evidence for the countercurrent hypothesis." American Journal of Physiology-Legacy Content **196**(4): 927-936.

Grantham, J. J. (1996). "The etiology, pathogenesis, and treatment of autosomal dominant polycystic kidney disease: recent advances." American journal of kidney diseases **28**(6): 788-803.

Graven, K. K., Q. Yu, et al. (1999). "Identification of an oxygen responsive enhancer element in the glyceraldehyde-3-phosphate dehydrogenase gene." Biochimica et Biophysica Acta (BBA)-Gene Structure and Expression **1447**(2-3): 208-218.

Greger, R., M. Bleich, et al. (1997). "Regulation of ion transport in colonic crypts." Physiology **12**(2): 62-66.

Gunshin, H., B. Mackenzie, et al. (1997). "Cloning and characterization of a mammalian proton-coupled metal-ion transporter." Nature **388**(6641): 482-488.

Guo, J.-K. and L. G. Cantley (2010). "Cellular maintenance and repair of the kidney." Annual review of physiology **72**: 357-376.

Haas, M. (1994). "The Na-K-Cl cotransporters." American Journal of Physiology-Cell Physiology **267**(4): C869-C885.

Haase, V. (2006). "The VHL/HIF oxygen-sensing pathway and its relevance to kidney disease." Kidney international **69**(8): 1302-1307.

Haase, V. H. (2006). "Hypoxia-inducible factors in the kidney." American Journal of Physiology-Renal Physiology **291**(2): F271-F281.

Haase, V. H. (2009). "The VHL tumor suppressor: master regulator of HIF." Current pharmaceutical design **15**(33): 3895-3903.

Haase, V. H. (2013). "Mechanisms of hypoxia responses in renal tissue." Journal of the american society of nephrology: ASN. 2012080855.

Hamm, L. L., Z. Feng, et al. (2010). "Regulation of sodium transport by ENaC in the kidney." Current opinion in nephrology and hypertension **19**(1): 98.

Hanaoka, K., O. Devuyst, et al. (1996). "A role for CFTR in human autosomal dominant polycystic kidney disease." American Journal of Physiology-Cell Physiology **270**(1): C389-C399.

Hanwell, D., T. Ishikawa, et al. (2002). "Trafficking and cell surface stability of the epithelial Na+ channel expressed in epithelial Madin-Darby canine kidney cells." Journal of Biological Chemistry **277**(12): 9772-9779.

Harhaj, N. S., E. A. Felinski, et al. (2006). "VEGF activation of protein kinase C stimulates occludin phosphorylation and contributes to endothelial permeability." Investigative ophthalmology & visual science **47**(11): 5106-5115.

Harten, S. K., D. Shukla, et al. (2009). "Regulation of renal epithelial tight junctions by the von Hippel-Lindau tumor suppressor gene involves occludin and claudin 1 and is independent of E-cadherin." Molecular biology of the cell **20**(3): 1089-1101.

Health, N. I. o. (2010). "US renal data systems: USRDS 2010 annual data report: atlas of end stage renal disease in the United States." http://www. usrds. org/2010/view/default. asp.

Higgins, D. F., K. Kimura, et al. (2007). "Hypoxia promotes fibrogenesis in vivo via HIF-1 stimulation of epithelial-to-mesenchymal transition." The Journal of clinical investigation **117**(12): 3810-3820.

Hille, B. (2001). Ion channels of excitable membranes, Sinauer Sunderland, MA.

Hirsilä, M., P. Koivunen, et al. (2005). "Effect of desferrioxamine and metals on the hydroxylases in the oxygen sensing pathway." The FASEB Journal **19**(10): 1308-1310.

Ho, K., C. G. Nichols, et al. (1993). "Cloning and expression of an inwardly rectifying ATP-regulated potassium channel." Nature **362**(6415): 31.

Holstein-Rathlou, N. and D. Marsh (1989). "Oscillations of tubular pressure, flow, and distal chloride concentration in rats." American Journal of Physiology-Renal Physiology **256**(6): F1007-F1014.

Hou, X., M. Mrug, et al. (2002). "Cystin, a novel cilia-associated protein, is disrupted in the cpk mouse model of polycystic kidney disease." The Journal of clinical investigation **109**(4): 533-540.

Huan, Y. and J. van Adelsberg (1999). "Polycystin-1, the PKD1 gene product, is in a complex containing E-cadherin and the catenins." The Journal of clinical investigation **104**(10): 1459-1468.

Huang, L. E., Z. Arany, et al. (1996). "Activation of hypoxia-inducible transcription factor depends primarily upon redox-sensitive stabilization of its α subunit." Journal of Biological Chemistry **271**(50): 32253-32259.

Huang, L. E., J. Gu, et al. (1998). "Regulation of hypoxia-inducible factor 1α is mediated by an O2-dependent degradation domain via the ubiquitin-proteasome pathway." Proceedings of the National Academy of Sciences **95**(14): 7987-7992.

Husted, R. F., H. Lu, et al. (2010). "Oxygen regulation of the epithelial Na channel in the collecting duct." American Journal of Physiology-Renal Physiology **300**(2): F412-F424.

Israeli, S., K. Amsler, et al. (2010). "Focal adhesion complex abnormalities in human autosomal recessive polycystic kidney disease (ARPKD)." Am. J. Physiol. Cell Physiol **298**: C831-C846.

Ivan, M., K. Kondo, et al. (2001). "HIFα targeted for VHL-mediated destruction by proline hydroxylation: implications for O2 sensing." Science **292**(5516): 464-468.

Jaakkola, P., D. R. Mole, et al. (2001). "Targeting of HIF-α to the von Hippel-Lindau ubiquitylation complex by O2-regulated prolyl hydroxylation." Science **292**(5516): 468-472.

Jain, M. and J. I. Sznajder (2005). "Effects of hypoxia on the alveolar epithelium." Proceedings of the American Thoracic Society **2**(3): 202-205.

Jat, P. S., M. D. Noble, et al. (1991). "Direct derivation of conditionally immortal cell lines from an H-2Kb-tsA58 transgenic mouse." Proceedings of the National Academy of Sciences **88**(12): 5096-5100.

Jin, X., A. M. Mohieldin, et al. (2014). "Cilioplasm is a cellular compartment for calcium signaling in response to mechanical and chemical stimuli." Cellular and molecular life sciences **71**(11): 2165-2178.

Jørgensen, P. L. (1990). "Structure and molecular mechanism of the Na, K." Monovalent Cations in Biological Systems: 117.

Jover, R., X. Ponsoda, et al. (1994). "Acute cytotoxicity of ten chemicals in human and rat cultured hepatocytes and in cell lines: Correlation between in vitro data and human lethal concentrations." Toxicology in vitro **8**(1): 47-54.

Kabra, R., K. K. Knight, et al. (2008). "Nedd4-2 induces endocytosis and degradation of proteolytically cleaved epithelial Na+ channels." Journal of Biological Chemistry **283**(10): 6033-6039.

Kago, T., N. Takagi, et al. (2006). "Cerebral ischemia enhances tyrosine phosphorylation of occludin in brain capillaries." Biochemical and biophysical research communications **339**(4): 1197-1203.

Kairaitis, L. K., Y. Wang, et al. (2005). "HIF-1α expression follows microvascular loss in advanced murine adriamycin nephrosis." American Journal of Physiology-Renal Physiology **288**(1): F198-F206.

Kaiser, M., S. Pereira, et al. (2015). "Chitosan encapsulation modulates the effect of capsaicin on the tight junctions of MDCK cells." Scientific reports **5**: 10048.

Kale, G., A. Naren, et al. (2003). "Tyrosine phosphorylation of occludin attenuates its interactions with ZO-1, ZO-2, and ZO-3." Biochemical and biophysical research communications **302**(2): 324-329.

Kamura, T., S. Sato, et al. (2000). "Activation of HIF1α ubiquitination by a reconstituted von Hippel-Lindau (VHL) tumor suppressor complex." Proceedings of the National Academy of Sciences **97**(19): 10430-10435.

Kang, J. J., I. Toma, et al. (2006). "Quantitative imaging of basic functions in renal (patho) physiology." American Journal of Physiology-Renal Physiology **291**(2): F495-F502.

Karihaloo, A., S. A. Karumanchi, et al. (2005). "Vascular endothelial growth factor induces branching morphogenesis/tubulogenesis in renal epithelial cells in a neuropilin-dependent fashion." Molecular and cellular biology **25**(17): 7441-7448.

Kellenberger, S., N. Hoffmann-Pochon, et al. (1999). "On the molecular basis of ion permeation in the epithelial Na+ channel." The Journal of general physiology **114**(1): 13-30.

Kiuchi-Saishin, Y., S. Gotoh, et al. (2002). "Differential expression patterns of claudins, tight junction membrane proteins, in mouse nephron segments." Journal of the american society of nephrology **13**(4): 875-886.

Koefoed-Johnsen, V. and H. H. Ussing (1958). "The nature of the frog skin potential." Acta Physiologica **42**(3-4): 298-308.

Koizumi, J.-i., T. Kojima, et al. (2007). "Changes of gap and tight junctions during differentiation of human nasal epithelial cells using primary human nasal

epithelial cells and primary human nasal fibroblast cells in a noncontact coculture system." Journal of Membrane Biology **218**(1-3): 1-7.

Kolb, R. J., P. G. Woost, et al. (2004). "Membrane trafficking of angiotensin receptor type-1 and mechanochemical signal transduction in proximal tubule cells." Hypertension **44**(3): 352-359.

KozMINSKI, K. G., K. A. Johnson, et al. (1993). "A motility in the eukaryotic flagellum unrelated to flagellar beating." Proceedings of the National Academy of Sciences **90**(12): 5519-5523.

Läuger, P. (1991). Electrogenic ion pumps.

Layton, A. T. (2012). "Modeling transport and flow regulatory mechanisms of the kidney." ISRN biomathematics **2012**.

Layton, A. T., H. E. Layton, et al. (2009). "The mammalian urine concentrating mechanism: hypotheses and uncertainties." Physiology **24**(4): 250-256.

Lea, T. (2015). Epithelial Cell Models; General Introduction. The Impact of Food Bioactives on Health: in vitro and ex vivo models. K. Verhoeckx, P. Cotter, I. López-Expósitoet al. Cham, Springer International Publishing**:** 95-102.

Lebeau, C., K. Hanaoka, et al. (2002). "Basolateral chloride transporters in autosomal dominant polycystic kidney disease." Pflügers Archiv **444**(6): 722-731.

Lee, K. L., M. D. Guevarra, et al. (2015). "The primary cilium functions as a mechanical and calcium signaling nexus." Cilia **4**(1): 7.

Leeuwen, I. S. L.-v., J. G. Dauwerse, et al. (2004). "Lowering of Pkd1 expression is sufficient to cause polycystic kidney disease." Human molecular genetics **13**(24): 3069-3077.

Lehman, J. M., E. J. Michaud, et al. (2008). "The Oak Ridge Polycystic Kidney mouse: modeling ciliopathies of mice and men." Developmental Dynamics **237**(8): 1960-1971.

Levenson, R. (1994). Isoforms of the Na, K-ATPase: family members in search of function. Reviews of Physiology, Biochemistry and Pharmacology, Volume 123, Springer**:** 1-45.

Levey, A. S., K.-U. Eckardt, et al. (2005). "Definition and classification of chronic kidney disease: a position statement from Kidney Disease: Improving Global Outcomes (KDIGO)." Kidney international **67**(6): 2089-2100.

Lewis, S. A. (1996). Epithelial electrophysiology. Epithelial Transport, Springer**:** 93-117.

Lewis, S. A. (1996). Epithelial structure and function. Epithelial Transport, Springer**:** 1-20.

Lewis, S. A., C. Clausen, et al. (1996). Impedance analysis of epithelia. Epithelial Transport, Springer**:** 118-145.

Leyssac, P. and L. Baumbach (1983). "An oscillating intratubular pressure response to alterations in Henle loop flow in the rat kidney." Acta Physiologica **117**(3): 415-419.

Li, H., I. A. Findlay, et al. (2004). "The relationship between cell proliferation, Cl− secretion, and renal cyst growth: a study using CFTR inhibitors." Kidney international **66**(5): 1926-1938.

Liedrke, C. (1989). "Regulation of chloride transport in epithelia." Annual review of physiology **51**(1): 143-160.

Lima, W. R., K. S. Parreira, et al. (2010). "ZONAB promotes proliferation and represses differentiation of proximal tubule epithelial cells." Journal of the american society of nephrology **21**(3): 478-488.

Lin, F., T. Hiesberger, et al. (2003). "Kidney-specific inactivation of the KIF3A subunit of kinesin-II inhibits renal ciliogenesis and produces polycystic kidney disease." Proceedings of the National Academy of Sciences **100**(9): 5286-5291.

Lingrel, J. B. (1992). "Na, K-ATPase: isoform structure, function, and expression." Journal of bioenergetics and biomembranes **24**(3): 263-270.

Lingrel, J. B., J. Van Huysse, et al. (1994). "Structure-function studies of the Na, K-ATPase." Kidney International Supplement(44).

Liu, J., R. Kesiry, et al. (2004). "Ouabain induces endocytosis of plasmalemmal Na/K-ATPase in LLC-PK1 cells by a clathrin-dependent mechanism." Kidney international **66**(1): 227-241.

Liu, W., N. S. Murcia, et al. (2005). "Mechanoregulation of intracellular Ca2+ concentration is attenuated in collecting duct of monocilium-impaired orpk mice." American Journal of Physiology-Renal Physiology **289**(5): F978-F988.

Loffing, J. and C. Korbmacher (2009). "Regulated sodium transport in the renal connecting tubule (CNT) via the epithelial sodium channel (ENaC)." Pflügers Archiv-European Journal of Physiology **458**(1): 111-135.

Lombardi, D., K. L. Gordon, et al. (1999). "Salt-sensitive hypertension develops after short-term exposure to angiotensin II." Hypertension **33**(4): 1013-1019.

Low, S. H., S. Vasanth, et al. (2006). "Polycystin-1, STAT6, and P100 function in a pathway that transduces ciliary mechanosensation and is activated in polycystic kidney disease." Developmental cell **10**(1): 57-69.

Lu, S., X. Gu, et al. (2002). "Identification of an additional hypoxia responsive element in the glyceraldehyde-3-phosphate dehydrogenase gene promoter." Biochimica et Biophysica Acta (BBA)-Gene Structure and Expression **1574**(2): 152-156.

Lübbers, D. W. and H. Baumgärtl (1997). "Heterogeneities and profiles of oxygen pressure in brain and kidney as examples of the pO2 distribution in the living tissue." Kidney international **51**(2): 372-380.

Lucking, K., J. M. Nielsen, et al. (1996). "Na-K-ATPase isoform (alpha 3, alpha 2, alpha 1) abundance in rat kidney estimated by competitive RT-PCR and ouabain binding." American Journal of Physiology-Renal Physiology **271**(2): F253-F260.

Luo, Y., P. M. Vassilev, et al. (2003). "Native polycystin 2 functions as a plasma membrane Ca2+-permeable cation channel in renal epithelia." Molecular and cellular biology **23**(7): 2600-2607.

Ma, T., J. R. Thiagarajah, et al. (2002). "Thiazolidinone CFTR inhibitor identified by high-throughput screening blocks cholera toxin–induced intestinal fluid secretion." The Journal of clinical investigation **110**(11): 1651-1658.

MacRobbie, E. A. and H. Ussing (1961). "Osmotic behaviour of the epithelial cells of frog skin." Acta Physiologica **53**(3-4): 348-365.

Magenheimer, B. S., P. L. S. John, et al. (2006). "Early embryonic renal tubules of wild-type and polycystic kidney disease kidneys respond to cAMP stimulation with cystic fibrosis transmembrane conductance regulator/Na+, K+, 2Cl− Co-

transporter–dependent cystic dilation." Journal of the american society of nephrology **17**(12): 3424-3437.

Magyar, C. E., K. E. White, et al. (2002). "Plasma membrane Ca2+-ATPase and NCX1 Na+/Ca2+ exchanger expression in distal convoluted tubule cells." American Journal of Physiology-Renal Physiology **283**(1): F29-F40.

Mairbäurl, H., K. Mayer, et al. (2002). "Hypoxia decreases active Na transport across primary rat alveolar epithelial cell monolayers." American Journal of Physiology-Lung Cellular and Molecular Physiology **282**(4): L659-L665.

Mairbäurl, H., K. Mayer, et al. (2002). "Hypoxia decreases active Na transport across primary rat alveolar epithelial cell monolayers." American Journal of Physiology-Lung Cellular and Molecular Physiology **282**(4): L659-L665.

Mairbäurl, H., R. Wodopia, et al. (1997). "Impairment of cation transport in A549 cells and rat alveolar epithelial cells by hypoxia." American Journal of Physiology-Lung Cellular and Molecular Physiology **273**(4): L797-L806.

Mandel, L. J., R. Bacallao, et al. (1993). "Uncoupling of the molecular'fence'and paracellular'gate'functions in epithelial tight junctions." Nature **361**(6412): 552.

Manotham, K., T. Tanaka, et al. (2004). "Transdifferentiation of cultured tubular cells induced by hypoxia." Kidney international **65**(3): 871-880.

Marshall Jr, E. and M. M. Crane (1924). "The secretory function of the renal tubules." American Journal of Physiology-Legacy Content **70**(3): 465-488.

Masson, N., C. Willam, et al. (2001). "Independent function of two destruction domains in hypoxia-inducible factor-α chains activated by prolyl hydroxylation." The EMBO journal **20**(18): 5197-5206.

Matter, K. and M. S. Balda (2003). "Functional analysis of tight junctions." Methods **30**(3): 228-234.

Maxwell, P. H., M. S. Wiesener, et al. (1999). "The tumour suppressor protein VHL targets hypoxia-inducible factors for oxygen-dependent proteolysis." Nature **399**(6733): 271.

McCarthy, K., S. Francis, et al. (2000). "Inducible expression of claudin-1-myc but not occludin-VSV-G results in aberrant tight junction strand formation in MDCK cells." Journal of Cell Science **113**(19): 3387-3398.

McDonough, A. A., K. Geering, et al. (1990). "The sodium pump needs its beta subunit." The FASEB Journal **4**(6): 1598-1605.

McKee, M., C. Scavone, et al. (1994). "Nitric oxide, cGMP, and hormone regulation of active sodium transport." Proceedings of the National Academy of Sciences **91**(25): 12056-12060.

Meer, G. v. and K. Simons (1986). "The function of tight junctions in maintaining differences in lipid composition between the apical and the basolateral cell surface domains of MDCK cells." The EMBO journal **5**(7): 1455-1464.

Mehta, R. L., J. A. Kellum, et al. (2007). "Acute Kidney Injury Network: report of an initiative to improve outcomes in acute kidney injury." Critical care **11**(2): R31.

Mercer, R. W. (1993). "Structure of the Na, K-ATPase." International review of cytology: 139-139.

Miettinen, H. M., K. Matter, et al. (1992). "Fc receptor endocytosis is controlled by a cytoplasmic domain determinant that actively prevents coated pit localization." The Journal of cell biology **116**(4): 875-888.

Mistry, A. C., B. M. Wynne, et al. (2016). "The sodium chloride cotransporter (NCC) and epithelial sodium channel (ENaC) associate." Biochemical Journal **473**(19): 3237-3252.

Molitoris, B. A. (1991). "Ischemia-induced loss of epithelial polarity: potential role of the actin cytoskeleton." American Journal of Physiology-Renal Physiology **260**(6): F769-F778.

Molitoris, B. A. (1993). "Na (+)-K (+)-ATPase that redistributes to apical membrane during ATP depletion remains functional." American Journal of Physiology-Renal Physiology **265**(5): F693-F697.

Molitoris, B. A., R. Dahl, et al. (1992). "Cytoskeleton disruption and apical redistribution of proximal tubule Na (+)-K (+)-ATPase during ischemia." American Journal of Physiology-Renal Physiology **263**(3): F488-F495.

Molitoris, B. A., R. Dahl, et al. (1996). "Cellular ATP depletion induces disruption of the spectrin cytoskeletal network." American Journal of Physiology-Renal Physiology **271**(4): F790-F798.

Morris, R. G. and J. A. Schafer (2002). "cAMP increases density of ENaC subunits in the apical membrane of MDCK cells in direct proportion to amiloride-sensitive Na+ transport." The Journal of general physiology **120**(1): 71-85.

Mosmann, T. (1983). "Rapid colorimetric assay for cellular growth and survival: application to proliferation and cytotoxicity assays." Journal of immunological methods **65**(1-2): 55-63.

Murakami, T., E. A. Felinski, et al. (2009). "Occludin phosphorylation and ubiquitination regulate tight junction trafficking and vascular endothelial growth factor (VEGF)-induced permeability." Journal of Biological Chemistry: jbc. M109. 016766.

Muto, S., M. Furuse, et al. (2012). "Claudins and renal salt transport." Clinical and experimental nephrology **16**(1): 61-67.

Muto, S., M. Hata, et al. (2010). "Claudin-2–deficient mice are defective in the leaky and cation-selective paracellular permeability properties of renal proximal tubules." Proceedings of the National Academy of Sciences **107**(17): 8011-8016.

Nadeau, J. L. (2017). Introduction to experimental biophysics: Biological methods for physical scientists, CRC Press.

Nag, S. and A. Resnick (2017). "Biophysics and biofluid dynamics of primary cilia: evidence for and against the flow-sensing function." American Journal of Physiology-Renal Physiology **313**(3): F706-F720.

Nag, S. and A. Resnick (2017). "Stabilization of hypoxia inducible factor by cobalt chloride can alter renal epithelial transport." Physiological reports **5**(24).

Nag, S. and A. Resnick (2018). "Paracellular Transport in the Mouse Kidney Cortical Collecting Duct Epithelial Monolayers Can Be Monitored By Measuring Transepithelial Resistance." The FASEB Journal **32**(1_supplement): 624.632-624.632.

Nag, S. and A. Resnick (2018). "Stabilization of Hypoxia Inducible Factor by Cobalt Chloride Can Alter Renal Epithelial Transport." The FASEB Journal **32**(1_supplement): 624.627-624.627.

Nangaku, M. (2006). "Chronic hypoxia and tubulointerstitial injury: a final common pathway to end-stage renal failure." Journal of the american society of nephrology **17**(1): 17-25.

Nangaku, M. and K.-U. Eckardt (2007). "Hypoxia and the HIF system in kidney disease." Journal of molecular medicine **85**(12): 1325-1330.

Nauli, S. M., F. J. Alenghat, et al. (2003). "Polycystins 1 and 2 mediate mechanosensation in the primary cilium of kidney cells." Nature genetics **33**(2): 129.

Niisato, N., A. Taruno, et al. (2007). "Aldosterone-induced modification of osmoregulated ENaC trafficking." Biochemical and biophysical research communications **361**(1): 162-168.

O'Connor, A. K., E. B. Malarkey, et al. (2013). "An inducible CiliaGFP mouse model for in vivo visualization and analysis of cilia in live tissue." Cilia **2**(1): 8.

O'Rourke, J. F., Y.-M. Tian, et al. (1999). "Oxygen-regulated and transactivating domains in endothelial PAS protein 1: comparison with hypoxia-inducible factor-1α." Journal of Biological Chemistry **274**(4): 2060-2071.

Obrien, W. J., J. B. Lingrel, et al. (1994). "Ouabain binding kinetics of the rat alpha two and alpha three isoforms of the sodium-potassium adenosine triphosphate." Archives of Biochemistry and Biophysics **310**(1): 32-39.

Ohannesian, L. and A. Streeter (2001). Handbook of pharmaceutical analysis, CRC Press.

Olsen, O., L. Funke, et al. (2007). "Renal defects associated with improper polarization of the CRB and DLG polarity complexes in MALS-3 knockout mice." J Cell Biol **179**(1): 151-164.

Oriolo, A. S., F. A. Wald, et al. (2007). "Intermediate filaments: a role in epithelial polarity." Experimental cell research **313**(10): 2255-2264.

Osathanondh, V. and E. L. Potter (1964). "Pathogenesis of polycystic kidneys. Survey of results of microdissection." Archives of pathology **77**: 510.

Pablo, J. L., P. G. DeCaen, et al. (2016). "Progress in ciliary ion channel physiology." The Journal of general physiology: jgp. 201611696.

Page, M., N. Bejaoui, et al. (1988). "Optimization of the tetrazolium-based colorimetric assay for the measurement of cell number and cytotoxicity." International journal of immunopharmacology **10**(7): 785-793.

Palm, F., J. Cederberg, et al. (2003). "Reactive oxygen species cause diabetes-induced decrease in renal oxygen tension." Diabetologia **46**(8): 1153-1160.

Palm, F. and L. Nordquist (2011). "Renal tubulointerstitial hypoxia: cause and consequence of kidney dysfunction." Clinical and Experimental Pharmacology and Physiology **38**(7): 474-480.

Palmer, L. G. (1995). "Epithelial Na channels and their kin." Physiology **10**(2): 61-67.

Patel, A. and E. Honoré (2010). "Polycystins and renovascular mechanosensory transduction." Nature Reviews Nephrology **6**(9): 530.

Paulmichl, M. and F. Lang (1988). "Enhancement of intracellular calcium concentration by extracellular ATP and UTP in Madin Darby canine kidney cells." Biochemical and biophysical research communications **156**(3): 1139-1143.

Pazour, G. J., B. L. Dickert, et al. (2000). "Chlamydomonas IFT88 and its mouse homologue, polycystic kidney disease gene tg737, are required for assembly of cilia and flagella." The Journal of cell biology **151**(3): 709-718.

Pazour, G. J., J. T. San Agustin, et al. (2002). "Polycystin-2 localizes to kidney cilia and the ciliary level is elevated in orpk mice with polycystic kidney disease." Current Biology **12**(11): R378-R380.

Perrone, R. D. (1985). "In vitro function of cyst epithelium from human polycystic kidney." The Journal of clinical investigation **76**(4): 1688-1691.

Phua, S. C., Y.-C. Lin, et al. (2015). "An intelligent nano-antenna: primary cilium harnesses TRP channels to decode polymodal stimuli." Cell calcium **58**(4): 415-422.

Pitts, R. F. (1968). Physiology of the kidney and body fluids: an introductory text.

Planès, C., M. Blot-Chabaud, et al. (2002). "Hypoxia and β2-agonists regulate cell surface expression of the epithelial sodium channel in native alveolar epithelial cells." Journal of Biological Chemistry **277**(49): 47318-47324.

Pouysségur, J. (1994). "Molecular biology and hormonal regulation of vertebrate Na+/H+ exchanger isoforms." Kidney and Blood Pressure Research **17**(3-4): 190-193.

Praetorius, H., J. Frokiaer, et al. (2003). "Bending the primary cilium opens Ca2+-sensitive intermediate-conductance K+ channels in MDCK cells." The Journal of membrane biology **191**(3): 193-200.

Praetorius, H. and K. R. Spring (2001). "Bending the MDCK cell primary cilium increases intracellular calcium." The Journal of membrane biology **184**(1): 71-79.

Praetorius, H. and K. R. Spring (2003). "Removal of the MDCK cell primary cilium abolishes flow sensing." The Journal of membrane biology **191**(1): 69-76.

Praetorius, H. A. and K. R. Spring (2003). "The renal cell primary cilium functions as a flow sensor." Current opinion in nephrology and hypertension **12**(5): 517-520.

Pratt, J. H. (2005). "Central role for ENaC in development of hypertension." Journal of the american society of nephrology **16**(11): 3154-3159.

Pressley, T. (1996). "Structure and function of the Na, K pump: ten years of molecular biology." Mineral and electrolyte metabolism **22**(5-6): 264-271.

Pruitt, M. E. C., M. A. Knepper, et al. (2006). "Effect of peristaltic contractions of the renal pelvic wall on solute concentrations of the renal inner medulla in the hamster." American Journal of Physiology-Renal Physiology **290**(4): F892-F896.

Quigley, R. (2012). "Chronic kidney disease: highlights for the general pediatrician." International journal of pediatrics **2012**.

Reilly, R. F. and D. H. Ellison (2000). "Mammalian distal tubule: physiology, pathophysiology, and molecular anatomy." Physiological reviews **80**(1): 277-313.

Resnick, A. (2011). "Chronic fluid flow is an environmental modifier of renal epithelial function." PloS one **6**(10): e27058.

Resnick, A. (2016). "HIF Stabilization Weakens Primary Cilia." PloS one **11**(11): e0165907.

Resnick, A. and U. Hopfer (2007). "Force-response considerations in ciliary mechanosensation." Biophysical journal **93**(4): 1380-1390.

Reuss, L., N. K. Wills, et al. (1996). Epithelial transport proteins. Epithelial Transport, Springer**:** 21-48.

Rohatgi, R., A. Greenberg, et al. (2003). "Na transport in autosomal recessive polycystic kidney disease (ARPKD) cyst lining epithelial cells." Journal of the american society of nephrology **14**(4): 827-836.

Roitbak, T., C. J. Ward, et al. (2004). "A polycystin-1 multiprotein complex is disrupted in polycystic kidney disease cells." Molecular biology of the cell **15**(3): 1334-1346.

Rosenbaum, J. L. and G. B. Witman (2002). "Intraflagellar transport." Nature reviews Molecular cell biology **3**(11): 813.

Rosenberger, C., M. Khamaisi, et al. (2008). "Adaptation to hypoxia in the diabetic rat kidney." Kidney international **73**(1): 34-42.

Rosivall, L., S. Mirzahosseini, et al. (2006). "Fluid flow in the juxtaglomerular interstitium visualized in vivo." American Journal of Physiology-Renal Physiology **291**(6): F1241-F1247.

Rotin, D. and L. Schild (2008). "ENaC and its regulatory proteins as drug targets for blood pressure control." Current drug targets **9**(8): 709-716.

Sabolic, I. and D. Brown (1995). "Water channels in renal and nonrenal tissues." Physiology **10**(1): 12-17.

Saeedi, B. J., D. J. Kao, et al. (2015). "HIF-dependent regulation of claudin-1 is central to intestinal epithelial tight junction integrity." Mol Biol Cell **26**(12): 2252-2262.

Sakai, T., D. A. Craig, et al. (1986). "Fluid waves in renal tubules." Biophysical journal **50**(5): 805-813.

Sands, J. M. and H. E. Layton (2000). "Urine concentrating mechanism and its regulation." The Kidney: Physiology and Pathophysiology **3**: 1175-1216.

Sarnak, M. J., A. S. Levey, et al. (2003). "Kidney disease as a risk factor for development of cardiovascular disease: a statement from the American Heart Association Councils on Kidney in Cardiovascular Disease, High Blood Pressure Research,

Clinical Cardiology, and Epidemiology and Prevention." Circulation **108**(17): 2154-2169.

Scavone, C., C. Scanlon, et al. (1995). "Atrial natriuretic peptide modulates sodium and potassium-activated adenosine triphosphatase through a mechanism involving cyclic GMP and cyclic GMP-dependent protein kinase." Journal of Pharmacology and Experimental Therapeutics **272**(3): 1036-1043.

Scholey, J. M. (2008). "Intraflagellar transport motors in cilia: moving along the cell's antenna." The Journal of cell biology **180**(1): 23-29.

Semenza, G. L. (2000). "HIF-1: mediator of physiological and pathophysiological responses to hypoxia." Journal of applied physiology **88**(4): 1474-1480.

Sgouralis, I. and A. T. Layton (2012). "Autoregulation and conduction of vasomotor responses in a mathematical model of the rat afferent arteriole." American Journal of Physiology-Renal Physiology **303**(2): F229-F239.

Sheng, S., M. D. Carattino, et al. (2006). "Furin cleavage activates the epithelial Na+ channel by relieving Na+ self-inhibition." American Journal of Physiology-Renal Physiology **290**(6): F1488-F1496.

Shillingford, J. M., N. S. Murcia, et al. (2006). "The mTOR pathway is regulated by polycystin-1, and its inhibition reverses renal cystogenesis in polycystic kidney disease." Proceedings of the National Academy of Sciences **103**(14): 5466-5471.

Sieuwerts, A. M., J. G. Klijn, et al. (1995). "The MTT tetrazolium salt assay scrutinized: how to use this assay reliably to measure metabolie activity of cell cultures in vitro for the assessment of growth characteristics, IC50-values and cell survival." Clinical Chemistry and Laboratory Medicine **33**(11): 813-824.

Siflinger-Birnboim, A., P. J. del Vecchio, et al. (1987). "Molecular sieving characteristics of the cultured endothelial monolayer." Journal of cellular physiology **132**(1): 111-117.

Simons, M., J. Gloy, et al. (2005). "Inversin, the gene product mutated in nephronophthisis type II, functions as a molecular switch between Wnt signaling pathways." Nature genetics **37**(5): 537.

Simons, M. and G. Walz (2006). "Polycystic kidney disease: cell division without ac (l) ue?" Kidney international **70**(5): 854-864.

Singla, V. and J. F. Reiter (2006). "The primary cilium as the cell's antenna: signaling at a sensory organelle." Science **313**(5787): 629-633.

Siroky, B. J., W. B. Ferguson, et al. (2006). "Loss of primary cilia results in deregulated and unabated apical calcium entry in ARPKD collecting duct cells." American Journal of Physiology-Renal Physiology **290**(6): F1320-F1328.

Smith, E. F. and R. Rohatgi (2011). Cilia 2010: the surprise organelle of the decade, American Association for the Advancement of Science.

Song, H.-A., Y.-S. Kim, et al. (2017). "Hypoxia Modulates Epithelial Permeability via Regulation of Vascular Endothelial Growth Factor in Airway Epithelia." American journal of respiratory cell and molecular biology **57**(5): 527-535.

Sparks, M. A., S. D. Crowley, et al. (2014). "Classical Renin-Angiotensin System in Kidney Physiology." Comprehensive Physiology.

Srinivasan, B., A. R. Kolli, et al. (2015). "TEER measurement techniques for in vitro barrier model systems." Journal of laboratory automation **20**(2): 107-126.

Srivastava, P. K. (2005). Elementary biophysics: an introduction, Alpha Science Int'l Ltd.

Staruschenko, A., D. V. Ilatovskaya, et al. (2016). Fundamentals of Epithelial Na+ Absorption. Ion Channels and Transporters of Epithelia in Health and Disease, Springer**:** 49-94.

Stefani, E. and M. Cereijido (1983). "Electrical properties of cultured epithelioid cells (MDCK)." The Journal of membrane biology **73**(2): 177-184.

Stein, W. D. and T. Litman (2014). Channels, carriers, and pumps: an introduction to membrane transport, Elsevier.

Steinhausen, M., K. Endlich, et al. (1997). "Electrically induced vasomotor responses and their propagation in rat renal vessels in vivo." The Journal of physiology **505**(2): 493-501.

Sullivan, L. P., D. P. Wallace, et al. (1998). "Epithelial transport in polycystic kidney disease." Physiological reviews **78**(4): 1165-1191.

Taglialatela, M. and A. M. Brown (1994). "Structural correlates of K+ channel function." Physiology **9**(4): 169-173.

Tanaka, T., N. Hanafusa, et al. (2003). "Hypoxia induces apoptosis in SV40-immortalized rat proximal tubular cells through the mitochondrial pathways, devoid of HIF1-mediated upregulation of Bax." Biochemical and biophysical research communications **309**(1): 222-231.

Tanaka, T., H. Kato, et al. (2006). "Hypoxia and expression of hypoxia-inducible factor in the aging kidney." The Journals of Gerontology Series A: Biological Sciences and Medical Sciences **61**(8): 795-805.

Taulman, P. D., C. J. Haycraft, et al. (2001). "Polaris, a protein involved in left-right axis patterning, localizes to basal bodies and cilia." Molecular biology of the cell **12**(3): 589-599.

Thiery, J. P. and J. P. Sleeman (2006). "Complex networks orchestrate epithelial–mesenchymal transitions." Nature reviews Molecular cell biology **7**(2): 131.

Thomson, R. B., S. Mentone, et al. (2003). "Histopathological analysis of renal cystic epithelia in the Pkd2 WS25/-mouse model of ADPKD." American Journal of Physiology-Renal Physiology **285**(5): F870-F880.

Thorens, B. (1993). "Facilitated glucose transporters in epithelial cells." Annual review of physiology **55**(1): 591-608.

Torkko, J. M., A. Manninen, et al. (2008). "Depletion of apical transport proteins perturbs epithelial cyst formation and ciliogenesis." Journal of cell science **121**(8): 1193-1203.

Trudel, M., Q. Yao, et al. (2016). "The Role of G-protein-coupled receptor proteolysis site cleavage of polycystin-1 in renal physiology and polycystic kidney disease." Cells **5**(1): 3.

Tufro, A., V. F. Norwood, et al. (1999). "Vascular endothelial growth factor induces nephrogenesis and vasculogenesis." Journal of the american society of nephrology **10**(10): 2125-2134.

Van Itallie, C. M., A. S. Fanning, et al. (2009). "ZO-1 stabilizes the tight junction solute barrier through coupling to the perijunctional cytoskeleton." Molecular biology of the cell **20**(17): 3930-3940.

van Meerloo, J., G. J. Kaspers, et al. (2011). Cell sensitivity assays: the MTT assay. Cancer cell culture, Springer**:** 237-245.

Veland, I. R., A. Awan, et al. (2009). "Primary cilia and signaling pathways in mammalian development, health and disease." Nephron Physiology **111**(3): p39-p53.

Vengellur, A. and J. LaPres (2004). "The role of hypoxia inducible factor 1α in cobalt chloride induced cell death in mouse embryonic fibroblasts." Toxicological Sciences **82**(2): 638-646.

Verghese, E., R. Weidenfeld, et al. (2007). "Renal cilia display length alterations following tubular injury and are present early in epithelial repair." Nephrology Dialysis Transplantation **23**(3): 834-841.

Verghese, E., J. Zhuang, et al. (2011). "In vitro investigation of renal epithelial injury suggests that primary cilium length is regulated by hypoxia-inducible mechanisms." Cell biology international **35**(9): 909-913.

Vivona, M. L., M. Matthay, et al. (2001). "Hypoxia reduces alveolar epithelial sodium and fluid transport in rats: reversal by β-adrenergic agonist treatment." American journal of respiratory cell and molecular biology **25**(5): 554-561.

Walker, A. M. and C. L. Hudson (1936). "The reabsorption of glucose from the renal tubule in amphibia and the action of phlorhizin upon it." American Journal of Physiology-Legacy Content **118**(1): 130-143.

Wang, L., R. Weidenfeld, et al. (2008). "Alterations in renal cilium length during transient complete ureteral obstruction in the mouse." Journal of anatomy **213**(2): 79-85.

Wang, W., W. L. Dentler, et al. (2001). "VEGF increases BMEC monolayer permeability by affecting occludin expression and tight junction assembly." American Journal of Physiology-Heart and Circulatory Physiology **280**(1): H434-H440.

Wang, W., H. Sackin, et al. (1992). "Renal potassium channels and their regulation." Annual review of physiology **54**(1): 81-96.

Wei, W., V. Popov, et al. (2006). "Evidence of angiogenesis and microvascular regression in autosomal-dominant polycystic kidney disease kidneys: a corrosion cast study." Kidney international **70**(7): 1261-1268.

Weimbs, T. (2006). "Regulation of mTOR by polycystin-1: is polycystic kidney disease a case of futile repair?" Cell cycle **5**(21): 2425-2429.

Weimbs, T. (2007). "Polycystic kidney disease and renal injury repair: common pathways, fluid flow, and the function of polycystin-1." American Journal of Physiology-Renal Physiology **293**(5): F1423-F1432.

Wenger, R. H., V. Kurtcuoglu, et al. (2015). "Frequently asked questions in hypoxia research." Hypoxia **3**: 35.

White, P., R. B. Doctor, et al. (2000). "Coincident microvillar actin bundle disruption and perinuclear actin sequestration in anoxic proximal tubule." American Journal of Physiology-Renal Physiology **278**(6): F886-F893.

Whitehead, R., P. VanEeden, et al. (1993). "Establishment of conditionally immortalized epithelial cell lines from both colon and small intestine of adult H-2Kb-tsA58 transgenic mice." Proceedings of the National Academy of Sciences **90**(2): 587-591.

Wills, N. K., L. Reuss, et al. (2012). Epithelial transport: a guide to methods and experimental analysis, Springer Science & Business Media.

Wilson, P. and D. Falkenstein (1995). The pathology of human renal cystic disease. Tubulointerstitial and Cystic Disease of the Kidney, Springer**:** 1-50.

Wilson, P. D. (2004). "Polycystic kidney disease." New England Journal of Medicine **350**(2): 151-164.

Wilson, P. D. (2011). "Apico-basal polarity in polycystic kidney disease epithelia." Biochimica et Biophysica Acta (BBA)-Molecular Basis of Disease **1812**(10): 1239-1248.

Wilson, P. D., M. A. Dillingham, et al. (1985). "Defined human renal tubular epithelia in culture: growth, characterization, and hormonal response." American Journal of Physiology-Renal Physiology **248**(3): F436-F443.

Wilson, P. D., L. Geng, et al. (1999). "The PKD1 gene product," polycystin-1," is a tyrosine-phosphorylated protein that colocalizes with alpha2beta1-integrin in focal clusters in adherent renal epithelia." Laboratory investigation; a journal of technical methods and pathology **79**(10): 1311-1323.

Wilson, P. D., A. Sherwood, et al. (1991). "Reversed polarity of Na (+)-K (+)-ATPase: mislocation to apical plasma membranes in polycystic kidney disease epithelia." American Journal of Physiology-Renal Physiology **260**(3): F420-F430.

Wodopia, R., H. S. Ko, et al. (2000). "Hypoxia decreases proteins involved in epithelial electrolyte transport in A549 cells and rat lung." American Journal of Physiology-Lung Cellular and Molecular Physiology **279**(6): L1110-L1119.

Xu, D.-Z., Q. Lu, et al. (1999). "The effect of hypoxia/reoxygenation on the cellular function of intestinal epithelial cells." Journal of Trauma and Acute Care Surgery **46**(2): 280-285.

Yamagata, K., M. Tagami, et al. (2004). "Hypoxia-induced changes in tight junction permeability of brain capillary endothelial cells are associated with IL-1beta and nitric oxide." Neurobiology of disease **17**(3): 491-499.

Yamaguchi, T., S. J. Hempson, et al. (2006). "Calcium restores a normal proliferation phenotype in human polycystic kidney disease epithelial cells." Journal of the american society of nephrology **17**(1): 178-187.

Yang, B., N. D. Sonawane, et al. (2008). "Small-molecule CFTR inhibitors slow cyst growth in polycystic kidney disease." Journal of the american society of nephrology **19**(7): 1300-1310.

Yoder, B. K., X. Hou, et al. (2002). "The polycystic kidney disease proteins, polycystin-1, polycystin-2, polaris, and cystin, are co-localized in renal cilia." Journal of the american society of nephrology **13**(10): 2508-2516.

Yoder, B. K., A. Tousson, et al. (2002). "Polaris, a protein disrupted in orpk mutant mice, is required for assembly of renal cilium." American Journal of Physiology-Renal Physiology **282**(3): F541-F552.

Young, D. K. and D. J. Marsh (1981). "Pulse wave propagation in rat renal tubules: implications for GFR autoregulation." American Journal of Physiology-Renal Physiology **240**(5): F446-F458.

Yu, A. S., S. A. Kanzawa, et al. (2008). "Tight junction composition is altered in the epithelium of polycystic kidneys." The Journal of pathology **216**(1): 120-128.

Yu, X., Y. Fang, et al. (2012). "The balance of beneficial and deleterious effects of hypoxia-inducible factor activation by prolyl hydroxylase inhibitor in rat remnant kidney depends on the timing of administration." Nephrology Dialysis Transplantation **27**(8): 3110-3119.

Yuan, S. and R. Rigor (2010). "Methods for measuring permeability." Regulation of Endothelial Barrier Function. San Rafael (CA).

Yuan, Y., G. Hilliard, et al. (2003). "Cobalt inhibits the interaction between hypoxia-inducible factor-α and von Hippel-Lindau protein by direct binding to hypoxia-inducible factor-α." Journal of Biological Chemistry **278**(18): 15911-15916.

Zerres, K., S. Rudnik-Schöneborn, et al. (1998). "Autosomal recessive polycystic kidney disease." Journal of molecular medicine **76**(5): 303-309.

Zhang, Q., P. D. Taulman, et al. (2004). "Cystic kidney diseases: all roads lead to the cilium." Physiology **19**(4): 225-230.

Zhong, H. and J. W. Simons (1999). "Direct comparison of GAPDH, β-actin, cyclophilin, and 28S rRNA as internal standards for quantifying RNA levels under hypoxia." Biochemical and biophysical research communications **259**(3): 523-526.